DEVELOPMENT OF CALCIUM OXIDE SOLID REACTANT FOR THE UT-3 THERMOCHEMICAL CYCLE TO PRODUCE HYDROGEN FROM WATER

By

BENJAMIN GRANT HETTINGER

A THESIS PRESENTED TO THE GRADUATE SCHOOL
OF THE UNIVERSITY OF FLORIDA IN PARTIAL FULFILLMENT
OF THE REQUIREMENTS FOR THE DEGREE OF
MASTER OF SCIENCE

UNIVERSITY OF FLORIDA

2005

ACKNOWLEDGMENTS

Many people have assisted me in the past year and a half with this thesis project here at the University of Florida. I could not have completed this task without the help these people who gave me their time, taught me knowledge, challenged me to think critically, and supported me throughout the project.

I thank Dr. D. Yogi Goswami for the opportunity to investigate this challenging research project and his encouragement to investigate all aspects of the project. I thank my committee members, S. A. Sherif, Dr. H. Ingley, and Dr. H. Hagelin-Weaver, for their advice and support throughout the project.

I thank Dr. Deshpande for his tireless efforts to aid me in understanding the subject of my research, for continuing to push me to stay diligent, for helping me write and edit my thesis, and for being a helpful advisor. He has been there at every step of this project and helped to impart academic knowledge in many aspects of research. He has especially helped me to more quickly grasp the chemical engineering and chemistry which encompass the majority of this project.

I thank Chuck G. for teaching me how to use many of the tools at the shop and also for imparting on me practical engineering knowledge and critical thinking. I also am grateful for the members of the lab group that advised me on solutions to problems in research, challenged me to investigate problems further, and who helped me to find and to use items in the lab.

I had a lot of help at the different facilities and with the variety of equipment I used. I thank Dr. Anghai and Tom Carter and those at the nuclear laboratory for the use of their facilities and friendly and helpful assistance. I also thank Dr. Hahn for the use of the his aid in understanding Raman spectroscopy and X- Ray diffraction. I thank Gary Scheiffele for his training on Raman spectroscopy and mercury porosimetry and his willingness to help me understand their use and limitations. I thank Gill Brubaker for his training on the NOVA machine for nitrogen adsorption analysis. I would also like to thank other people at the Particle Science Engineering building who helped to orient me with use of their equipment. I acknowledge financial support from the US Department of Energy which allowed me to investigate this project. Without these people I could not have finished my project.

I thank my parents, Jean and Glenn Hettinger, and the rest of my family in their constant support of my education. I thank my friends and Kappa Sigma fraternity brothers for their support and help over the years. Most of all I thank my Lord Jesus Christ who has sustained me through life thus far especially during the tough times.

TABLE OF CONTENTS

LIST OF TABLES

LIST OF FIGURES

LIST OF SYMBOLS

Chemical Elements

Br	Bromine
Ca	Calcium
C	Carbon
Cl	Chlorine
Fe	Iron
H	Hydrogen
I	Iodine
Mn	Manganese
Na	Sodium
O	Oxygen
S	Sulfur
Si	Silicon
Ti	Titanium
Zn	Zinc
Zr	Zirconium

Calcium Compounds

$CaBr_2$	Calcium Bromide
$CaCO_3$	Calcium Carbonate
$Ca(OH)_2$	Calcium Hydroxide

CaO	Calcium Oxide
$CaTiO_3$	Calcium Titanate

Other Chemistry Symbols

$+\delta$	Positive partial charge
$-\delta$	Negative partial charge
e^-	Electron
M	Metal Atom
m	Stoichiometric symbol
n	Stoichiometric symbol
R	Organic molecule
x	Stoichiometric symbol
y	Stoichiometric symbol

Other Symbols

γ	Mercury surface tension [degrees]
θ	Mercury contact angle [dyne/cm]
C_V	Concentration of vacant sites on reaction surface [mol/L]
$C_{N2\text{-}S}$	Concentration of sites with nitrogen adsorbed [mol/L]
$C_{subscript}$	Concentration [mol/L]
H_{H2}	Power of hydrogen produced based on HHV [MW]
H_{He}	Heat input from helium [MW]
H_R	Heat recovered [MW]
HX	Heat exchanger
Int	Relative intensity of light [counts]

k_A	Adsorption rate coefficient [1/(psia*s)]
K_A	Equilibrium adsorption constant [1/psia]
MT	Metric tons
P	Pressure [psia]
P_c	Power consumed [MW]
P_o	Ambient pressure [psia]
P_{N2}	Pressure of nitrogen [psia]
r_{3s}	Rate of reaction 3 [mol/(L*s)]
r_{AD}	Rate of adsorption [mol/(L*s)]
R	Universal gas constant [J/(gmol*K)]
R1-R4	Reactors 1 through 4 respectively
S1-S2	Separators 1 and 2
T	Temperature[K or °C]
X	Conversion

Abstract of Thesis Presented to the Graduate School
of the University of Florida in Partial Fulfillment of the
Requirements for the Degree of Master of Science

DEVELOPMENT OF CALCIUM OXIDE SOLID REACTANT FOR THE UT-3 THERMOCHEMICAL CYCLE TO PRODUCE HYDROGEN FROM WATER

By

Benjamin Grant Hettinger

December 2005

Chair: D. Yogi Goswami
Major Department: Mechanical and Aerospace Engineering

Hydrogen may be the answer to meeting the world's energy demand as it increases and the fossil fuel sources run out. The University of Tokyo #3 (UT-3) thermochemical cycle is being researched as a means of producing hydrogen from water. In order to make the UT-3 thermochemical cycle economically feasible, the operating temperatures for the reactions must be reduced. In order to study this cycle, the solid reactant must be in a form that will allow the reactions to take place efficiently. A procedure to make the solid reactant for the UT-3 thermochemical cycle has been developed using outlines from previous researchers. The procedure includes chemical procedures to make the precursors, drying and preheating, molding, and sintering procedures.

Sol-gel chemistry was used to create the particulate precursors for the pellets. The liquor resultant from the chemistry procedure was dried via evaporation and then preheated to 430°C to eliminate volatiles. The resultant powder was molded into pellets

using a compression mold which had been fabricated. The pellets were then sintered to temperatures above the highest operation temperature of the UT-3 cycle, 760°C in order to strengthen the pellets.

The characteristics of the fabricated pellets were used to gauge the success of the process and modify it as necessary to yield better characteristics. The characteristics of the pellets which were used to evaluate the procedure were the porosity, the composition, and the strength. The porosity was evaluated by mercury porosimetry and nitrogen adsorption. The composition was determined qualitatively by Raman spectroscopy and X-ray diffraction and quantitatively by a chemical procedure. The strength was evaluated qualitatively.

Based on these characteristics a number of changes were made to the procedure including a new chemical procedure, a redesigned molding assembly, and the addition of a preheating step. Correlations were also made between certain characteristics and procedural parameters. One correlation showed that there was an increase in strength with sintering temperature but a decrease in both macro and micro porosity. Another correlation showed that the strength of the pellets decreased with an increase in the ratio of calcium to titanium used in the pellets.

Though these pellets seem to have acceptable characteristics, more characteristics including reactivity and degradation need to be studied. These pellets may not hold up structurally or may not react as well as they must. Further study needs to be done to truly determine the success of this process. More importantly, the pellets are just the first step toward studying the UT-3 thermochemical cycle.

CHAPTER 1
INTRODUCTION

The world energy consumption is rising as more and more countries become industrialized. Currently the most abundantly used sources of energy are fossil fuels. These, however, are limited and most projections show that the production of oil will not meet the need within the next 10 to 25 years. This presents a major problem to energy consumers around the world but especially for transportation where oil is almost the sole energy source. Looking ahead the United States is seeking the solution in hydrogen powered transportation. The U.S. government along with automobile manufacturers is pushing researchers to investigate hydrogen to meet this upcoming need. Hydrogen has been shown to be 40 to 50% efficient in fuel cells and is environmentally friendly producing steam as its only by-product. There are many problems that must be solved in order to make the "hydrogen economy" feasible. A large amount of research is being conducted to investigate hydrogen production, fuel cells, storage, safety, and infrastructure.

This research focuses on a small but important aspect of one of the potential hydrogen production processes. In this chapter an overview of the present methods for hydrogen production is presented and discussed.

Current Hydrogen Production Methods

There are a number of methods that can be used to produce hydrogen. These methods include steam methane reformation (SMR), partial oxidation of fuels (POX)

coal and biomass gasification, electrolysis, thermal decomposition, thermochemical processes, biological, and other processes. Some of these have been found to be impractical, such as, thermal decomposition. Others are established means of hydrogen production and still others are currently being investigated and may be viable options in the future. Ideally a process is sought that is a cost effective and energy efficient means to produce hydrogen using a renewable energy source. This would allow utilization of all the benefits of hydrogen as a fuel.

Fossil Fuels

The most cost effective way to produce hydrogen is to use one of the fossil fuel processes. Though these processes are efficient and cost effective, they also eliminate on of the major advantages of hydrogen. The green house gas CO_2 is still being produced if hydrogen is produced in this manner. Though, biomass is not considered a fossil fuel it has been included with coal gasification because of the similarity in the processes. It is considered a carbon neutral means of hydrogen production. Also the reason hydrogen is being researched as a fuel source is because of the depleting fossil fuel sources.

Steam methane reformation

Steam methane reformation (SMR) has many benefits and is the most economical method of producing hydrogen now. It is a process in which steam and methane are combined at high temperatures (700°C to 925°C) using a catalyst. A sulfur separation step is needed so that the catalyst will not be destroyed. After the first reaction an equilibrium shift reaction is added to produce more oxygen in the cycle. The total process result is 96-98% pure hydrogen with an efficiency of 65-75% (Goswami et al., 2003). The heat is supplied by burning fossil fuels. There are two drawbacks to this method. First the method is not “clean” or “green”. It produces the green house gas, CO-

$_2$. Second it relies on the limited amount of methane on the earth. As the supply dwindles the feedstock cost will rise and make SMR less economical than other processes. The chemical scheme for SMR can be seen below in Equations 1.1 and 1.2 (Cox and Williamson, 1977-1979).

$$C_n \cdot H_m + n \cdot H_2 \cdot O = n \cdot CO + \left(\frac{2 \cdot n + m}{2}\right) \cdot H_2 \quad (1.1)$$

$$CO + H_2O = CO_2 + H_2 \quad (1.2)$$

Partial oxidation method

The next most popular method of hydrogen production is partial oxidation of heavy hydrocarbons (POX). This method is very similar to SMR with the addition of a step. In this additional step heavy hydrocarbons are partially burned with pure oxygen and water. Simultaneously, the heavy hydrocarbons are broken down into less complex hydrocarbons such as methane which is reacted with steam in a similar manner as in SMR. The resulting products are CO, CO_2, H_2O, H_2. After a desulphurization step the shift reaction is again used to produce more hydrogen. POX produces hydrogen with a purity of 96-98% and an efficiency of about 50% (Goswami et al., 2003). The same problems exist with POX as did with SMR. The additional step of oxygen separation increases the cost of this process compared to SMR.

$$C_n \cdot H_m + \frac{n}{2} \cdot O_2 = n \cdot CO + \left(\frac{m}{2}\right) \cdot H_2 + \text{Heat} \quad (1.3)$$

$$C_n \cdot H_m + n \cdot H_2 \cdot O + \text{Heat} = n \cdot CO + \left(\frac{2 \cdot n + m}{2}\right) \cdot H_2 \quad (1.4)$$

$$CO + H_2O = CO_2 + H_2 + \text{Heat} \quad (1.5)$$

Coal and biomass gasification

Coal and biomass gasification are very similar to POX with the differences of a higher temperature range (1100°C -1300°C), higher pressures, and there is very little

oxygen present. The high carbon content of coal and biomass is converted to CO2, H2, and CO. After a desulphurization step the shift reaction is again used to produce more H2. Purity of hydrogen of up to 97% has been obtained using coal gasification (Goswami et al., 2003). Coal is the most abundant fuel on earth and supplies will probably not be a concern for a century from now. Like those mentioned before, this process produces the greenhouse gas, CO2.

Using biomass as the fuel other benefits and problems exist. Benefits include valuable byproducts such as ammonia, better pollution control, and lower operating costs. Biomass is also considered a carbon neutral fuel because the CO2 would be produced through natural decomposition anyway. The problems lie in transporting the solid fuel and disposing of the large quantities waste ash that are produced.

$$2C+O_2 \rightarrow 2CO \quad (1.6)$$

$$C+H_2O \rightarrow CO+H_2 \quad (1.7)$$

$$C+CO_2 \rightarrow 2CO \quad (1.8)$$

All these processes based on fossil fuels produce CO2. Presently they are the most cost effective ways to produce hydrogen. The main benefit of hydrogen as a fuel is that it does not produce any harmful by products when used to make energy. If it is produced in a manner in which CO2 is created this benefit is essentially eliminated. Alternative methods must be used if this benefit is wanted.

Electrolysis

Electrolysis of water is the next most commonly used means to produce hydrogen. In electrolysis a voltage is supplied so that electricity flows through a medium and ions are conducted across a membrane. H_2 is produced by combing H^+ ions and two electrons at the cathode as shown in Equation 1.9. Water is split at the anode so that O2

is produced along with H^+ ions and electrons as seen in Equation 1.10 (Cox and Williamson, 1977-1979)

$$H_2O \rightarrow .5\ O_2 + 2H^+ + 2e^- \qquad \text{Anode} \qquad (1.9)$$

$$2H^+ + 2e^- \rightarrow H_2 \qquad \text{Cathode} \qquad (1.10)$$

Electrolysis has been researched extensively and some ideas presently being considered are the electrolysis of sea water and efficiency increase with temperature variance. Electrolysis has been seen to be 94% efficient based on the electrical power input to the system (Goswami et al., 2003). This electricity however comes from another source. Solar produced electricity is a very good source to use for electrolysis. Almost all the electricity produced by solar means can be used to make hydrogen. This creates a clean way to produce hydrogen and can eliminate any fossil fuels from the process.

Thermal Decomposition of Water

When water is heated to very high temperatures some of the steam decomposes to O2, H2, OH, O, and H. At first glance this process seems very simple, but it has many problems. A large amount of energy has to be supplied to heat water to the needed temperatures. The steam does not even fully dissociate until a temperature above 4000K is reached. The mixture of dissociated gases is also highly explosive which creates a very serious danger. Finding containers that can withstand the temperatures needed for the operation also presents a problem. High temperature gas separation is also hard to do. Quenching can be done but the heat lost during the process can not be recovered and makes the process too costly to operate. Only 2.1% efficiency has been recorded using the thermal decomposition of water to produce hydrogen and only a 40% theoretical

efficiently has been calculated (Goswami et al., 2003). Obviously, this process is not feasible unless solutions are found to these problems.

Thermochemical Processes

In thermochemical processes water is input along with heat and oxygen and hydrogen are produced. The overall result then is the same as that of thermal decomposition. These processes are much different, however, and much more practical. The processes have been theoretically modeled to be up to 50% efficient dwarfing the 2.1% efficiency of the thermal decomposition of water (Sakurai et al. 1996). Much lower temperatures can also be used and hydrogen and oxygen can be produced in different steps eliminating an explosive mixture of gases. Each thermochemical process however has its own problems that must be considered to make the process feasible.

Inside this black box system a series of heat driven chemical reactions are used to produce hydrogen and oxygen. There are thousands of proposed processes but only a few which have been studied extensively and even fewer that hold promise in large scale implementation. Some of these processes are discussed later in this chapter.

Photoelectrical and Photochemical Hydrogen Production

Photoelectrical systems couple a solar voltaic cell with electrolysis. A photo anode absorbs sunlight creating a current to flow and electrolysis to occur. Hybrids of this system have reported efficiencies of up to 18% (Goswami et al., 2003). In photochemical systems semiconductors are paired with photosensitive organic particles. When light hits the photosensitive particles electrons are excited and are directly used to carry out the reduction and oxidation reactions to create hydrogen. There are problems in the catalyst and photosensitive material degrading, back reactions, and the separation of hydrogen and oxygen. Photochemical systems have yet to reach 10% efficiency

(Goswami et al., 2003). More investigation must be conducted to evaluate the feasibility of these hydrogen production methods.

Biological Hydrogen Production

There are two general biological methods that are used to produce hydrogen. The first is the fermentation of bacteria. In this process organic substances are converted to oxygen and hydrogen without sunlight or oxygen. The theoretical efficiency for this process is only 33% (Goswami et al., 2003). Treatment of the polluted process water may also be a problem which should be addressed when considering this process.

The second method is called biophotolysis. In this process micro-algae-cynobacteria and green algae are exposed to sunlight and water. Through organic processes they produce hydrogen and oxygen. There are two types of bacteria, nitrogenase and hydrogenase. The first of the two uses ATP molecules and coverts them to ADP molecules releasing H+ ions in the process which form hydrogen. Hydrogenase produces hydrogen by breaking down carbohydrates in a photosynthesis system. Both will die in the presence of a small amount of oxygen (Goswami et al., 2003).

Thermochemical Cycles

There are thousands of thermochemical processes. The processes vary widely in many different aspects though some are very similar. Many of the processes are slight modifications of a previous cycle, including a substitute reaction or reactions and/or an imposed voltage. Processes with imposed voltages are known as hybrid thermochemical cycles.

Ispra Mark Processes

The first thoroughly researched process is the Ispra Mark I process shown below. As can be seen mercury is used in this process. Mercury is known to be a very toxic

element and research on this process was discontinued because on a larger scale use the process would be too much of a safety risk for consideration. The process was important, however, as it was a harbinger of the exploration of thermochemical cycles. It was the first process demonstrated to give reasonable amount of hydrogen at an acceptable efficiency. Other processes followed the Ispra Mark I and there are now 17 Ispra Mark processes some of which have different sub-processes. The series of Ispra Mark processes are some of the most promising thermochemical processes.

Ispra Mark I

$$CaBr_2+2H_2O \rightarrow Ca(OH)_2+2HBr \quad (730°C) \quad (1.12)$$

$$2HBr+Hg \rightarrow HgBr_2+H_2 \quad (250°C) \quad (1.13)$$

$$HgBr_2+Ca(OH)_2 \rightarrow CaBr_2+HgO+H_2O \quad (200°C) \quad (1.14)$$

$$HgO \rightarrow Hg+.5O_2 \quad (600°C) \quad (1.15)$$

Much work has been done in exploring the possibility of using iron-chloride in processes. Ispra Mark processes 7, 7A, 7B, 9, 14, and 15 contain iron-chloride. Problems in these processes have been found and generally stem from either the thermal decomposition of $FeCl_3$ (Eq. 1.17) or the hydrolysis of $FeCl_2$ (Eq. 1.18). Much research has been conducted to eliminate these problems but no viable solution has been found. The iron-chloride family of reactions was deemed uneconomical and research has been focused elsewhere. Ispra Mark 7B can be seen below.

Ispra Mark 7B

$$2Fe_2O_3+6Cl_2 \rightarrow 4FeCl_3+3O_2 \quad (1000°C) \quad (1.16)$$

$$2FeCl_3 \rightarrow 2FeCl_2+Cl_2 \quad (420°C) \quad (1.17)$$

$$3\,FeCl_2 + 4H_2O \rightarrow Fe_3O_4 + 6\,HCl + H_2 \quad (650°C) \quad (1.18)$$

$$Fe_3O_4 + O_2 \rightarrow 6Fe_2O_3 \quad (350°C) \quad (1.19)$$

Another focus area of research was the sulfur family processes, mostly concerning the decomposition of sulfuric acid. The Ispra Mark 4, 10,11,12,13, 16 and 17 processes all use sulfur, but the ones that focus on the decomposition of sulfuric acid are 11, 13, 16, and 17. Each process starts with the thermal decomposition of sulfuric acid but there are 4 different schemes to finish the respective processes, three of which are shown below.

Decomposition of Sulfuric Acid

$$H_2SO_4 \rightarrow 2SO_2+2H_2O+O_2 \quad (1.20)$$

Ispra Mark 11 (also known as Westinghouse)

$$SO_2 + 2H_2O + elec \rightarrow H_2SO_4 + H_2 \quad (1.21)$$

Ispra Mark 13

$$2H_2O+Br_2+SO_2 \rightarrow H_2SO_4 + 2HBr \quad (1.22)$$

$$2HBr+elec \rightarrow Br_2 + H_2 \quad (1.23)$$

Ispra Mark 16 (also known as the General Atomic Process and the sulfur-iodine process)

$$2H_2O+ I_2+SO_2 \rightarrow H_2SO_4+2HI \quad (1.24)$$

$$2HI \rightarrow I_2+H_2 \quad (1.25)$$

The Ispra Mark 16 process is also known as the General Atomic (GA) process because of GA's extensive work on it. It shows much potential and is one of the most researched processes.

Sulfur-Iodine or Mark 16 or GA Process

$$I_2+SO_2+H_2O \rightarrow 2HI+H_2SO_4 \quad (100\ ^\circ C) \quad (1.26)$$

$$2HI \rightarrow H_2+I_2 \quad (420^\circ C) \quad (1.27)$$

$$H_2SO_4 \rightarrow H_20+SO_2+ .5O_2 \quad (850\ ^\circ C) \quad (1.28)$$

The GA process has many desirable aspects. Three reactions are used at relatively low thermochemical process temperatures. The reactions can also be arranged

to create a continuous process. Many people have studied this reaction and it has been well researched. Theoretical efficiencies have been predicted to be approximately 50%. There are expensive separation and purification steps that needed to be considered. This process also uses highly acidic chemicals. In addition there have been problems with hydriodic acid decomposition. At 700K there is only a 25% dissociation which cannot be greatly increased with temperature. This, therefore, makes it necessary for the products to be recirculated creating thermal losses. Another factor that must be considered is the possibility of side reactions which can form sulfur and hydrogen sulfide. Despite these problems, this process is being studied at a number of places and has arguably the most potential of thermochemical processes to be used to produce hydrogen (Sakurai et al., 1999, 2000)

Metal Oxides

$M_xO_y = xM + y/2\ O_2$ (High Temperature reduction reaction) (1.29)

$xM + yH2O = M_xO_y + yH_2$ (Low Temperatures oxidation reaction) (1.30)

Another large area of research within thermochemical processes is being conducted on metal oxide reduction-oxidation (redox) processes. Metals are reduced with heat creating a pure metal and releasing oxygen. The metal is oxidized with water to form a metal oxide once again. The metal steals the oxygen from the water so that hydrogen is released. There are a number of metals and alloys being considered at this time. The simplicity of the processes seems appealing, having only 2 reactions. Most of the oxidizing reactions proceed without problem. An undesirable requirement of these processes is that the reduction reaction occurs at very high temperatures. Much of the

work being done is to find an alloy that will significantly lower the temperature of the reduction reaction.

One of the most promising is the zinc oxide reaction. Reported conversion efficiencies have been as high as 50% (Weidenkaff et al., 2000). The temperature for the reduction reaction however is 2300K. The process is depicted below in Figure 1.

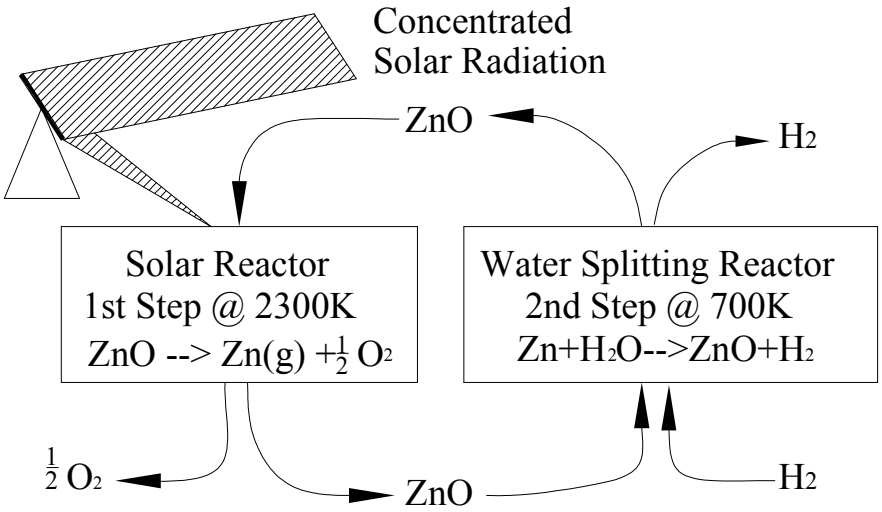

Figure 1.1 Two-Step Water-Splitting Oxides Reduction Processes
(Weidenkaff et al., 1999)

Other metals and alloys considered are listed below with their reduction temperature. Some of the temperatures have been reported over a range of temperatures. For simplicity, one value was chosen and the actually temperatures will vary somewhat based on the experimental design. The Table is just to show typical temperature values for thermochemical metal oxide processes.

Table 1.1: Reduction Temperatures for Researched Metal Oxides

Metal or Alloy	[K]	[°C]	References
ZnO	2000	1727	Weidenkaff et al., 2000 & Hauter et al., 1999
Mn2O3	1835	1562	Meier et al., 1996 & Sturzenegger and Nuesh, 1998
Fe3O4	2300	2027	Steinfeld et al., 1999
MnFe2O4	1273	1000	Ehrensberger et al., 1995
Na3(MnFe2)O6	1073	800	Kaneko et al., 2001,2002

Miscellaneous Processes

There are other processes that have been researched by different groups. Most groups are found either at universities or scientific labs around the world.

One group at the University of Tokyo developed one of the most promising processes. They have done extensive research on the process and up-scaled their laboratory scale model. It is predicted to be the first thermochemical process that will actually be used for large scale hydrogen production. This process is know as the UT-3 process and will be discussed in more detail in the next chapter.

Another process that might have potential is the Julich Center EOS shown below.

$$2Fe3O4+6FeSO_4 \rightarrow 6Fe_2O_3+6SO_2+O_2 \quad (800°C) \quad (1.31)$$

$$3FeO+H_2O \rightarrow Fe3O4+H_2 \quad (700°C) \quad (1.32)$$

$$Fe_2O_3+SO_2 \rightarrow FeO+FeSO_4 \quad (200°C) \quad (1.33)$$

It is in the beginning stages of research and has many desirable attributes. Reactants in this cycle are not corrosive. Besides oxygen and hydrogen, the only elements used are sulfur and iron which are very abundant on the earth. Early testing shows the reactions go as written. Not much current research is being conducted on this process, however. This may be due to other significant problems encountered (Brown et al., 2002).

CHAPTER 2
THE UT-3 THERMOCHEMICAL PROCESS

The University of Tokyo #3 thermochemical (UT-3) process was proposed in 1978 by Kameyama and Yoshida at the 2nd World Energy Conference (Kameyama and Yoshida, 1978). A UT-3 cycle is composed of a series of four thermochemical reactions which are shown below. The operating temperatures are relatively lower than those found in other thermochemical cycles, the highest being 760°C. When the reactions proceed in the correct order all the solid reactants are regenerated, except water which is split into hydrogen and oxygen and separated from the system. The flow schematic of the UT-3 Thermochemical process is shown in Figure 2.1 below and the reactions are enumerated below:

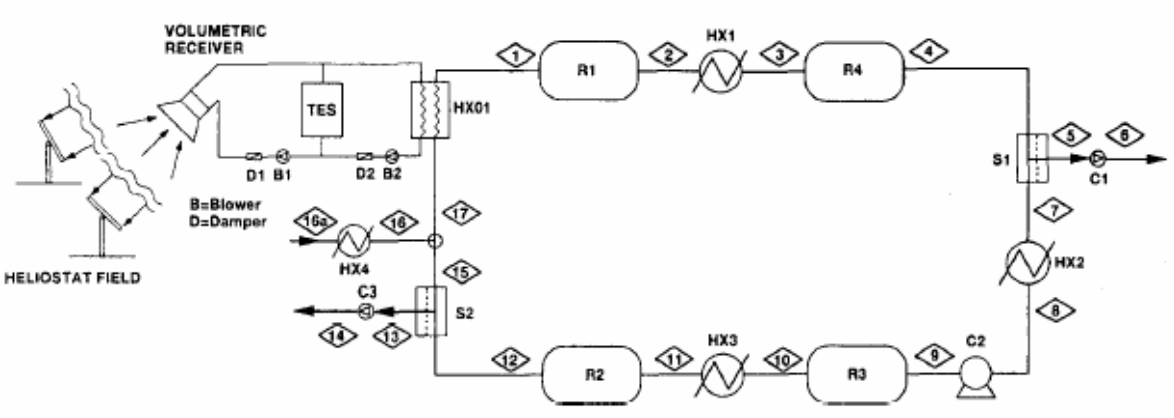

Figure 2.1 Flow Sheet of the Solar UT-3 Thermochemical Process (Sakarai et al., 1996)

The UT-3 System starts with water being pumped into the system <16>, heated into steam in HX01, and pumped into the reactor R1 where reaction (2.1) occur with

$CaBr_2$ to generate HBr. This reaction is reported to take one hour to reach equilibrium. Surplus steam along with other gaseous products (primarily HBr) is routed to reactor R4 where reaction (2.4) takes place with the release of H_2 and additional HBr.

(Reactor R1, 760°C)	$CaBr_2+H_2O(g) \rightarrow CaO + HBr(g)$	(2.1)
(Reactor R2, 570°C)	$CaO+Br_2(g) \rightarrow CaBr + .5O_2\ (g)$	(2.2)
(Reactor R3, 220°C)	$Fe_3O_4+8HBr(g) \rightarrow 3FeBr_2+4H_20(g)+Br_2(g)$	(2.3)
(Reactor R4, 560°C)	$FeBr_2+4H_2O(g) \rightarrow Fe_3O_4+6HBr(g)+H_2(g)$	(2.4)

Hydrogen is separated from the main process stream at S1. The balance flow primarily containing HBr reacts with Fe_3O_4 in reactor R3 to form Br_2 as shown in the reaction (2.3). Br_2 then reacts with CaO in reactor R2 to release O_2 as shown in the reaction (2.2). O_2 is separated in S2 and the balance of the stream flows with the make-up water, at <16> , back to reactor 1 completing the cycle.

The prominent features of the process path are listed below.

1. Only water is fed through the stream <16> which is consumed and split into H_2 and O_2.

2. Reactors R1 and R4 (hydrolysis reactors) produce H2 and Reactors R1 and R2 and R3 (bromination reactors) produce O2.

3. The products of reactors R1 and R4 are reactants in the reactors R2 and R3 respectively. As reaction equilibrium is reached in the reactors, the flow direction is reversed, where reactors R2 and R3 now function as the hydrolysis reactors (producing hydrogen) and reactors R1 and R4 serve as the bromination reactors (producing O2). This switch over approach can be repeated multiple times for continuous operation.

History of Research on the UT-3 Thermochemical Process

Through the years the reactions and process have been studied extensively by groups in Japan. The UT-3 process may have potential as a means to commercially produce hydrogen in a carbon free and energy efficient manner. However, in order to

evaluate this potential, a number of different aspects of the UT-3 process have to be investigated. For discussion these aspects are categorized into process and simulation studies, membrane and separation techniques, iron solid reactants, and calcium solid reactants.

Process and Simulation Studies

The first investigation (Kameyama and Yoshida, 1978) examined the Gibbs free energy of each of the reactions in the UT-3 process. An experimental set up was reported but no significant system study was made.

In 1981, a conceptual design of a large scale UT-3 thermochemical process hydrogen production plant to be coupled with a high temperature nuclear power plant was given (Kameyama and Yoshida, 1981). The facility would include three main sections (Figure 2.2). The first two consisting of a reaction tower for the calcium reactants and another for the iron reactants. The third section would be a tower for heat exchangers to bring high temperature heat to the reactors and recover waste heat from other reactors. The design includes a provision for using solid reactants in the form of honeycomb-shaped tubes with inert materials as binders. The honeycomb-shaped solid reactants would be put into a fixed bed reactor. The reactions can occur along honeycomb channels isolating the process stream from the reactor walls. Thus this would eliminate the need for expensive materials of construction such as titanium. In this paper a simulation was also done to determine the reaction zone as well as investigate heat exchanger design.

Results from the performance of the MASCOT (Model Apparatus for Studying Cyclic Operation in Tokyo) bench scale UT-3 plant were reported in 1984 (Nakayama et al., 1984). Most of the paper focused on the experimental setup for the MASCOT plant

(Figure 2.3). The plant was designed to produce 3 normal liters of H_2 per hour. It was run for 2 cycles with a peak performance of 2 normal liters per hour (Figure 2.4).

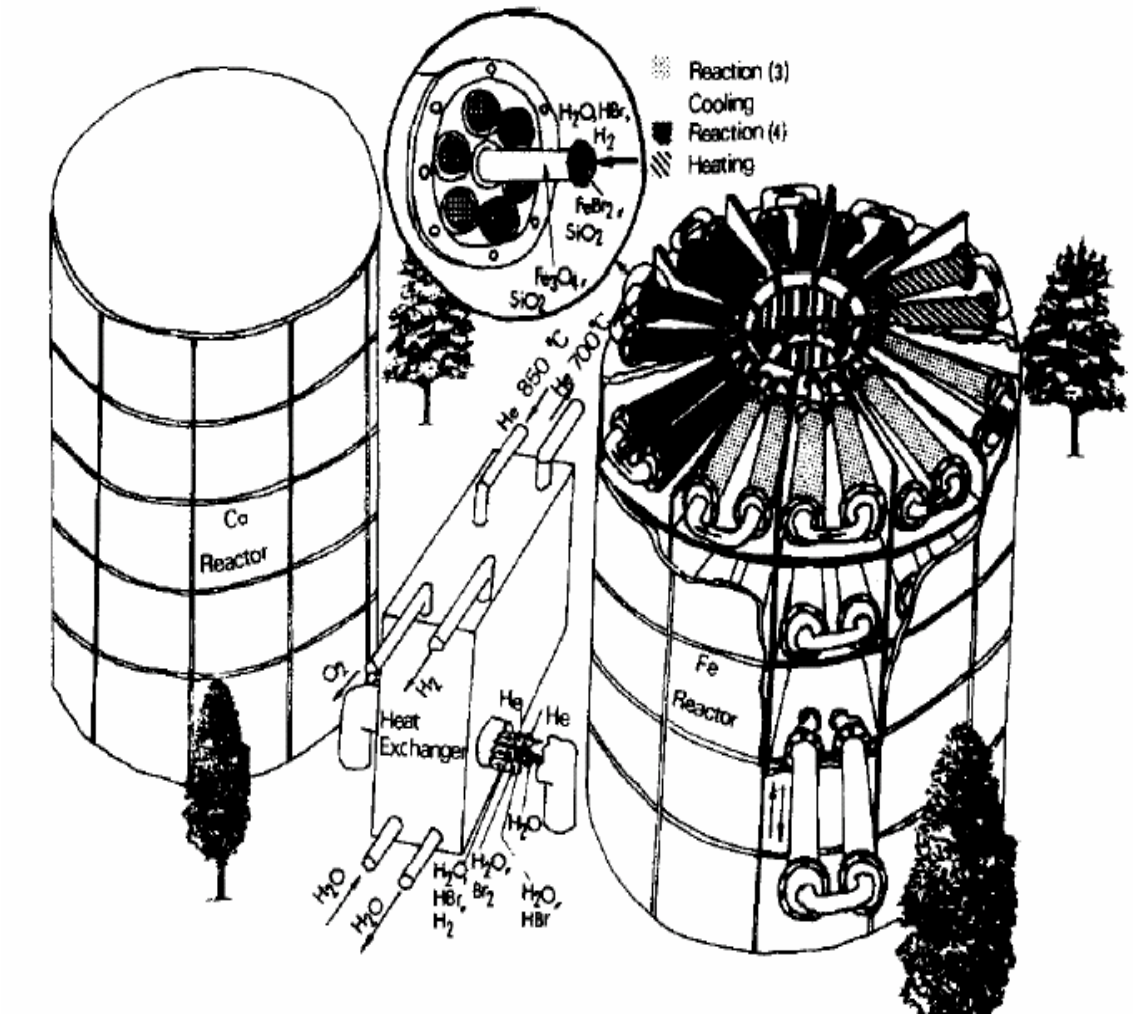

Figure 2.2 Conceptual Illustration of Whole Plant (Kameyama and Yoshida, 1981)

A change in the process flow was subsequently introduced so that the HBr from reaction 1 would not have to be separated from surplus H_2O before entering reaction 4 (Kameyama et al.,1989). Rather the HBr is carried through reactor 4 and proceeds to reactor 3. Figure 2.5 shows the original (a) and the modified schemes (b). The modified scheme reduces the flow complexity found in the original process.

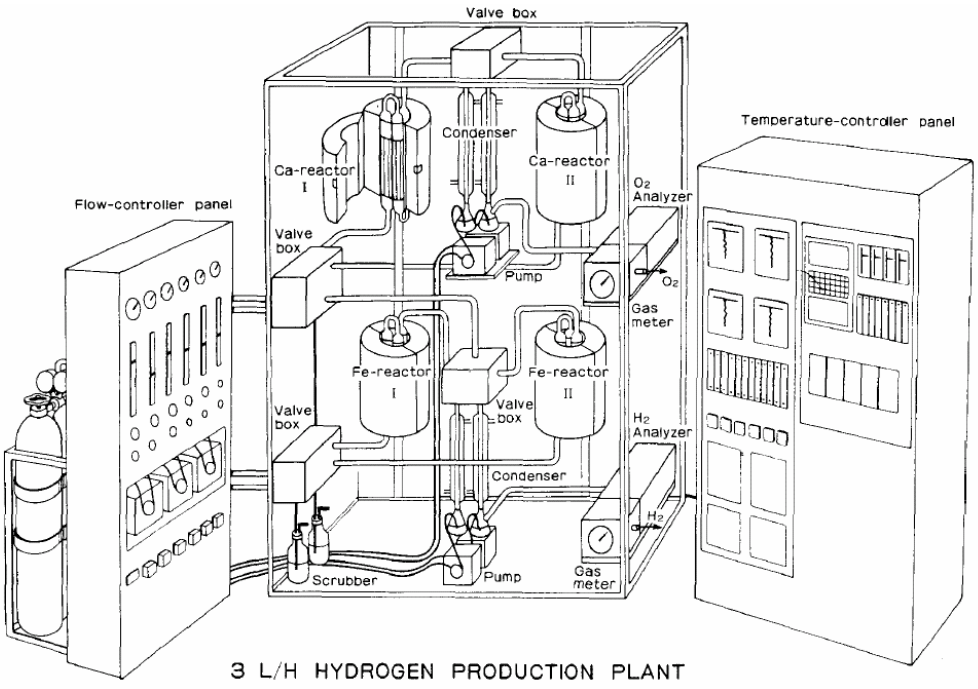

Figure 2.3 Illustrative Diagram of the MASCOT Plant (Nakayama et al., 1984)

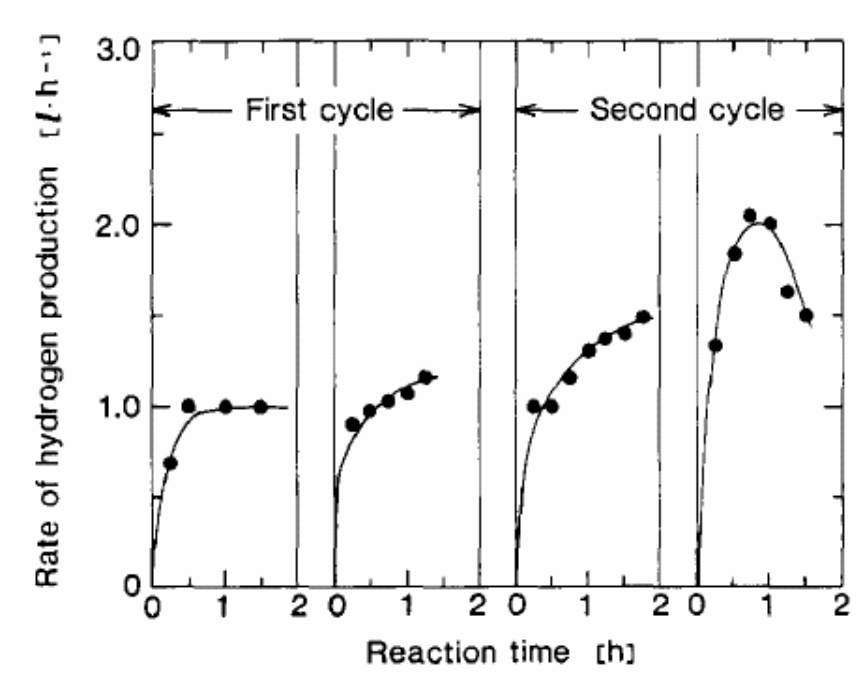

Figure 2.4 Time Histories of the Rate of Hydrogen Production (Nakayama et al., 1984)

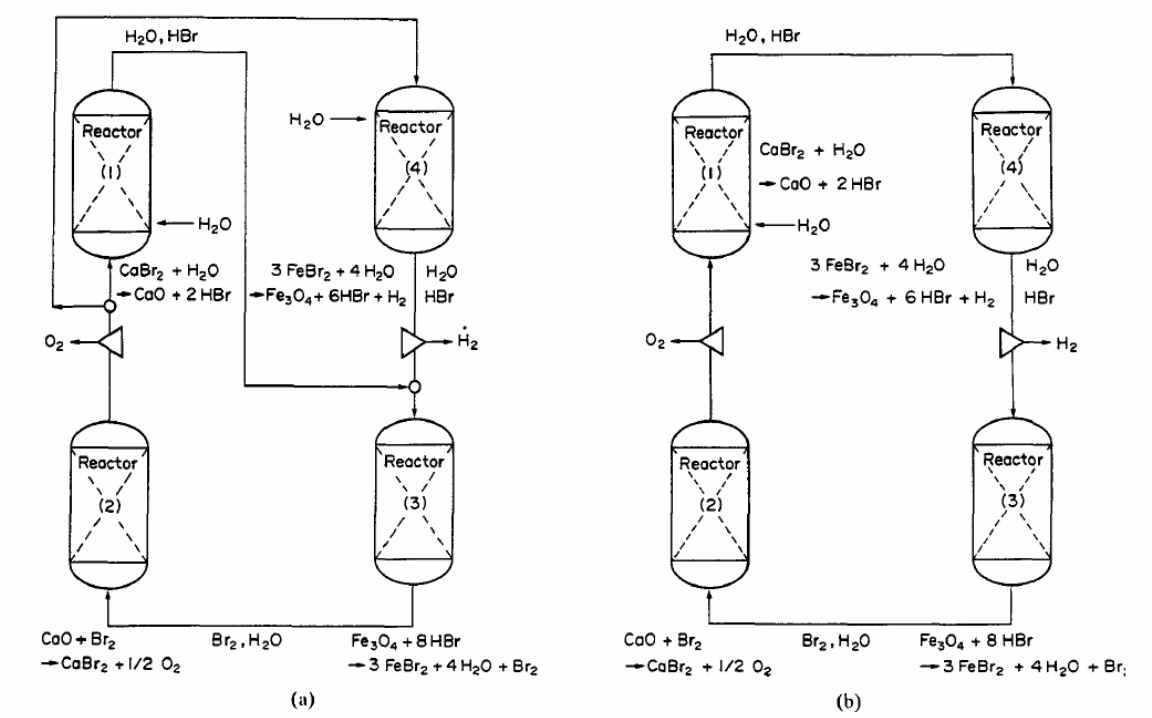

Figure 2.5 Original (a) and New (b) Flow Sheets of the UT-3 Process (Kameyama et al., 1989)

In 1989 an in-depth efficiency study was done on the whole cycle (Aochi et al., 1989). The study projected greater than 40% thermal efficiency if power generation from waste heat was 25% or greater. An energy balance was also done showing the breakdown of the energy usage assumed to obtain this efficiency (Figure 2.6).

$$\eta_T = \frac{H_{H2}}{H_{He} - \left(H_R - \frac{P_c \cdot 860.6}{\eta_{sp}} \right)} \tag{2.5}$$

H_{H2} is the energy per unit time of the hydrogen produced in the plant, at the higher heating value in MW. H_{He} is the Input heat to the chemical process from the high temperature gas reactor (HTGR) plant by helium gas in MW. H_R is the heat recovered in MW. P_C is the power consumed within the plant in MW and 860.6 is a conversion factor. η_{SP} is the power generation efficiency, which means the efficiency of the

conversion of recovered heat into electricity or for driving steam turbines. η_T is the overall total efficiency as defined by Aochi et al.

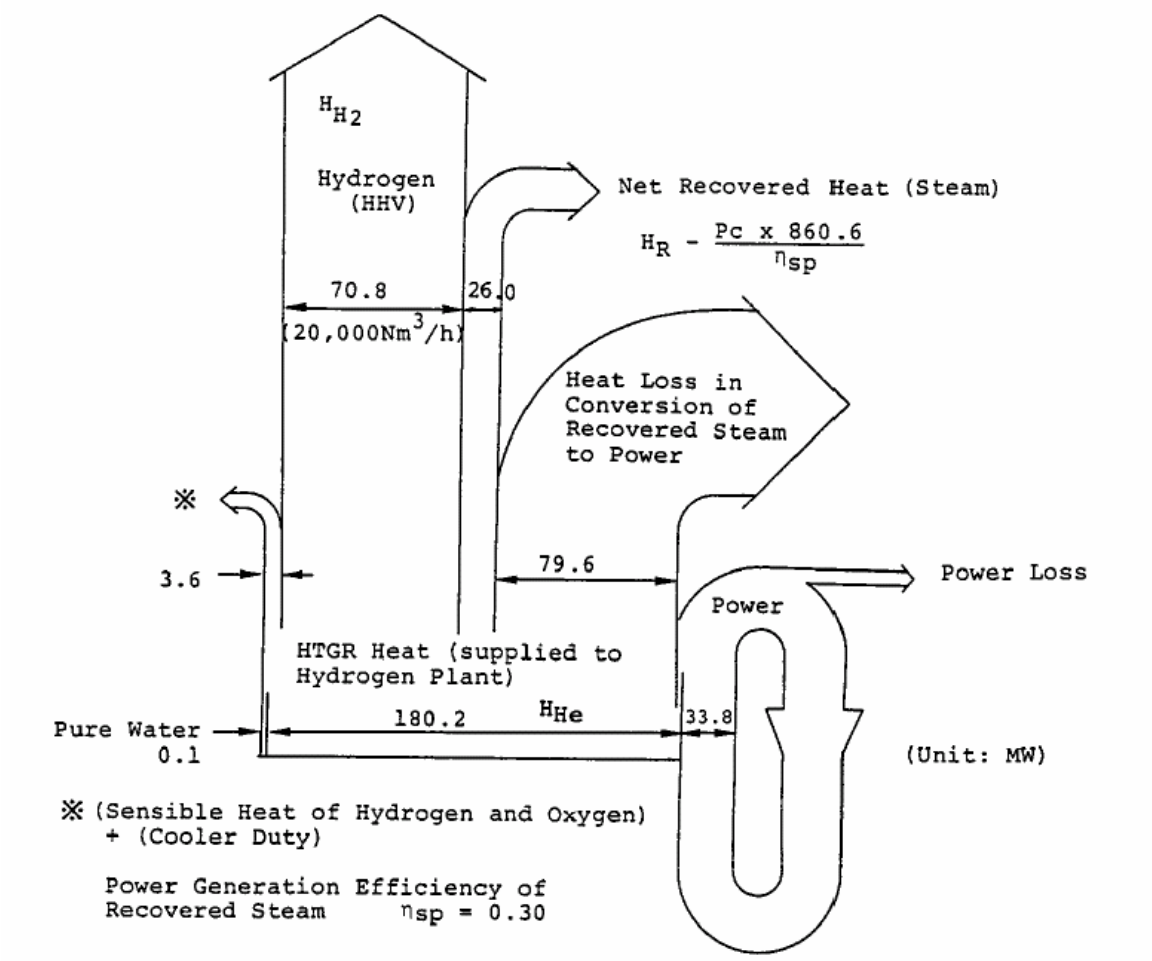

Figure 2.6 Energy Balance of the UT-3 Hydrogen Plant (Aochi, et al. 1989)

The MASCOT was operated with the new flow scheme for 11 cycles continuously (Sakurai et al., 1992). It was found that there was close to a 2 to 1 ratio between hydrogen and oxygen produced. The system appeared to operate steadily though slight fluxuations existed. The yield seems to be lower in this experiment than that reported in 1984 by Nakayama et al. but the cyclic run time is not given for this experiment. The run time for the other cycles was approximately 2 hours though, so it would seem that the run time would be at least 1 hour and that the yield would be around

1 to 2 liters per cycle. It is thought that the new flow scheme would not affect the hydrogen output so drastically. The reason for this discrepancy is unknown, though cycle times of only about 10 to 20 minutes would reconcile the two sets of data.

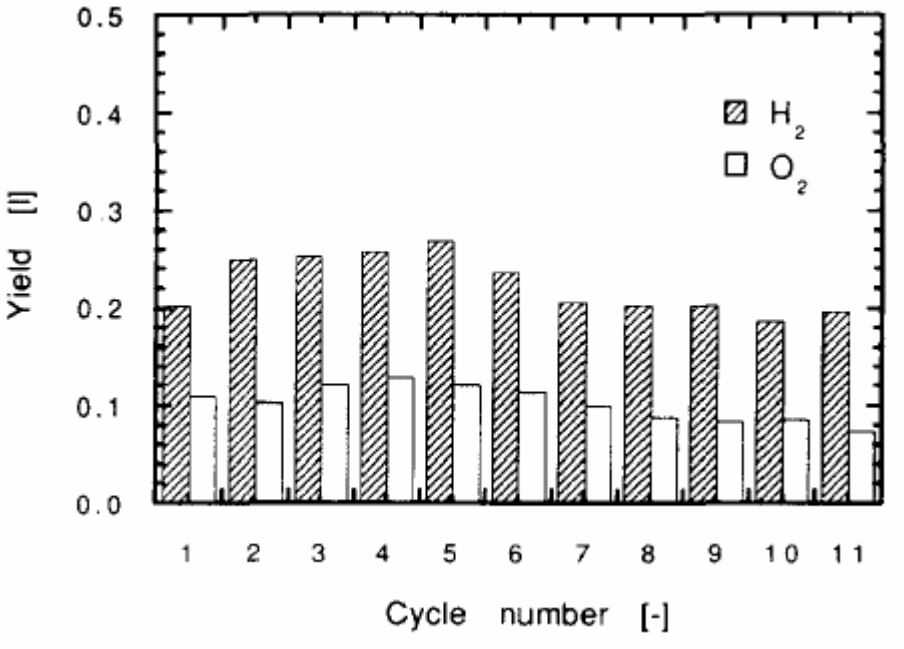

Figure 2.7 History of Total Gas Production by Cyclic Operation (Sakurai et al., 1992)

Most of the research from 1996 onward focused on simulations of the UT-3 Process. In 1996 Sakurai, Bilgen et al. published 2 papers. The first discusses the possibility of using a solar concentrator to supply the heat for the cycle. They conclude that it will be feasible to operate with a thermal storage unit and 24 hour operation. The second discusses an adiabatic model of the UT-3 Cycle. A computer simulation is run and first and second law efficiencies are found to be 48.9% and 53.2% respectively. The next year a technical evaluation of an industrial scale plant for the UT-3 thermochemical cycle is reported by Tadokoro et al. (1997). The main focus of the paper was the improvement in the overall thermal efficiency with membrane separation. Figure 2.8 illustrates their predicted efficiencies. They concluded that the use of a membrane for

separation will increase efficiency and therefore improve the economics of hydrogen production by the UT-3 thermochemical process.

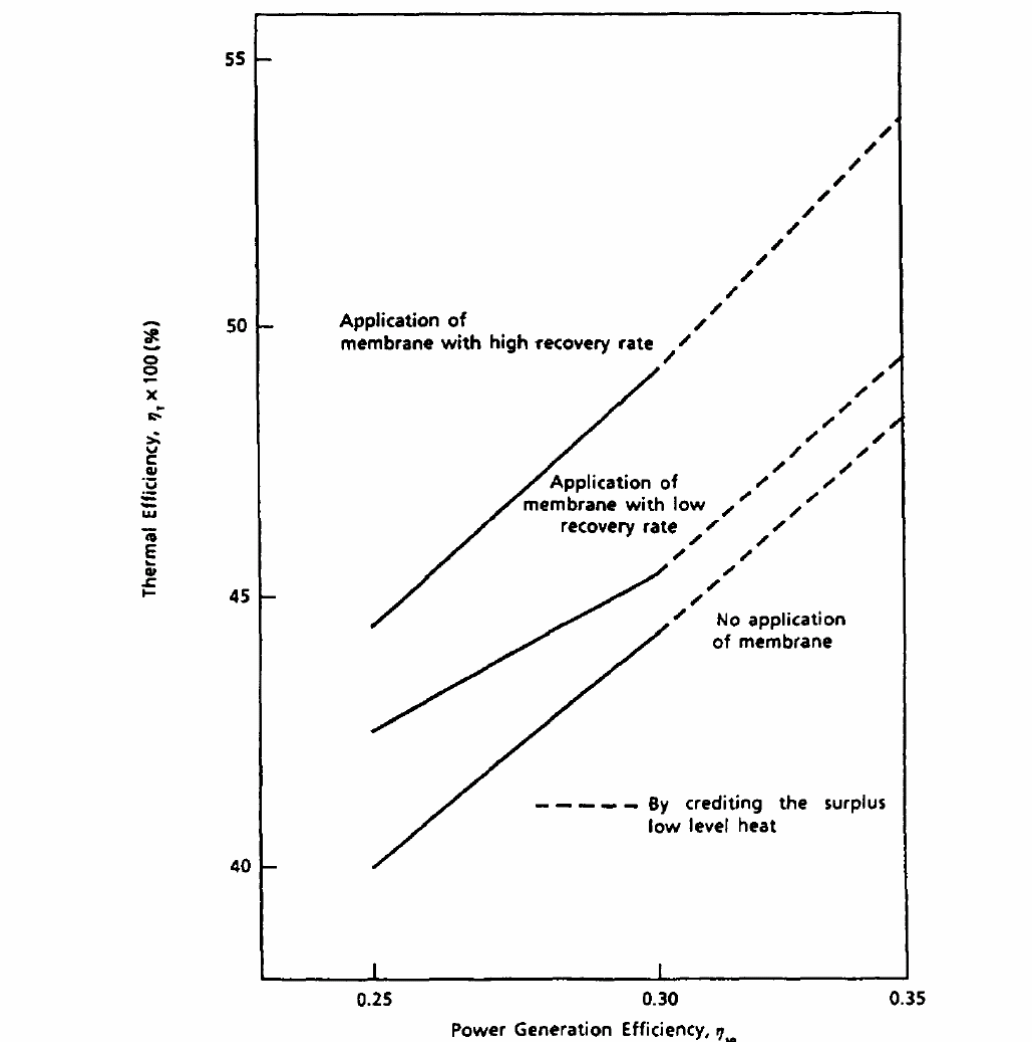

Figure 2.8 Thermal Efficiency of UT-3 Hydrogen Plant Having Membrane Separation (High Heating Value Basis) (Tadokoro et al., 1997)

After 1997 there is not much published on the UT-3 process. Teo et al. (2005) carried out an analysis on the UT-3 process efficiency. Their analysis included practical considerations of equipment efficiencies (compressors, heat exchangers), separation membranes and associated pressure loses, incomplete conversions for the reactions, low temperature heat, and the impracticality of isothermal operation in the iron reactors.

Their value for process efficiency from solar heat was less than 7%. To give more credibility to this paper, in the postscript the authors tell of feedback from the research and development community that indicated it is well known that the efficiency of the UT-3 thermochemical process is much lower than claimed by original researchers. The authors indicated that this has not been published in a public domain until now. They also indicated that other thermochemical processes should be evaluated in a similar manner to weigh the questions: Should work be done on these processes? And if so which ones?

Membrane, Separation Techniques, and Materials

One of the most important factors affecting the energy efficiency of the process is the separation of hydrogen and oxygen from the process stream. The hydrogen is produced in a reaction with a temperature of 570°C. Hydrogen has to be separated from stream containing hydrogen bromide and nitrogen or steam (used in excess). Separation can be accomplished (if nitrogen is not used) by condensation of water and hydrogen bromide. This, however, is highly energy inefficient means of separation since this condensed stream has to be reheated before it is sent to the bromination reactor R3 (Figure 2.1).

Alternatively, research has focused on developing high temperature corrosion resistance ceramic membranes to separate hydrogen from the other gases. This has also proven difficult because of the incompatibility of hydrogen bromide with most membrane material. The list of hydrogen bromide compatible materials is further shortened due to the high temperatures at which desired separations should occur. The pressure drop across the membranes is high and the separated H_2 has to be compressed which required additional energy.

To meet these needs a zirconia-silica composite was studied for the separation of hydrogen (Ohya et al., 1997, 1994). The study found that hydrogen bromide and steam were able to permeate the membrane much more than the hydrogen. Thus the hydrogen could be separated in the reject stream and the hydrogen bromide and water could be separated out through the membrane. Separation factors between 6 and 36 were obtained using different pressure gradients and temperatures ranging from 423K-773K (250°C-500°C). The HBr-H_2O-H_2 separation was also investigated by Morooka et al. in 1996. The approach used an α-alumina support with a silica membrane and was tested up to 400°C with effective results. The hydrogen bromide could not pass through the membrane and the separation factor between hydrogen and water was over 100. Though these membranes still do not function at the reaction temperature of 570°C they allow for a much more energy efficient separation of hydrogen.

Materials for piping and other parts also need to be considered. Not many materials can withstand the corrosive components such as Br_2 and HBr at such high temperatures. Titanium would work but the cost is too high to make the system economical to produce hydrogen. Ceramic materials are also being developed for use with the UT-3 cycle. Sasaki and Hirai (1994) coated stainless steel with TiC-SiC film using vapor deposition techniques and tested it in a Br_2- O_2- Ar environment up to 800°C. The temperature was cycled between 500°C and 800°C. Corrosion was still present but greatly reduced.

Another proposed plan to reduce materials of construction cost is to run the system with excess steam or nitrogen or a mixture of the two. This is what is currently

done in the UT-3 process. No reports of corrosion problems appear in the literature, though it is suspected that corrosion may occur over time.

Solid Reactants

A pellet form has been chosen to meet the strength and reactivity demands of the cyclic UT-3 process for both the iron and calcium reactants. Even in the first proposal of the UT-3 process Kameyama and Yoshida (1978) emphasized the importance of developing durable solid reactants. Their development and improvements are outlined here.

Iron reactants

In 1978 Kameyama and Yoshida tested three supports for the iron reactants. These supports included 120 micron glass beads, Bentonite (a type of clay), and Kaolin (high quality clay used to make china). The pellets were made into 15mm spheres. The bentonite supported material seemed to have the best conversion to $FeBr_2$ which was about 45%.

In 1981 Kameyama and Yoshida reported on their studies of the iron solid reactants and their chemistry. The iron oxide pellets were made by mixing Fe_3O_4 and silicasol (Cataloid-S-OH), adding a saturated solution of ammonium carbonate, then drying, molding, and calcination. It was reported that reaction 3 was found to be composed of two stages represented by

$$Fe_3O_4+2HBr \rightarrow Fe_2O_3+ FeBr_2+H_2O \quad (2.6)$$
$$Fe_2O_3+6HBr \rightarrow 2FeBr_2+3H_2O+Br_2 \quad (2.7)$$

Taking into consideration the mass and heat transfer resistances from the gas film, product layer and surface chemical reaction these researchers came up with two equations for reaction rates for different temperature regions. The reaction rates use the shrinking

core and assumed to precede topochemically. These reactions are shown here in Eq. 2.8 and Eq. 2.9 where a is the surface area of the reaction in cm^2.

$$r_{3\cdot s} = 38.2\cdot a\cdot\left(C_{Fe3O4} - .00150\right)\cdot C_{HBr} \qquad \text{(210C-255C)} \qquad (2.8)$$

$$r_{3\cdot s} = 1.78\,10^{-8}\cdot\exp\left(\frac{13.0}{RT}\right)\cdot a\cdot\left(C_{Fe3O4} - .00150\right)\cdot\left(C_{HBr}\right)^{.5} \qquad \text{(255C-300C)} \qquad (2.9)$$

A more detailed iron pellet formulation procedure is given by Yoshida et al. (1990). Figure 2.9 shows an outline of this formulation along with that of the contemporary calcium pellet formulation procedure of that time. The reaction rates of all four reactions were also evaluated experimentally. A tabulation of these rates can be seen in Table 2.1 below.

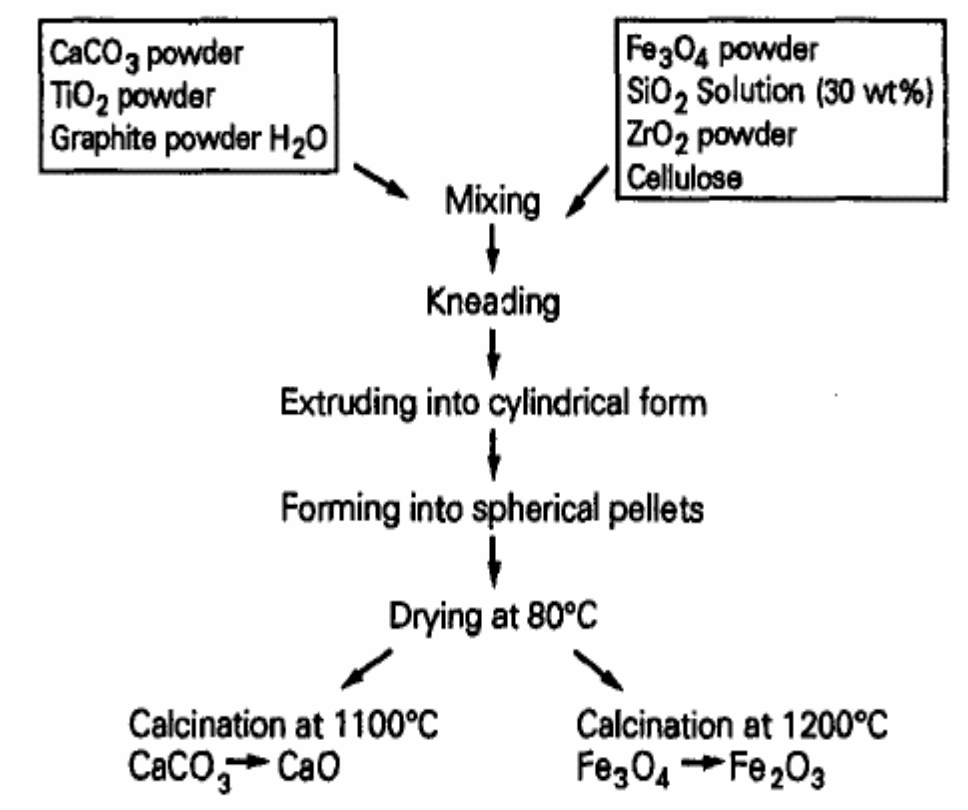

Figure 2.9 Process for Pelletizing Solid Reactants (Yoshida et al. 1990).
Table 2.1 Comparison of Initial Rates of the UT-3 Thermochemical Process Yoshida et al. (1990).

Reaction	Reaction temp. t[°C]	Gas concen. C[mol·m^{-3}]	Solid concen. C[mol·m^{-3}]	Reaction constant k	Rate equation	Initial rate r[mol·m^{-3}·s^{-1}]
$CaO + Br_2 \rightarrow CaBr_2 + 1/2O_2$	550	7 33	3.45×10^3	4.62×10^{-4}	$r = kC_{CaO}C_{Br_2}$	11 53
$CaBr_2 + H_2O \rightarrow CaO + 2HBr$	700	251	3.45×10^3	6.10×10^{-5}	$r = kC_{CaBr_2}C_{H_2O}$	53
$Fe_3O_4 + 8HBr \rightarrow 3FeBr_2 + 4H_2O + Br_2$	220	81 195	1.20×10^3	2.25×10^{-4}	$r = kC_{Fe_3O_4}C_{HBr}$	22 53
$3FeBr_2 + 4H_2O \rightarrow Fe_3O_4 + 6HBr + H_2$	580 400	286 362	3.60×10^3 3.60×10^3	4.28×10^{-3} 3.12×10^{-4}	$r = kC^{3/4}_{FeBr_2}C_{H_2O}$	569 53

Total pressure = 20 atm.

In 1992 another paper was published on the procedure of making the iron pellets (Amir et al., 1992). The paper highlights the use of graphite to increase porosity by more than 5 times. Specific pore volume with no graphite was .06 cc/g and was increased to .35 cc/g when 20% by weight graphite is used. Figure 2.10 shows a linear relationship between the total cumulative pore volume and the percent of graphite added

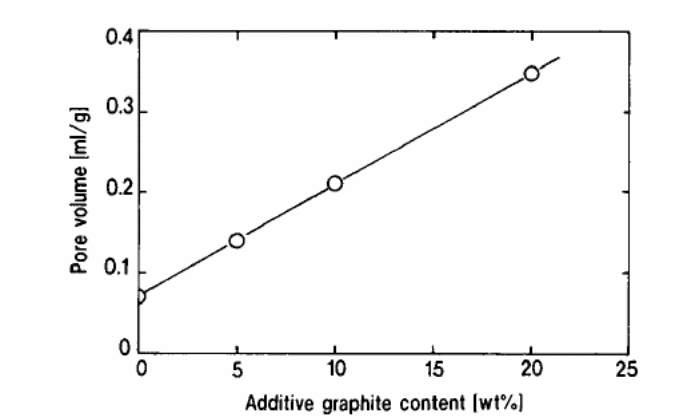

Figure 2.10 Relationship Between Pore Volume and Additive Graphite Content in Pellet (Amir et al., 1992)

In 1993 Amir et al. published results comparing 8 different ceramic supports for the iron reactants. The analysis included the chemical composition, hardness, porosity, and reactivity of the pellets. A Table of the results can be seen in Table 2.2 below. Degradation of reactivity occurred over a number of cycles. It was concluded that some $FeBr_2$ sublimes at the high temperature of the reactions. This reduces the iron content and also plugs the pores as it leaves. There is also agglomeration of iron oxide particles

which reduces surface area and damages the structure of the pores both of which have an adverse effect on reactivity. This is the last study which focused on the iron reactants.

Table 2.2 Properties of Calcined Iron Solid Reactant Pellets (Amir et al., 1993)

Pellet	Raw material: Reactant	Raw material: Support	Mole ratio Fe:(Zr:Si)/(TZ−Y)	Density (kg m^{-3})	Iron content (mol m^{-3} pellet^{-1})	Hardness (kg mm^{-2})	Pore volume (ml g^{-1})
1	Fe_3O_4	SiO_2 + ZrO_2	1:4.2:4.2	1.8×10^3	5.4×10^3	8	0.45
2	Fe_3O_4	$ZrSiO_4$	1:4.2	1.8×10^3	5.4×10^3	8	0.35
3	Fe_3O_4	TZ−3Y	1:4	3.7×10^3	15.2×10^3	11	0.12
4	Fe_3O_4	TZ−8Y	1:4	3.6×10^3	14.3×10^3	17	0.12
5	Fe_3O_4(UFP)	TZ−3Y	1:4	1.7×10^3	6.9×10^3	9	—
6	$FeC_4H_2O_4$	TZ−3Y	1:4	1.6×10^3	6.5×10^3	<1	—
7	$FeC_{15}H_{21}O_6$	TZ−3Y	1:4	8.9×10^2	3.6×10^3	<1	—
8	$FeC_6H_{18}O_{15}N_3$	TZ−3Y	1:4	1.3×10^3	5.6×10^3	<1	—

Calcium reactants

The reaction rates of reactions 1 and 2 were reported in 1989 (Kameyama et al.) and then again in 1990 (Yoshida et al., Table 2.1 on previous page). Kameyama et al. (1989) used X-ray microanalyzer and found that after the bromination reaction calcium bromide was equally distributed throughout the pellet confirming their prediction of a homogenous reaction.

Table 2.1 give the findings of Yoshida et al. (1990). The formulation of the calcium pellets was first reported by Yoshida et al. (1990). It is thought that this procedure had been used for a number of years before but only reported in 1990. Figure 2.9 above outlines this procedure. The process uses a mixture of calcium carbonate and titanium dioxide with some graphite. The mixture is made into pellets and heated to 1100°C so that the calcium carbonate loses CO_2 leaving CaO, the needed solid reactant (Eq. 2.10). At this temperature some of the calcium oxide will also bond with the titanium dioxide form calcium titanate (Eq. 2.11).

$$CaCO_3 \rightarrow CaO + CO_2 \quad (2.10)$$

$$CaO + TiO_2 \rightarrow CaTiO_3 \quad (2.11)$$

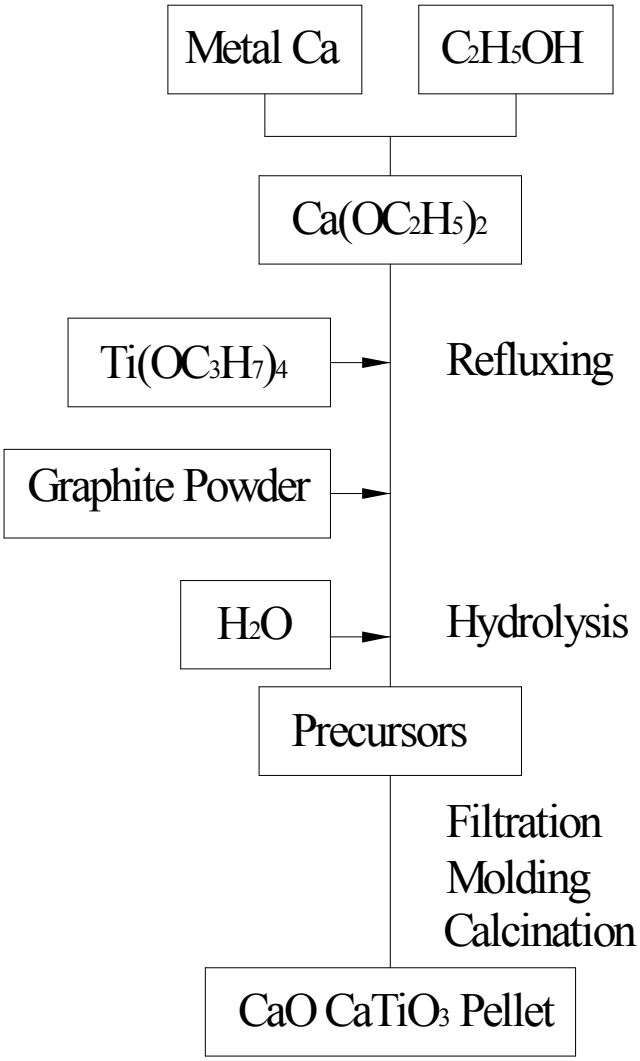

Figure 2.11 Production Process of the Pellet Using Ca and Ti Alkoxide (Aihara et al., 1990)

A new method for fabrication of calcium pellets was reported in 1990 by Aihara et al. This method uses alkoxide chemistry to create calcium titanate and calcium oxide (Figure 2.11). Pellets were made from both the old and new methods and their performance in the cycle was compared. The new method had a much higher reaction rate which reduced the time to maximum conversion. This can bee seen in Figure 2.12 below.

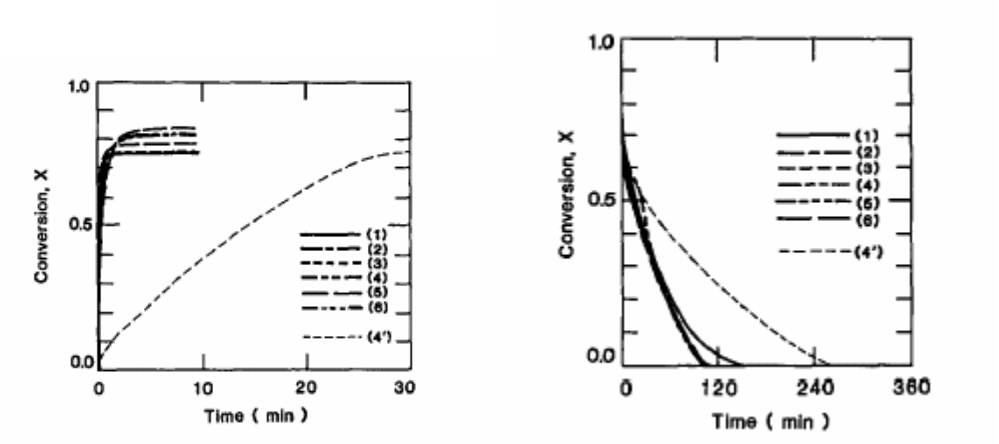

Figure 2.12 Solid Conversion Profiles of Bromination (left) and Hydrolysis (right) by Cyclic Operation (Aihara et al., 1990)

In the new pellets the calcium oxide was distributed in smaller particles in a more even arrangement. This reduced pore clogging significantly and therefore decreased the conversion times. Figure 2.13 illustrates the reduction in pore volume after one run for the old and new methods respectively.

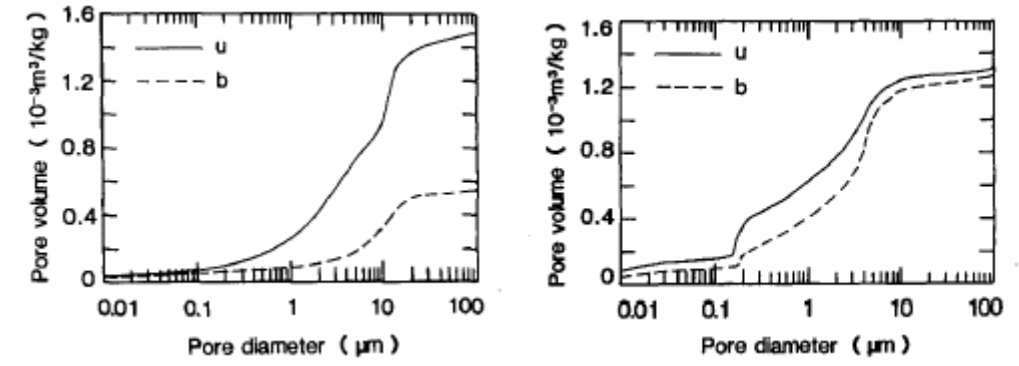

Figure 2.13 Pore Size Distribution of Unreacted (u) and Brominated (b) Pellets Made from the Old Method (Left) and the New Alkoxide Method (Right) (Aihara et al., 1990)

In 1992 Sakurai et al. studied the rates of reaction with the pellets made using alkoxide chemistry. The reaction rates were proportional to first order of both the bromide and calcium oxide concentrations. It was also found that bromination (Eq. 2.2)

should take place above 590°C to prevent formation of by products, though these by products are not specified.

In 1995 Sakurai et al. reported another significant improvement in the formation of the calcium oxide pellets. A very similar approach to Aihara et al. was taken but a dispersion chain of chemistry was added. The same alkoxide chemistry was used to create the calcium titanate. Then another formulation was added to make very small particles of calcium oxide. This separated the synthesis of CaO and $CaTiO_3$ in two processes and then the mixing of the two form the final product. The CaO particles are much smaller than those produced from the previous method and better dispersed in the $CaTiO_3$ matrix. An outline of this procedure is shown below in Figure 2.14. The left part of the Figure is the calcium oxide dispersion chain.

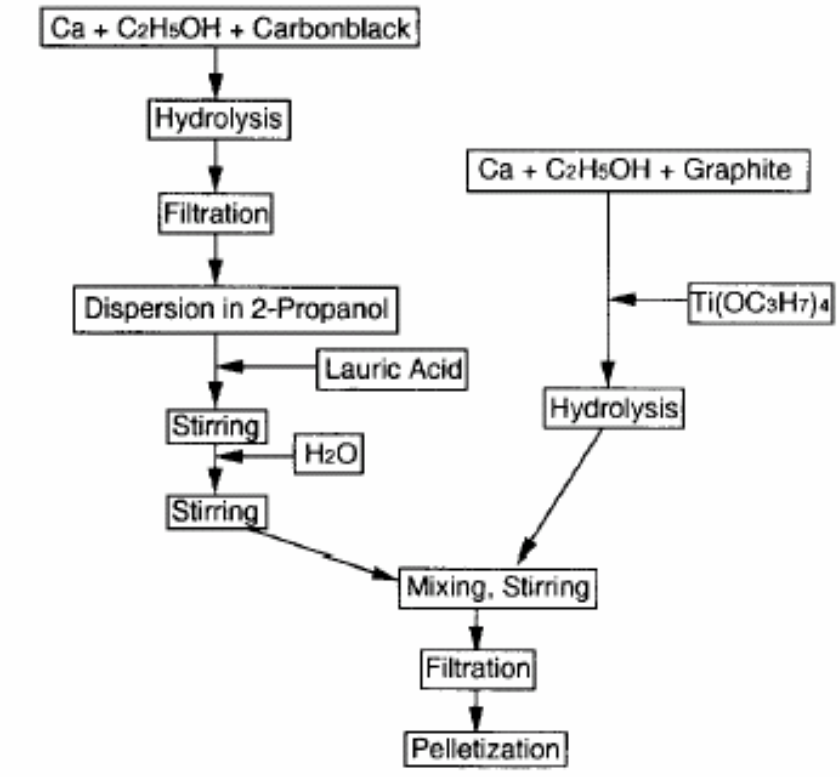

Figure 2.14 Flow Chart of a Modified Method for the Preparation of a Pellets Using Alkoxide Method with a Dispersion Chain (Sakurai et al., 1995)

Again pellets were made by both methods (conventional and modified) and their performances were compared. The conventional method refers to the first alkoxide chemistry method outlined above in Figure 2.11 above and the modified method refers to the alkoxide chemistry method with the dispersion chain outline in Figure 2.14 above. The most dramatic improvement can probably be seen in the rates for hydrolysis (Figure 2.15). Though there is improvement in the bromination it is insignificant compared to the increase in rate of hydrolysis. The production is governed by the slowest reaction (hydrolysis reaction). The improvement in the hydrolysis rate therefore improved the H_2 production rate significantly.

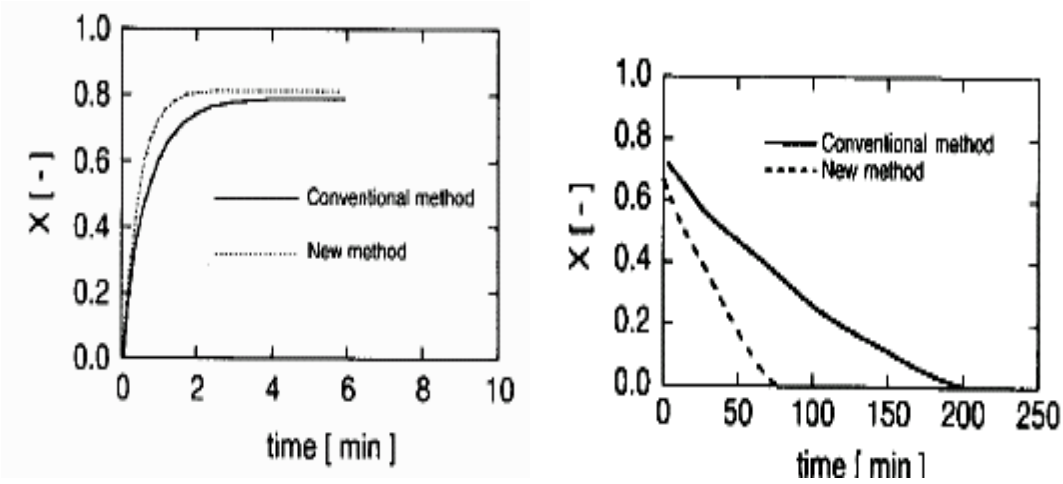

Figure 2.15 Comparison of the Solid Conversion Profiles of Bromination (Left) and Hydrolysis (Right) Between the Conventional Method (Alkoxide) and Modified Method (Alkoxide with Dispersion Chain) (Sakurai et al., 1995)

Sakurai et al. (1995) also experimentally found the effect of the ratio of calcium oxide to calcium titanate on the conversion. Of the four ratios tested the .76 CaO/CaTiO3 had the highest conversion at about 80% conversion. Figure 2.16 shows their data.

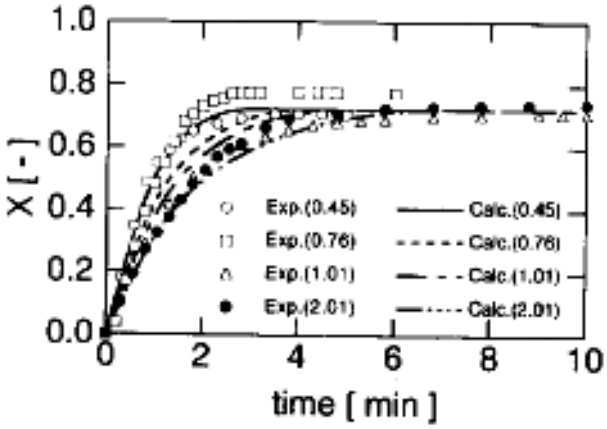

Figure 2.16 Comparison Between Computed and Observed Time Histories of Bromination ($CaO/CaTiO_3$= .45, .76, 1.01, 2.01) (Sakurai et al.,1995)

Sakurai et al. (1996) reported results from an in-depth study on porosity of pellets made from the alkoxide method (Aihara et al., 1990). These pellets were subjected to a number of cycles and the porosity was measured after each cycle (Figure 2.17). The differential porosity from .01 μm to 354 μm is shown (Figure 2.18) for sample pellets before and after bromination. It can be seen that most of the pore volume in concentrated in the 1 to 5 micron range. This was the latest significant data published on the calcium pellets.

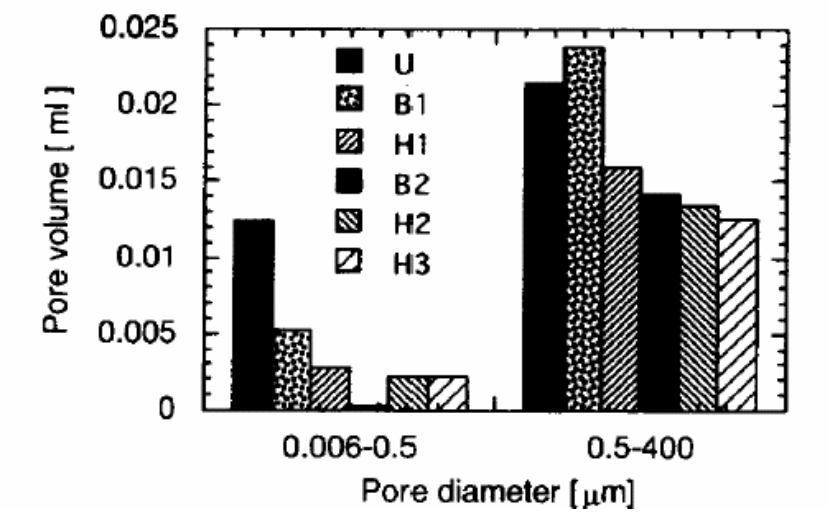

Figure 2.17 Change of Pore Volume in Cyclic Operation (U; Unreacted, B1 and B2; After 1st and 2nd Bromination, H1, H2, and H3; After 1st, 2nd, and 3rd Hydrolysis, Respectively) (Sakurai et al., 1996)

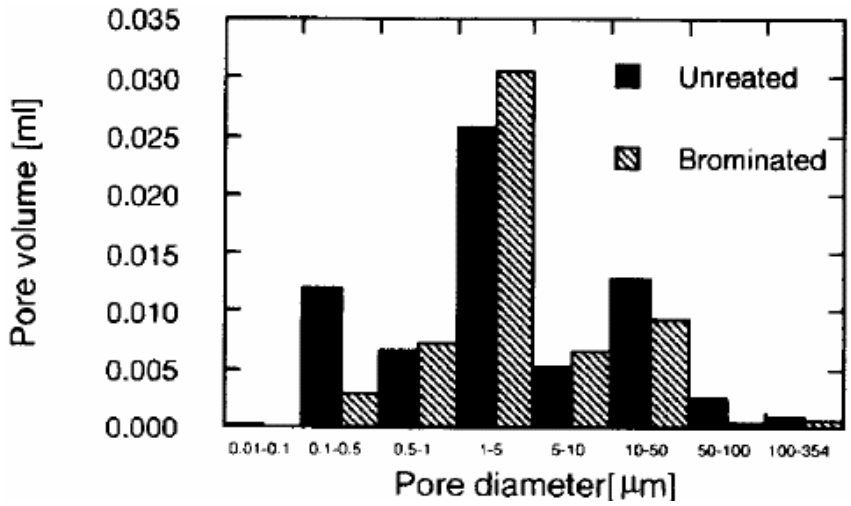

Figure 2.18 Change of Pore Volume During Bromination (Sakurai et al., 1996)

Throughout these Studies, the Hydrolysis of CaO (Eq. 2.1) is rate limiting. It determines H_2 production rate in the UT-3 process. It is also the highest temperature reaction. The current study therefore attempts to formulate CaO pellets with more favorable characteristics.

Strengths and Weaknesses of the UT-3 Thermochemical Process

The UT-3 thermochemical cycle can be a commercially viable process. Simulation indicates that it is energy efficient and can become cost competitive as the prices of fossil fuels rise. The process has relatively low temperatures for a thermochemical process which can be achieved through solar concentrators or through helium from high temperature nuclear reactors. If the heat for the process is supplied in this manner no carbon dioxide will be produced. Another advantage of the process is that the solid reactants remain stationary in the reactors eliminating the need for moving bed reactor which would otherwise add a great deal of operation complexity.

There are weaknesses of the UT-3 process as well. The process is in batch mode and is limited by the slowest reaction which is about 1 hour. There are still problems that

have to be solved in hydrogen separation at high temperatures from corrosive gas. This problem, however, is inherent in most thermochemical cycles. In addition both the calcium and iron pellets need to be durable and have a cyclic life that would make them economical. This may be a major drawback of the process. Despite these weaknesses the UT-3 thermochemical process is one of the two non-hybrid cycles being studied, the other being the General Atomic process mentioned earlier.

Teo et al. (2005) were skeptical of the possibility of the UT-3 thermochemical process as a feasible means to produce hydrogen. They did an analysis which predicts a much lower efficiency of less than 7%.

Calcium Oxide Solid Reactant

When designing a solid reactant for the UT-3 thermochemical process a number of characteristics had to be considered within the confines of the process. The UT-3 thermochemical process is cyclic. A solid reactant that can continue to react from one cycle to the next had to be designed. UT-3 researchers selected a pellet configuration where the solid reactants were dispersed on a solid porous substrate. Such formulation prevents the carry over of solid reactant in the gaseous stream. Proper formulation of a porous substrate and high dispersion of the solid reactant can increase the conversion and improve the reaction rates. A pellet form of solid reactant with minimal degradation can also be used in a standard fixed bed reactor. Many interdependent physical and chemical processes will be considered when designing the pellets.

The design characteristics which need to be considered are similar to those considered when designing a catalyst. These characteristics are interdependent so that they need to be considered together and cannot be isolated to a large degree. These characteristics and their interdependencies will be discussed below.

Physical Characteristics

Physical characteristics refer to those properties that have to do with the physical geometry and mechanics of the material. Porosity and strength are two important physical characteristics that must be considered when designing the pellets.

Porosity

Porosity is the term for the characterization of the pores of a material. The porosity of a material is explained using a few different statistics. The first is the total surface area which is important because it is proportional to the number of available chemical reaction sites. The second is the pore size which affects the diffusion rates through a material. All these parameters can be correlated using the BJH equation to manipulate isotherm data which will be explained in the analytic research tools section in Chapter 4. Thus a pore size distribution can be created. This allows the researcher to understand what size pores are in the material. Pore sizes have been split up into two groups. Microporosity describes pores smaller than 0.5 μm whereas macroporosity refers to pores larger than 0.5 μm. Macropores contribute to diffusion characteristic inside the pellet while micropores increase the surface area on which the solid reactant can be dispersed. Macropores are also necessary to prevent plugging of diffusion path due to volume change of the reactants during the cyclic process.

Strength

The strength obviously refers to the strength of the pellets to resist disintegration. Strength of the pellets must also be considered with the thermal shock that comes with the cyclic oscillations of the UT-3 process. Strength also refers to the ability of the material to keep its porous structure intact on a micro level. The “micro” strength helps to prevent reduction in pore surface area and pore volume. Further, the pellets must support

the weight of other similar pellets. If they are crushed within the fixed bed they will cause a higher pressure gradient in the reactor leading to a lower flow rates and greatly reduce reaction surface area leading to lower conversion.

Chemical Characteristics

Chemical composition

Chemical composition refers to the chemical make up of the final pellets. This is important in this particular application because one of the components, calcium oxide, is a chemical reactant. Generally, reaction rates are proportional to the concentration of reactants, thus a greater concentration usually yields a higher reaction rate. The solid reactant, calcium oxide should be maximized but must be balanced with the characteristic strength of the pellet, especially on the smaller scale. The calcium titanate forms the porous substrate on which the calcium oxide is dispersed. If these structures collapse the surface area is greatly reduced and thus the reaction rates are greatly reduced.

Reactivity

Reactivity refers to the ability of the solid reactant, CaO or $CaBr_2$, to react with the gaseous reactant, Br_2 or H_2O respectively. This parameter depends on the surface of the solid reactant that is dispersed and the diffusion path to the solid reactant and out of the pellet. The reactivity is highly dependent on the porosity of the material as both overall surface area and diffusion rates are determined from porosity. Reactivity can also depend on the concentration of the reactant and so the amount of reactant should be increased as much as possible without sacrificing the other needed characteristics especially the strength. The rate of reaction and conversion are the main measure of reactivity. The reaction rates are generally dependant on concentrations of reactants and products and temperature. Conversion is a quantity to describe the extent of reaction.

Temperature, pressure, reaction rates, type of reactor, and concentrations all have an effect on the conversion.

Degradation

Degradation refers to the loss of reactivity from cycle to cycle. This can happen in a number of ways. Degradation is usually due to pore clogging or pore structure breakdown. Pore clogging occurs when larger particles react and bond to a site formerly occupied by a smaller particle. The molecules volume of $CaBr_2$ is greater than CaO which could lead to pore clogging after the bromination reaction. Pore clogging can also occur do to growth of agglomerates which usually happens at high temperatures through sintering. Pore structures can breakdown due to external forces (fixed bed weight) and also small forces from the gases entering and exiting and molecules forming and reforming break the bonds which maintain the integrity of the pores.

Research Objective

The objective of the research project at the University of Florida is to investigate the feasibility of the UT-3 thermochemical process and explore the possibility of lowering the operating temperature. The highest temperature reaction is reaction 1 (Eq. 2.1) at 760°C in which CaBr2 is converted to CaO. Solid reactants with acceptable characteristics must be developed to evaluate the performance of the UT-3 process. This research is therefore focused on developing the solid reactant for the calcium reactions (Eq. 2.1, 2.2).

The objective of the present research is to develop a method of producing the calcium solid reactant for the UT-3 process. The solid reactant will be made into pellets for our research. It is a common practice to make catalyst into pellet materials for use in fixed bed reactors. Pellets provide a good surface area, low degradation, and even

transport of gaseous reactants and products through the reactor. Though the solid reactants are not catalysts in the UT-3 process, pellets are a good choice for the form of the solid reactant. If designed and fabricated correctly they can provide the same benefits as in a catalyst system.

There are many steps that need to be taken in order to create pellets for the UT-3 thermochemical process. A summary of the strategy to make the pellets is presented below for both the chemical formulation and physical procedures. Both will again be explained in greater detail in the procedural section.

Chemistry Formulation

A chemical procedure will be used to make two different sizes of agglomerates. The first will be larger particle of $CaTiO_3$ and second will be the smaller will be CaO. In the final formation the larger agglomerates will have space between them which will result in macroporosity. These larger agglomerates themselves are not solid though. They have microporosity as well. In this way the pellets will have the bimodal porosity. The smaller agglomerates of CaO will be dispersed into the micropores which will give a good reaction area for the pellets while at the same time maintaining the macroporosity needed for diffusion.

This chemical procedure is complex. The $CaTiO_3$ agglomerates must be made big enough to create the macroporosity in the pellet. The agglomerates themselves should have microporosities for CaO dispersion. The CaO particle must be very small in order to be dispersed into the micropores of the $CaTiO_3$ and not clog them. Parameters which will be examined are mixing ratios and heating procedures. The effect of these parameters will be evaluated by porosity, strength, and chemical composition measurements.

Physical Formation

After the chemical procedure is developed and mixture of $CaTiO_3$ and CaO obtained, the mixture must be formed into pellets. The precursors must be dried to a solid powder form. The powder then will be molded in a compression mold to create pellets. The pellets will then be heated to a temperature to achieve controlled sintering and adjust the porosity distribution and strength of the pellets. Parameters which will be examined are mold compression force, drying temperature, sintering temperature and duration. Porosity and strength will be the dependent variables by which the effect of these parameters will be evaluated.

CHAPTER 3
SOLID REACTANT

Presented in this chapter are the procedures to produce the precursors for pellets, including the original chemical formulation, the modified chemical formulation used by UT-3 cycle researchers, and the physical method to mold and treat the pellets. There have been several problems during the course of the work leading to a number of changes to both the chemical and physical procedures. These problems, their causes, and procedural changes are also discussed in this chapter.

Sol-Gel Chemistry

The sol-gel process is an approach for preparing thermally, chemically, and mechanically stable materials with controlled porosities used in the area of gas separation, catalysis, membrane reactors, sensors, and absorbents. Starting from a molecular precursor (sol), an oxide network (gel) is obtained via inorganic polymerization reactions. These reactions occur in solution and hence the term "sol-gel processing" is used (Brinker and Scherer).

As compared to the conventional "powder" route these processes offer many advantages:

1. Homogeneous multi-component systems can easily be obtained by mixing the molecular precursor solutions with better kinetics and yields.
2. The scale of mixing is considerably smaller which enables greater dispersion
3. The temperatures required in sol-gel processes are markedly low.

4. Careful manipulation of operating parameters (temperature, pH, water content) can yield products suitable for diverse applications.

5. The deformation properties of the sol or gels allow the formation of fibers, films or composites by such techniques as spinning, dip-coating or impregnation.

An alkoxide is "an ionic compound formed by the removal of hydrogen ions from the hydroxyl (OH^-) group in an alcohol using reactive metals." (Frostburg) The alkoxide used in the current chemical process is calcium ethoxide ($Ca(C_2H_5O)_2$) . Metal alkoxides $M(OR)_n$ are versatile molecular precursors for the sol-gel synthesis of metal oxides. There are known alkoxides from many metals including the transition metal elements. The difference in transition metal sol-gel chemistry compared to the rest of the metal elements arises from two factors:

- The higher electropositivity of transition metals leads to a much higher electrophilic characters of the metal.
- The possibility exists for most transition metals to exhibit several coordinations so that full coordination is usually not satisfied in the precursors (alkoxides). This increases the probability of adding ligands to the transition metal ion which leads to diverse physical and chemical properties.

As a result, transition metal alkoxides are much more reactive. They must be handled with care, in the absence of moisture. They readily form precipitates (particles) rather than gels (networks) when water is added. The sol-gel process primarily proceeds in two steps: hydrolysis, then condensation.

Hydrolysis

The electronegative alkoxo groups (OR) make the metal atom relatively electropositive and therefore highly prone to nucleophillic attack. Metal alkoxides are therefore extremely reactive with water leading to the formation of hydroxides or hydrous oxides. The overall reaction can be written as:

$M(OR)_n + nH_2O \rightarrow M(OH)_n + nROH$

The stepwise progress of hydrolysis is shown here (Sanchez et al., 1988).

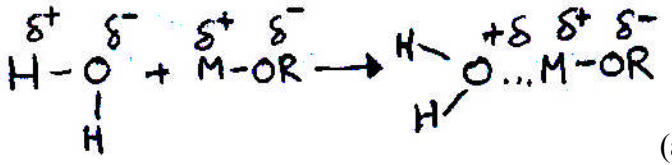

(a)

1. The first step (a) is a nucleophillic addition of a water molecule to the positively charged metal atom M. This leads to a transition state (b) where the coordination number of M has increased by one.

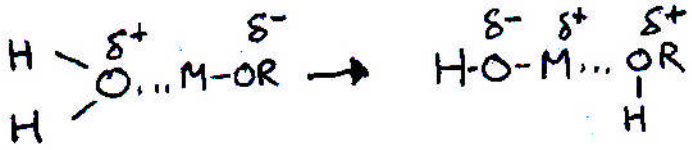

(b)

2. The second step involves a proton transfer with (b) leading to the intermediate (c). A proton from the entering water molecule is transferred to the negatively charged oxygen of the adjacent OR group.

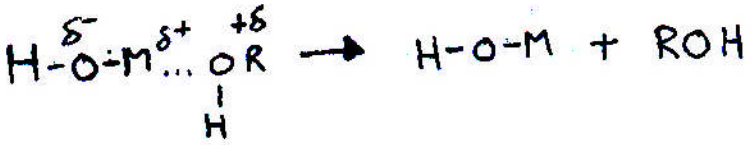

(c)

3. The third step is the departure of the more electropositive group within the transition state (c).

Condensation

Condensation is a complex process and can occur as soon as hydroxo groups are generated from hydrolysis. Depending on experiment, three competitive mechanisms have to be considered, namely: alcoxolation, oxolation, and olation (Livage et al., 1988)

1. Alcoxolation is a reaction by which a bridging oxo group is formed through the elimination of an alcohol molecule.

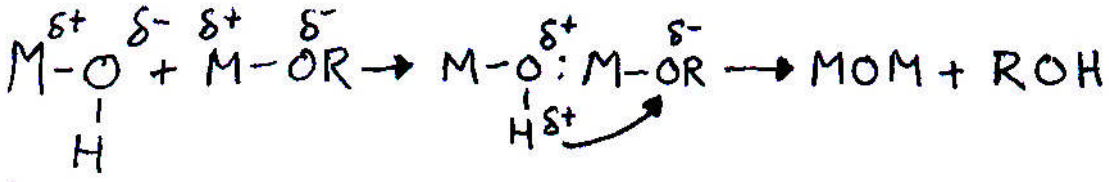

2. Oxolation follows the same mechanism as alcoxolation, but the R group of the leaving species is a proton and the leaving group is water.

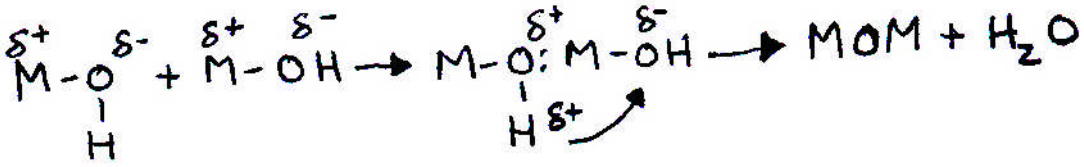

3. Olation can occur when the full coordination of the metal atom is not in the alkoxide. In this case bridging hydro groups can be formed through the elimination of a solvent molecule (ROH or water)

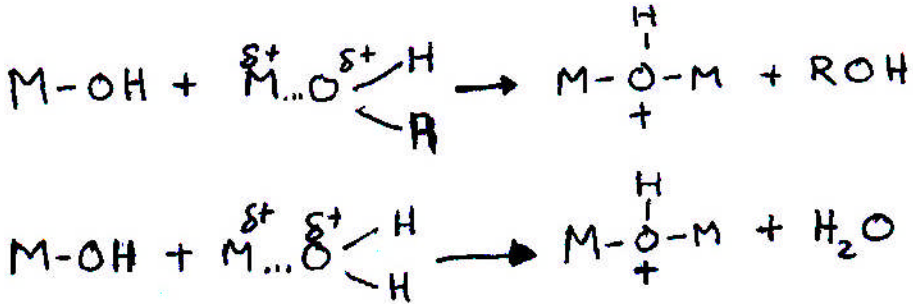

The condensation reaction can continue to build larger and larger molecules through polymerization. A polymer contains hundreds of thousands of units called monomers which are capable of forming at least two bonds with neighboring molecules. The polymerization may result into compact particle structure or extended structure (network). Particles can be easily molded to form pellets. High water/alkoxide molar ratios, high pH, and high temperatures promote particle formation (Brinker et al., 1994). Low water/alkoxide molar ratios, moderate acidity, and low temperatures promote extended structures.

This experiment has the following expected reactions:

1. Formation of Calcium Ethoxide

$$Ca + 2C_2H_5OH \rightarrow Ca(C_2H_5O)_2 + H_2 \quad (3.1)$$

2. Hydrolysis of Ca(OC2H5)2 and Ti(OC3H7)4

$$H_2O + Ca(OC_2H_5)_2 \rightarrow Ca(OC_2H_5)(OH) + C_2H_5OH \quad (3.2)$$

$$H_2O + Ti(OC_3H_7)_4 \rightarrow Ti(OC_3H_7)_3(OH) + C_3H_7OH \quad (3.3)$$

3. Condensation by oxalation

$$Ca(OC_2H_5)(OH) + Ti(OC_3H_7)_3(OH) \rightarrow (OC_2H_5)Ca\text{-}O\text{-}Ti(OC_3H_7)_3 + H_2O \quad (3.4)$$

4. Further condesation

$$(OC_2H_5)Ca\text{-}O\text{-}Ti(OC_3H_7)_3 + \text{Heating} \rightarrow CaTiO_3 \text{ Network} \quad (3.5)$$

It should be noted that this is very complex chemistry which cannot be completely predicted. Equation 3.2 shows one hydroxyl group replacing one alkoxo group on each the titanium and calcium metal atoms. In actuality this reaction may occur more than once. The number of hydroxyl and alkoxo groups shown as reactants for condensation will also likewise vary (Eq. 3.4). Equation 3.5 simply states that more condensation occurs through chemistry, drying, and heating which ultimately forms the $CaTiO_3$ network.

Chemical Formulation

The chemical formulation of the precursors for the pellets is a very sensitive and important step in the process. Sol-gel processing described above is used. Within this method there are a number of parameters that can be changed which can greatly affect the properties of the resultant product. These parameters include molar ratios between calcium, ethanol, water, and titanium isopropoxide, pH, temperature, and procedural steps. The procedures developed by Aihara et al. published in 1990 and later in more detail 2001 were used as guidelines in the current work of synthesis of the precursors.

Qualitative investigation

A qualitative study was conducted to observe the reactions. The reactants were mixed with each other to see what could be expected. Table 3.1 shows the qualitative observations of this investigation. All these experiments were conducted at room temperature in air.

Table 3.1 Qualitative Reaction Study

	Ca	Eth.	Ti. Iso.	D.W.
Calcium	XXXXXXXX	GWP	NAR	VED
Ethanol	GWP	XXXXXXXX	WFP	DFS
Titanium Isopropoxide	NAR	WFP	XXXXXXXX	SFWP
Dionized Water	VED	DFS	SFWP	XXXXX

GWP -Globular white precipitate forms (after stirring)
NAR- No apparent reaction
VED- Ca violently exothermically dissolves in dionized water producing bubbles
WFP- White fibrous precipitate forms
SFWP- Spontaneous reaction with white precipitate and gas evolution
DFS- Dissolves forming a solution

Original procedure

The procedure details given in the original publication (Aihara et al., 1990) are far from complete. Figure 3.1 shows an outline of this procedure. This outline was followed except graphite powder was not added. Graphite is used as an additive to increase porosity during calcination. This parameter was eliminated at this time to increase understanding of the other parameters affecting the porosity.

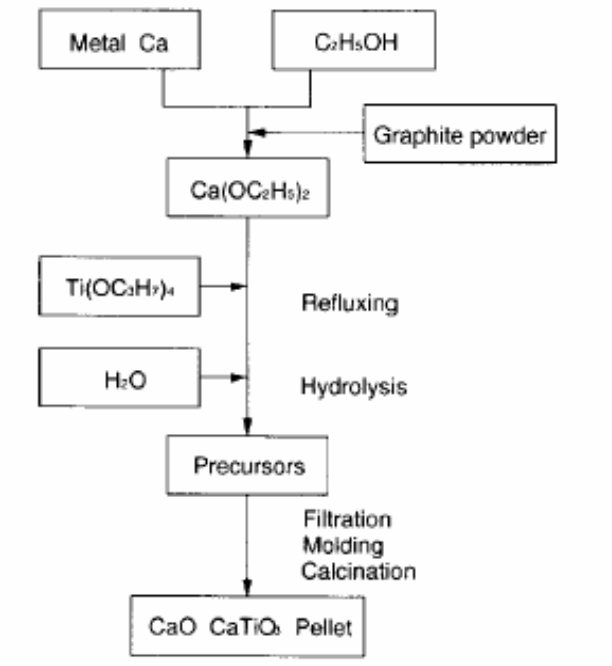

Figure 3.1 Production Process of the Pellet Using Ca and Ti Alkoxide (Aihara et al., 1990)

Though, this procedure looks fairly easy to follow there were many difficulties in performing the necessary steps. This first step, combining metal calcium and ethanol to form calcium ethoxide proved to be a major difficulty. Calcium does not react readily with ethanol. In order to try to remedy this situation two solutions were proposed.

1. Heat the ethanol and calcium mixture to see if the reaction would proceed quicker at a higher temperature. This was done but no reaction was observed up to boiling temperatures of ethanol. Because of the loss of ethanol to evaporation and boiling the mixture would dry out if it was left for long periods of time. No appreciable reaction was seen in this time frame. Later, it was found that there actually is a noticeable reaction that occurs between 73°C and the boiling point of ethanol 79°C. The reaction forms bubbles of hydrogen. This may have been overlooked as a slow boil because the temperature is so close to boiling of ethanol.

2. Stir the solution covered to see if the reaction would proceed faster while stirred. Again, there was no appreciable reaction observed. This mixture was left and the evaporation rate was slower in this set up. Thus, the reaction could be observed over a longer period of time. A white precipitate could be seen after about two days. The white precipitate thought to be the calcium ethoxide was finally formed. The precipitate seemed to be white and globular and settled to the bottom of the beaker after several hours. This method was adopted as the first step of the original chemical formulation.

The amount of calcium that would react in ethanol was very small. Later through a 10 day test the reaction limit was found to be about 0.0015g/mL. This was done by taking 0.38 grams calcium and adding ethanol over a number of days until the calcium was reacted. After 10 days the volume of ethanol added to react all the calcium was 250

mL. To try to increase the concentration of calcium some ethanol could be evaporated without signs of black calcium reforming. However, other calcium compounds may have been formed.

Next, 18 mL of titanium isopropoxide was added to 40 mL of this mixture. A stringing precipitate was spontaneously formed. The beaker became noticeably warmer indicating that this was an exothermic reaction. This precipitate appeared to be the same that was found in the qualitative study of reaction between ethanol and titanium isopropoxide (Table 3.1). The mixture was stirred for 5 minutes and the stringy precipitate broke apart very easily.

Next the mixture was hydrolyzed using 12 mL of dionized water. The beaker again became warmer indicating an exothermic reaction. The water seemed to react with the precipitate forming a powder-like precipitate. The mixture was again stirred for 5 minutes.

Drying procedures described later in this chapter were then followed to eliminate ethanol and water from the liquor leaving a powder. The powder was molded into pellets. The feedback from this pelletization study was used to improve the pellet mold and pelletization technique and to determine affects of sintering temperature. This procedure was expected to yield CaO dispersed in CaTiO3 matrix. However, since the ratio of calcium to titanium was small, it is suspected (and later confirmed via Raman spectroscopy) that not much calcium titanate or calcium oxide was formed. Most of the solid was anatase or rutile titanium oxide. Another indication that calcium titanate did not form is that calcium titanate exists in different colors ranging from orange to black but it cannot be bright white as the resultant powder was. This indicated that the powder

was TiO_2 which was later confirmed by Raman spectroscopy to be TiO_2 (anatase and rutile). Thus, a new chemical procedure had to be designed. This design needed to increase the calcium in the precursors.

Modified procedure

A paper by one of the original UT-3 authors (Aihara et al., 2001) gives more detail into the methods used for the chemical formulation of the calcium titanate (CaTiO3) precursor. This procedure implied that the reactions within the alkoxide procedure are very sensitive to water and possibly sensitive to oxygen. A new setup was constructed to perform the anhydronous formulation. The setup is shown below in Figure 3.2.

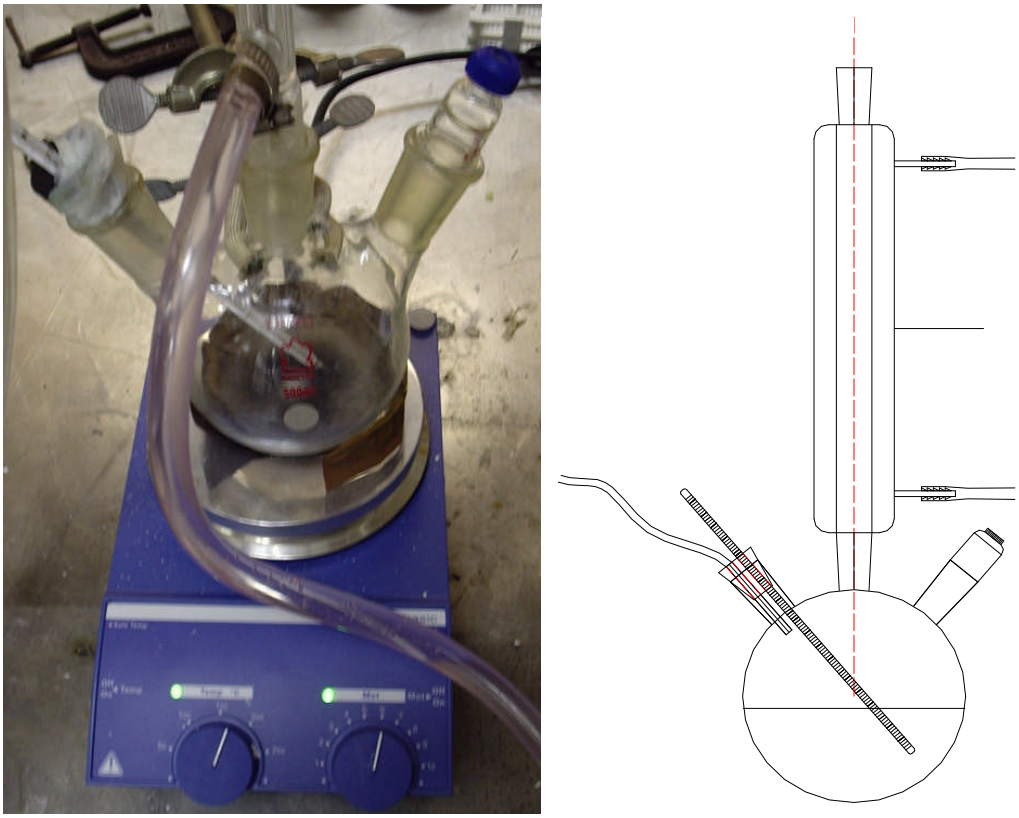

Figure 3.2 Three Mouthed Flask on Stirring Heater

A three mouthed flask is used as the vessel to carry out the new procedure. The first opening has a rubber stopper covered with parafilm with a tube and a mercury thermometer. The tube is connected to a nitrogen supply and used to purge the flask with nitrogen. The thermometer is used to monitor the temperature of the fluid inside the beaker. The second opening has a condenser to condense any vapor that could evaporate or boil from the system due to heating. The third opening has an adaptor with a silicon septum. Chemicals are added through the septum by a syringe to insure an anhydronous and oxygen free environment during the entire process. The flask is placed on a hot plate which provides the heat for the reflux processes. All of the equipment is properly supported using metal stands and clamps.

Aihara et al. (2001) used a nitrogen environment and followed the steps shown below in Figure 3.3. The ratios of the reagents are presented in Table 3.2. The molar ratios are shown with respect to Ca metal. The * indicates that in step 7 dionized water and ethanol are added in a solution.

Table 3.2 Original Mixing Ratios for Modified Chemical Formulation Procedure

Procedural Step	Substance	Amount	Units	Molar Ratio
Step 1	Calcium Metal	1.00	[g]	1
Steps 2, 4, & 7	Anhydronous Ethanol	14.6	[mL]	10
Step 5	Titanium Isopropoxide	7.4	[mL]	1
Step 7*	Dionized Water	1.8	[mL]	4
Step 7*	Ethanol	7.2	[mL]	4.9

The refluxing step in Aihara's, et al. procedure (step 3) was investigated to see how long the reaction took to fully react. An appreciable reaction occurred from about 73°C to about 78°C. Bubbles are observed forming on the calcium. This is the hydrogen product from the reaction shown in Eq. 3.1. In the 30 minute time that Aihara et al. prescribe much of the black calcium powder remained though an appreciable amount of white powder also could be seen. The reaction was watched for 5 hours without much

change. It was concluded that the reaction had reached equilibrium as no noticeable change was observed between 30 minutes and 5 hours. Therefore, the time of 30 minutes for step 3 was adopted.

Figure 3.3 Flow Diagram of Procedure Outlined by Aihara et al. (2001)

Stringent steps below were taken to ensure oxygen free and anhydronous condition.

1. Clean and dry flask, condenser, and other equipment.

2. The calcium sample is measured on the electronic scale and then dropped into the flask through the opening with the nitrogen and thermometer.

3. The Teflon stir bar is dropped into the flask through the opening with the nitrogen and thermometer

4. The condenser and septum adaptor are coated with a thin layer of petroleum jelly to prevent seizing before connecting to the flask.

5. The nitrogen valves are opened to allow a very small flow to the flask.

6. Water to the condenser is turned on.

7. Wait 5 minutes for nitrogen to purge system.

8. Anhydronous ethanol is extracted by syringe from its container and discharged into the system through the silicon septa.

9. The heater stirrer is turned on to raise the temperature of the mixture to between 72°C and 76°C. A noticeable reaction occurs in this temperature range forming a white/gray precipitate. The stirrer is set to maintain good stirring.

10. Heating proceeds for 30 minutes.

11. The mixture is diluted using the same amount of ethanol as in step 9.

12. Titanium isopropoxide is extracted from its container via syringe. The correct proportion is injected into the flask again through the silicon septa. The mixture is heated between 72°C and 76°C for 30 minutes.

13. A solution of 20% by volume of water in ethanol is made in a beaker.

14. A syringe is used to insert the water ethanol solution into the flask in order to maintain an oxygen free environment. A reaction occurs spontaneously turning most of the precipitate a bright white.

15. The mixture is stirred and heated for another hour. In this hour all of the precipitate becomes white except for a small amount when the calcium to titanium ratios are 3 and 4.

A problem encountered with this procedure was the formation of a purple rather than white/gray precipitate forming in step 9. The problem was thought to be in the cleaning of the flask from run to run. A new cleaning procedure for step 1 was considered so that the chemistry would not be affected by residue in the container from previous runs or residue from the actual cleaning agent. A rigorous cleaning was done including both an acid bath and base bath. However, the purple precipitate again formed. It was suggested that the rubber stoppers plugging the flask may be the problem. They were covered with parafilm and the purple precipitate ceased to form. In the interest of time a less thorough cleaning procedure can be used which does not affect the chemistry.

Mixing ratios

The initial mixing ratios for the new procedure came from Aihara et al. (2001). However, that procedure was designed to make calcium titanate and therefore uses a 1 to 1 ratio between calcium and titanium. In order to also make calcium oxide more calcium had to be used. Ratios of calcium to titanium of 2, 3, and 4 were used. Other parameters were changed because of the equipment setup and to accommodate for the extra calcium. These quantities can be seen in Appendix C. The original ratios used by Aihara et al. are presented in grams, milliliters, and moles in Table 3.2 above.

Physical Procedures

The synthesized precursors were molded into pellets. A procedure was developed which consists of first drying, then molding, and finally sintering. These three steps will be described in detail in the following sections.

Drying

The liquor from the precursor synthesis has a significant amount of ethanol and water left in it. The liquor is stirred to evenly distribute the particles in the container.

The liquor is poured into petri dishes. These petri dishes are set under an exhausting fume hood. Most of the liquid evaporates off after 18-20 hours, though the resultant powder is still slightly moist. The powder is put into a quartz crucible and heated in a furnace to 430°C for 1 hour. It was found that pellets molded using the powder disintegrated when heated between 300°C and 400°C. It was suspected that there were volatiles in the pellets which contribute to the pellet failure. Therefore, a preheating step was added. The pellets maintained their integrity at higher temperatures during the sintering step described later. This step was necessary before molding the pellets. It also eliminates any water or ethanol which was not evaporated in the overnight drying.

Molding

Hydraulic press

A hand pumped uni-axial hydraulic press (Figure 3.4) is used to supply the compression force to the mold assembly. It is a Carver hydraulic model # 3912 with a 5-1/8" maximum ram stroke. The press is located in room 1A of the Nuclear Field Building. There are two parallel plates on the press. The upper is plate on a screw and fixed in place using nuts. The bottom plate is connected to a hydraulic cylinder which is raised to supply the force as the lever arm is pushed down. A force gauge on the press in units on metric tons is rated up to 11 metric tons.

A 304-SS mold assembly (Figure 3.5) was fabricated and used in the hydraulic press described above to make pellets of 3/16" D x 4/16"-6/16" H. Compression force on the press was varied from 0.3 MT (metric tons) to 2 MT. Problems with plastic yielding and seizing of the plunger with the mold were experienced at axial loads greater than 1.0 MT and so the pellets were cast with forces less than 1 MT. A step by step procedure of this process can be seen in Appendix C.

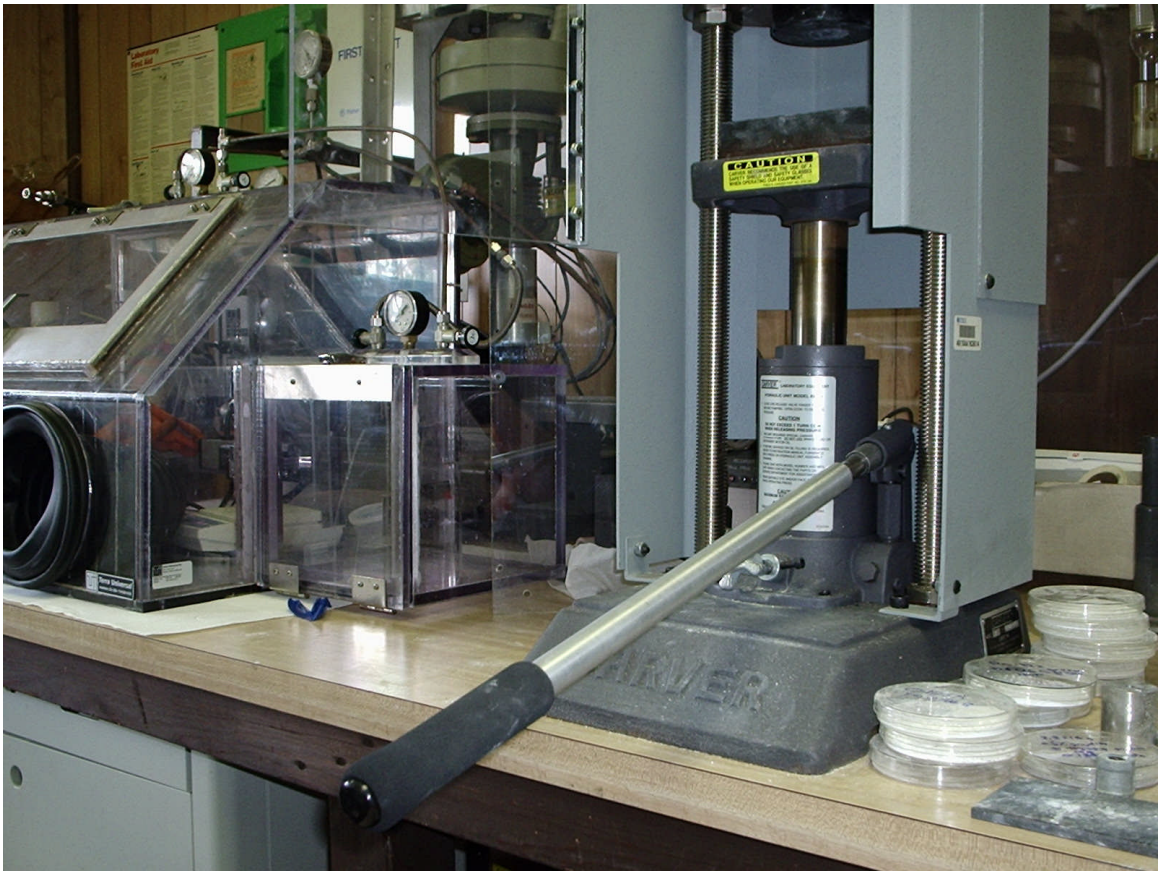

Figure 3.4 Hand Pumped Uni-Axial Hydraulic Press for Pellet Production

Original mold

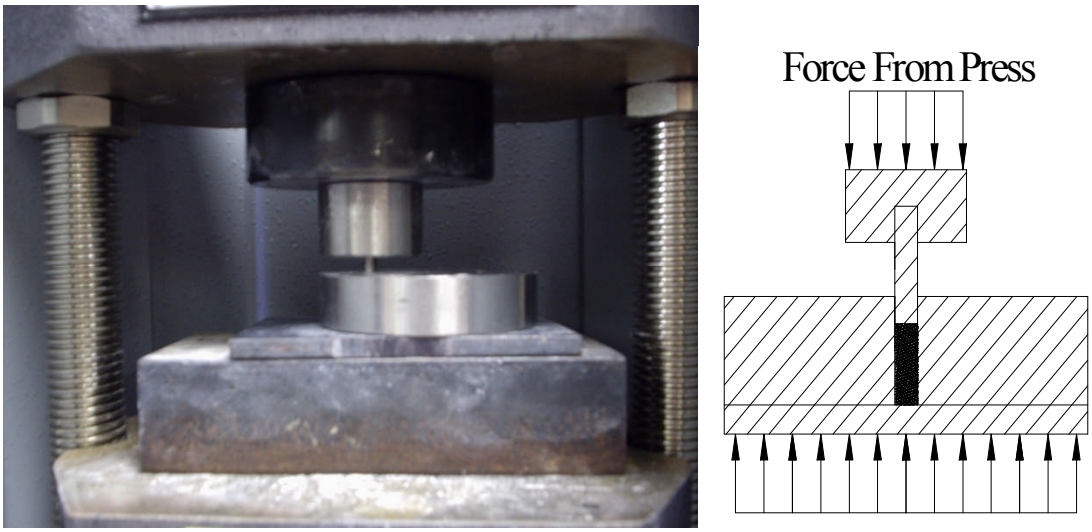

Figure 3.5 Pellet Mold Assembly

The mold assembly consisted of 5 parts as shown in Figure 3.6 which are the plate, plungers, cap, mold, and extraction piece. The plate was the bottom piece on which the mold was supported and was the surface the pellet was compressed against. It also helped to move the full assembly in and out of the press.

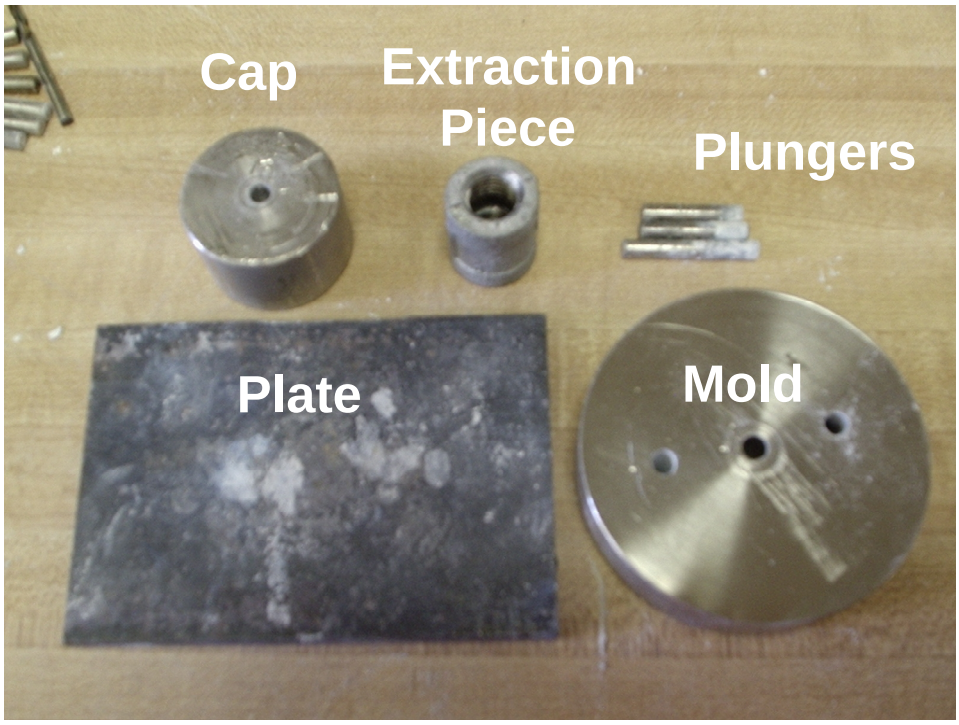

Figure 3.6 Pellet Molding Assembly Parts

The plungers were used in two different manners and so two different length plungers were fabricated. The shorter plungers were used to compress the pellets. Generally, the shorter plungers had a greater compression force on them. The shorter lengths helped to prevent bending from any eccentric forces. The longer plungers could be used to push the pellets out of the mold and could be pulled out easily because their extra length allowed room for gripping. The cap was the top piece which held the plungers vertical which also helped to reduce non-axial forces which would lead to buckling and bending. It has a hole drilled about 0.5” in depth with a 0.1875” drill bit and a 0.1895” reamer. The mold has bores where the powder is positioned and

compacted. These bores are made slightly larger than those in the cap. The bores were observed to expand after multiple uses at compression forces close to 1 metric ton. The bores were made using 0.2031" drill bit and reamer. The extraction piece is only used to extract the pellet. It is essentially a spacer between the mold and the top surface of the press. It has is a hollow cylindrical piece which transfers the force to the outer molding while giving no resistance in the center where the pellet is extracted. The extraction piece allows the pellet to be pushed out into the hollow space it contains.

As discussed in chapter 2, a low compaction force is expected to yield higher porosity in the pellet. However, lower compaction force may also reduce the strength of the pellet. These two factors were considered to arrive at the optimum molding procedure.

For the original chemical formulation procedure a force close to 1 metric ton gave the best strength. Whole pellets were formed with forces as low as 0.5 metric tons but a noticeable depreciation in strength was observed during handling the pellets. It was found that pellets made from precursors with 0.25-2 percentage of graphite could be made with a compaction force of only 0.3 metric tons. Also stearic acid and ammonium carbonate were both tried as binders at 3% by weight. Both actually degraded the strength of the pellet when compared with pellets made with the same compression without the binders.

For the modified chemical formulation procedure a force of only 0.25 metric tons was needed to give approximately the same strength as the pellets compressed at 1 metric ton using the previous chemistry. No graphite or binders were used with the modified chemical formulation.

Modifications in mold and molding procedure

Many problems were encountered during the fabrication of the mold and the development of the molding procedure. The most prevalent operational problem was the seizing of the plungers in the mold. This was attributed to two design aspects. The first was the length of the mold. The original mold was 1-1/16" This original mold bore also had a very low radial clearance between it and the plunger so that there would be minimum flow of the powder into the space between the bore in the mold and the plunger. The friction from the powder wedging between the mold and the plungers led to seizing.

To eliminate this problem a procedure which limited the insertion length of the plunger was used to prevent seizure during the compression process. The compressed pellets however could not be removed due to the friction forces between the walls of the mold and the consolidated powder. A slightly larger hole was drilled to see if pellets could be made. The same problems occurred, though the plunger rarely seized during the compression phase. When the pellets were extracted they fell apart. It was thought that an uneven distribution of pressure in the powder along the height of the mold due to friction led to the failure of these pellets.

A new mold was made that was 11/16" in height. The holes on this mold were drilled slightly larger than 0.1875" at 0.2031". A procedure was used with the new mold so that the powder would be compressed stepwise using multiple compactions. The plunger was removed after every incremental compaction and more powder was added to fill the hole to the top. The powder was again compressed. This was repeated until the desired height of the pellet was reached. This process resulted in some long pellets. However, most pellets would shear during extraction into small fragile disk shapes or

separate into shorter pellets. The seizing between the mold and the extraction plunger also occurred sometimes.

The procedure was further modified as follows. Only one fill was used. The powder was compressed by hand as much a possible and filled to the top. The press was then used to compress the mold assembly with the desired force. Seizing has not occurred using this procedure during compression or extraction. This procedure is now used and generally produces whole pellets with the average dimensions ~3/16" D x 5/16" H though this height varies slightly from run to run. If correctly executed this procedure yields a usable pellet every time. Seizing probably does not occur because of the relatively short compression length into the powder at high pressures. Most of the compression is at low pressures. Thus the powder in the gap between the plunger and the bore is loosely packed except for the bottom. When the plunger is being extracted it has some play in the axial direction which can loosen the tightly packed powder near its lower face. The surface area of the plunger exposed to tightly packed powder was also small. Similarly, during extraction the surface area of the tightly packed powder causing the friction was reduced due to the shortened length of the pellets. Thus no seizing occurred. The pellets hold together better also because they are compressed all together. The previous method compresses different sections. These sections don't seem to hold together well. Thus the current method eliminates seizing and provides a reliable way to produce pellets.

Sintering

The pellets are sintered in a furnace to increase strength in the structure of the pellet. An increase in temperature promotes growth of the titanium network. The particles form intermolecular bonds which help to create a web-like structure increasing

the structural strength of the pellets. However, in the process the particles become larger, which often leads to pore clogging. Therefore, there is an optimum sintering procedure which will give the needed strength but without forfeiting the desired porosity.

A tubular furnace with a controller is used for sintering. An ATS (Applied Test Systems) 3310 series furnace is used and is also located in room 1A of the Nuclear Field Building. It can be seen in Figure 3.7 below. The furnace range is up to 1300°C. The operation of the furnace can be programmed using a PID controller (Kanthal Super 33, PC-120/240-20 controller). The controller has an offset error and temperature set points must be above 95°C. A recalibration was done in order to try to eliminate this offset error but it still persisted. During the calibration the error range in the temperature was found to be plus or minus 10°C. A quartz crucible attached to a quartz hanger is used to lower the pellets and powder into the furnace. It is approximately 18" in length and the crucible has a diameter of 1.5" and a height of 2".

There are a number of different heating schemes used to vary the temperature and the duration of heating. The heating schemes are presented in Figure 3.8. The heating schemes have been modified based on the behavior of the pellets with respect to strength and microporosity. The original procedure was a 100°C step every hour up to 700°C. This was used to first find the volatiles addressed earlier in this chapter between 300°C and 400°C and to determine if there were any other disintegration temperatures. The next scheme that was used went to 1000°C over a number of hours. The ramp times were to allow any reactions to occur slowly so they would not to break the pellets. The slow ramp increase was also to prevent thermal shock from breaking the pellet. After 1000°C heating the porosity of the pellet was only about 3% of that of the 700°C pellet. However,

the 1000°C heated pellet was stronger than the 700°C pellet. A medium temperature above the reaction temperature of 760°C was sought that would increase strength yet give a better porosity. Both 800°C and 900°C heating schemes were then used to investigate this parameter shown in Figure 3.8 as the medium schemes. The results in chapter 5 show acceptable characteristics within these temperatures.

Figure 3.7 Furnace Used for Sintering Process

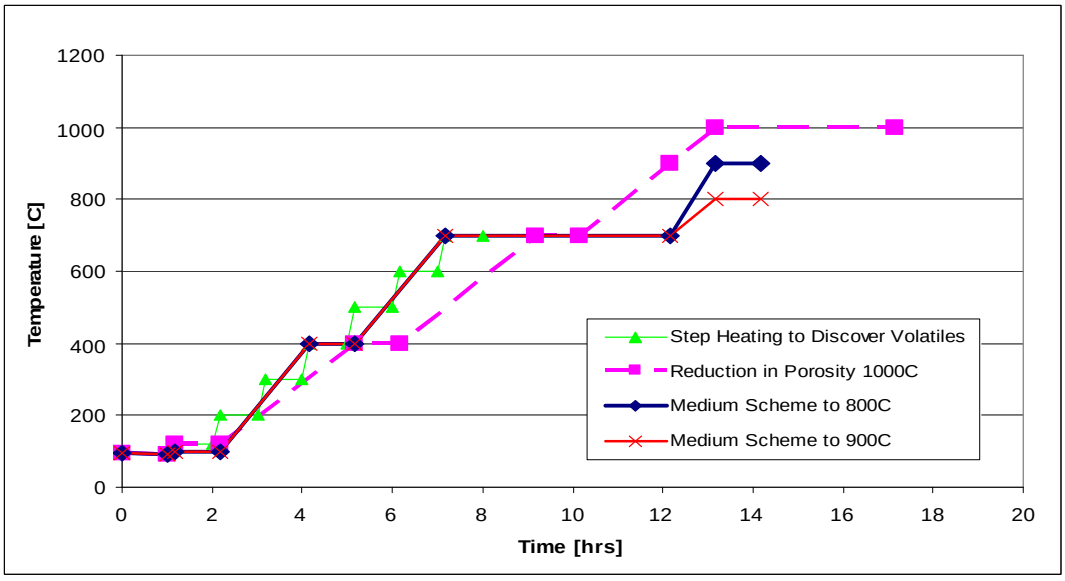

Figure 3.8 Heating Schemes for Pellets

CHAPTER 4
ANALYTICAL TOOLS

The theory and procedures for the analytical tools used are presented in this chapter. The theory presented in this chapter is meant to give an understanding of some of the methods used to characterize the pellets. The procedure is an outline of the steps taken for each instrument to give a basic understanding of its operation. More detailed procedures can be seen in Appendix D.

Presented in this chapter are three analytical tools. There are two porosity tests. The first, Nitrogen Adsorption, measures micropores using theory to predict distribution of pore sizes between 2 nm and 0.1 μm. The second, called Mercury Porosimetry, measures macropores using mercury under pressure and theory to predict distribution of pore sizes between 2 nm and ~100 μm. Though mercury porosimetry can intrude into small pore sizes, BET measurements are generally taken as a better measurement of micropores smaller than 50nm. The third tool is Raman spectroscopy which is used to determine the chemical composition of the pellets. In addition to these tools a chemical procedure was developed to help quantify the chemical composition of the pellets.

Nitrogen Adsorption

Theory

The nitrogen inside the sample tube is able to condense on the pore surface. This has been modeled by a number of scientists over the years. There are monolayer models and multi- layer models. Some account for capillary effects in pores and others do not.

One of the most widely used models is the BET multilayer adsorption model which builds upon the Langmuir monolayer model.

The Langmuir model relates the concentration of vacant sites and filled sites in adsorption process. The model has a form similar to a kinetic rate law. For nitrogen it is:

$$r_{AD} = k_A \cdot \left(P_{N2} \cdot C_v - \frac{C_{N2-S}}{K_A} \right) \tag{4.1}$$

where r_{AD} is the rate of adsorption. k_A is rate coefficient for adsorption. P_{N2} is the pressure of nitrogen. C_v is the concentration of vacant sites. $C_{N2\text{-}S}$ is the concentration of sites which are filled by a N_2 molecule. K_A is the equilibrium adsorption constant. Though, the pressure for nitrogen can be monitored all the other parameters must be known from earlier experimentation. However, when nitrogen is adsorbing on a surface the rate is different than if it is forming a multilayer on previously condensed nitrogen. Thus once the total surface is covered the rate is fairly constant and can be seen as the linear middle section in the plotted BET isotherm in Figure 4.1. The beginning of this linear region can be used to estimate the total surface area based on the volume adsorbed.

BET Isotherm

A BET (Brunauer, Emmett, and Teller, 1938) Isotherm describes the multilayer adsorption case for most surfaces. However, in materials with small pores this equation becomes less accurate due to capillary forces across the pores. Thus another calculation scheme has been developed by Barrett, Joyner, and Halenda (BJH).

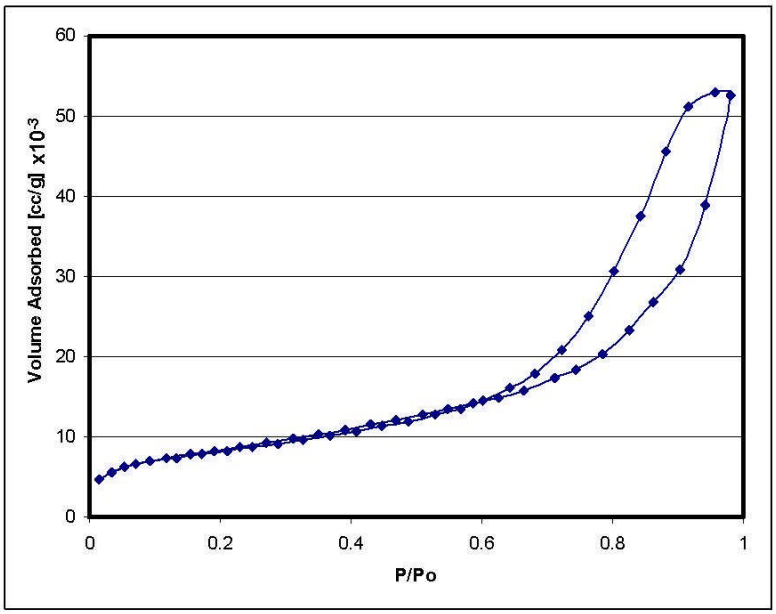

Figure 4.1 Typical BET Isotherm

BJH Pore Size Distribution

Barrett, Joyner, and Halenda (BJH) derived a relationship that can be used to create pore volume distributions or pore area distributions over a range of pore sizes (Barrett et al., 1951). In their derivation they used the proposed mechanism by BET for multilayer adsorption but account for capillary condensation. There are two main assumptions that are used in this derivation. The first is that all the pores are cylindrical. The second is that nitrogen is adsorbed by two means being condensation on the pore walls and capillary condensation. The derivation also uses the Kelvin equation relating pressure, surface tension, and pore radius. This method gives results within 1 to 5% of the BET total surface area measurement.

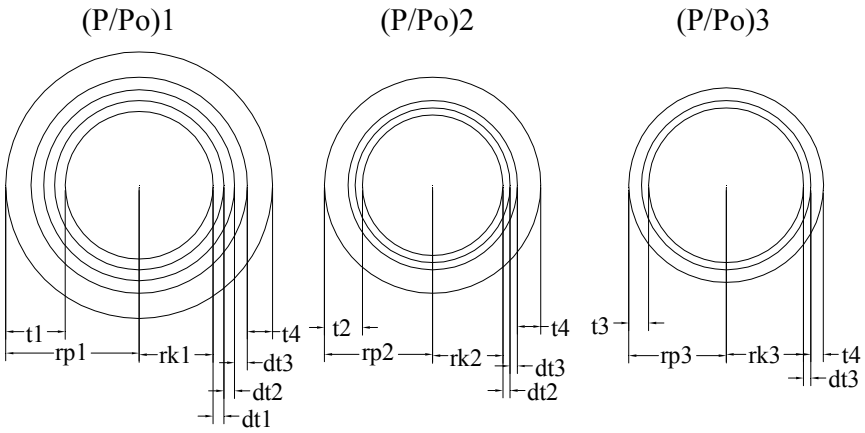

Vp1=R1*dV1 Vp2=R2*dV2-R2*dT2*Ac1

Vpn=Rn*dVn-Rn*dtn SUM[j=1 to n] (Acj)

Figure 4.2 Schematic Representation of Assumed Desorption Mechanism Showing Three Different Pores and Demonstrating the Thinning of the Physically Adsorbed Layer Over the First Three Decrements (Barrett et al., 1951)

The pressure is increased gradually until the sample is saturated or has reached the preset pressure. The pressure is then reduced stepwise so that a certain volume of condensate is emptied from a certain pore size range; The condensate layer thickness is reduced or the capillary condensate is emptied. A volume of gas at a given pressure is measured. This volume can be converted to condensate volume knowing the liquid and vapor densities of nitrogen. Thus the pore volume can be found. This is a simplified explanation of the theory. Detailed treatment of the theory is available by Barrett, Joyner, and Halenda (1951). Nitrogen adsorption and mercury porosimetry are also explained clearly and compared by Westermarck. (2000)

Procedure

A Quantachrome NOVA 1200 machine located at the Particle Science Engineering building was used for nitrogen adsorption tests. Two to three pellets are placed in a sample cell (similar to a test tube). The cell is placed into an airtight station in the NOVA machine. It is then vacuum outgassed for a duration which depends on the

sample. The sample is heated to 200°C during the outgassing procedure. Outgassing elutes the moisture from the sample, making the pore surface available for nitrogen adsorption.

At this point the mass and the density of the sample are entered in the instruments software. The sample cell is moved to the analysis station. A dewar (container) of liquid nitrogen is raised so that the cell is surrounded by liquid nitrogen. Starting from very low pressures, nitrogen is incrementally added into the cell. Some of this nitrogen is adsorbed into the pores of the sample. The pressure is increased until atmospheric pressure (770 mm Hg) is reached. The pressure is then reduced stepwise. A certain amount of nitrogen desorbs at each pressure. This is measured through pressure reading and/or air flow out of the cell. The amount of desorbed nitrogen can be correlated to pore size using theory.

Mercury Porosimetry

Theory

The theory behind the mercury porosimeter is relatively simple compared to that of Nitrogen Adsorption. Mercury porosimetry uses the capillary relationship given by Washburn equation (Eq. 4.2) to calculate pore size based on pressure.

$$D = -4 \gamma \cos(\theta) / P \qquad (4.2)$$

Knowing the contact angle of mercury (θ=140°) and surface tension (γ= 480 dyne/cm), the pore diameter can be correlated to the pressure inside the chamber. Mercury porosimetry like nitrogen adsorption, assumes that the pores are cylindrical. It also assumes constant mercury properties.

Procedure

The Quantachrome Autoscan 60 Mercury Porosimeter in the Particle Science Engineering Building was used to measure the porosity of the pellets. A porous sample is placed in a small glass container with a long thin tube at one end. The air is evacuated from the system using a vacuum pump. Mercury is then pushed up the long thin tube until the container and the tube are full. The mercury porosimeter works by measuring the capacitance of the mercury in the tube. As the pressure is increased in the chamber more mercury is pushed into the pores of the pellet. As the column of mercury is decreased, the capacitance changes by a certain amount which is calibrated so that a volume can be calculated. The pressure in the system is increased slowly so that more mercury intrudes into smaller pores. Using the pressure and Washburn equation the pore size can be calculated. Thus, a volume from the measured capacitance can be obtained and correlated to the pore size calculated from the capacitance. The pore size distributions are generated in this manner.

Raman Spectroscopy

Theory

Raman spectroscopy is a light scattering technique to determine the composition of molecules. A laser is focused onto a surface. The light is then inelastically scattered according to the bonds of the molecule. This is called the Raman effect. The Raman effect only occurs for about 1 in 10 million incident photons and is therefore a weak signal. Inelastic scattering occurs when a photon gains or loses energy from the vibration energy of bonds in a molecule (Eq. 4.3). If the photon loses energy it will have a higher wavelength than the exciting light. This is called the Stokes line and is generally what is measured. If a photon gains energy it will have a lower wavelength than the exciting

light. This is called the anti-stokes line and is generally very week and hard to detect. The change in wavelength of the stokes and anti-stokes line is related to the vibrational energy spacing. Thus these changes can be used to directly measure the vibrational energies of the molecule. In order to detect these weak signals a high powered monochromatic light source such as a laser is used.

$$h/\lambda_{in} + E_{vib} = h/\lambda_{out} \quad (4.3)$$

This scattered light is detected over a spectrum of wavelengths. The spectra for materials are different based on their bonds. This can be seen in the spectra for different materials. Characteristic peaks will indicate the presence of particular types of molecules. Raman spectroscopy also has a signal in which the relative intensities of the characteristic peaks can be correlated to the concentration of a certain substance. In order to do this, spectrum must be taken from known concentrations of species of interest.

Procedure

A sample of powder is prepared and put into a melting point capillary tube. A computer is attached to the Raman spectrometer. A program called OMNIC is used to adjust the laser light so that the best signal is obtained. The laser is focused onto the sample and the scattered light is reflected to a spectral detector. This signal can be measured for different lengths of time. OMNIC also averages a number of signals which can be varied. A number of other parameters affecting strength of the laser and the signal detection can be changed. A spectrum is then obtained for each sample. Characteristic peaks at certain wavelengths will indicate the presence of a particular substance. Sometimes the strength of the signal can also be correlated to the concentration of the particular substance of interest if calibrated using known concentrations.

Chemical Testing

Theory

Chemistry can be used to determine the amount of CaO present in the pellets. The two main components in the pellets are CaO and $CaTiO_3$. CaO reacts with HBr to form $CaBr_2$ yet $CaTiO_3$ does not react with HBr or H_2O. The percentage of CaO can be found using the molecular weights CaO and $CaBr_2$ and the difference is weight after a reaction with HBr and evaporation of volatiles.

Procedure

Samples were made of powder produced with modified chemistry and heating procedures. Each sample was placed in a sample container and weighed. An excess molar amount of hydrobromic acid was added to each container via a 48% by weight solution of hydrobromic acid in water. The mixtures were then subjected to 80°C heating for 18 hours. The heating temperature was increased to 100°C for 4 hrs and to 200°C for an additional 2 hours. All the chemicals were volatile except for the calcium compounds. The amount of CaO can be quantified by finding the change in weight resulting from the added HBr solution because $CaTiO_3$ does not react with HBr. The extent of the reaction was determined by using laboratory grade CaO and performing the same procedure. The extent of the reaction was found to be 98%. This procedure was used to determine the amount of CaO in each sample. An error of about 5% is estimated using this procedure. Though, small amounts of $CaCO_3$ and TiO_2 can be present in the pellet most of it is composed of CaO and $CaTiO_3$. Thus, after the CaO is calculated the amount of $CaTiO_3$ can be approximated as the remainder of the composition.

CHAPTER 5
EVALUATION OF PARAMETERS

The effect of various parameters on the pellet characteristics—the porosity, the chemical composition, and the strength—was studied to develop the molding and heating procedures. The parameters are listed in Table 5.1 and are associated with the chemical formulation, molding procedure, and pellet heat treatment. Correlations have been made between procedural parameters and the resultant characteristics of the pellet. The optimum procedure has been chosen based on these correlations. These correlations and the optimum procedure parameters are presented in this chapter.

Correlations from Original Chemistry

The original chemistry was helpful for determining a general range of parameters for the heating procedures and molding procedures. However, this procedure had to be modified to attain the desired composition in the pellets. Figure 5.1 is a diagram that illustrates how the parameters were evaluated based on the resulting characteristics. Within each of these general categories describing the procedure there are parameters which can be seen in Table 5.1. The parameters with a (1) are ones which were varied to characterize the pellets using the original chemistry. Likewise, a (2) indicates parameters for the modified chemistry. An (M) indicates the parameters which were changed as a direct result of feedback from the characteristics of the resulting pellets. Parameters without any of these designations were established in the original procedure and not significantly changed or varied to investigate how the characteristics of the pellet changed.

Table 5.1 Parameters in the Main Categories Shown in Figure 5.1

Chemistry (M)	Molding	Heating Procedures
Ca/Ti Ratio (2)(M)	Compression Force (1) (M)	Drying Time & Temp.
pH	Binder Additive (1)	Preheating Time & Temp (M)
Water/Ca (M)		Max Sintering Time & Temp.(1) (2)
Ethanol/Ca (M)		Temp. Ramping Scheme (M)
CondensationTime and Temp.		

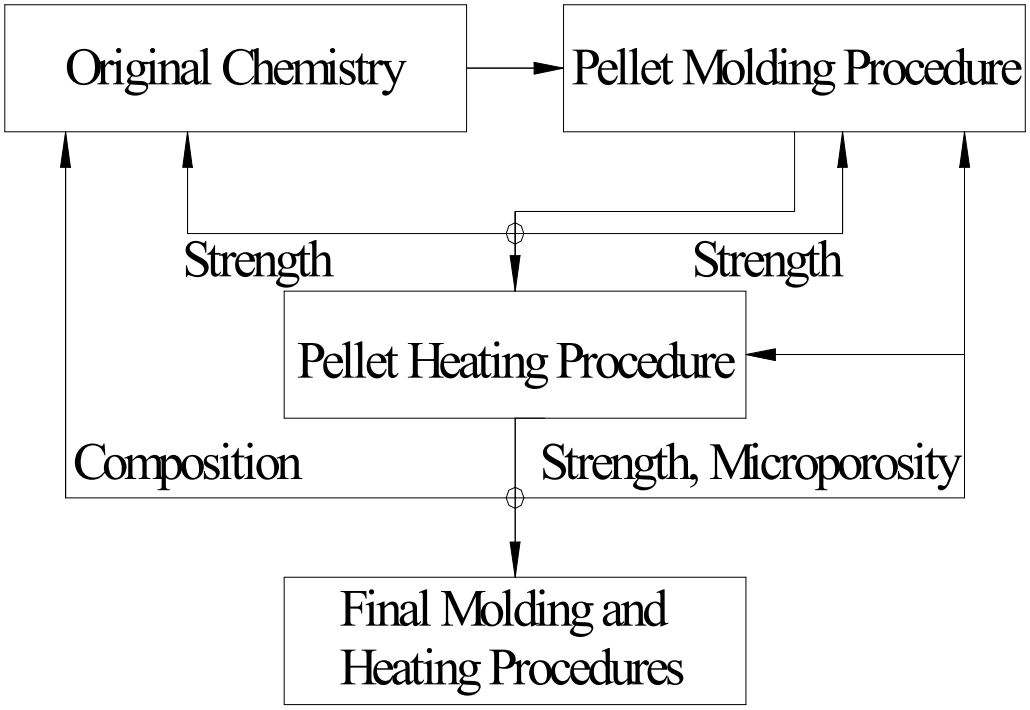

Figure 5.1 Flow Diagram Indicating How Characteristics Were Used as Feedback to Modify the Parameters to Arrive at the Final Procedures

Molding Procedure: Strength

The strength was qualitatively be analyzed. If the extruded pellet fell apart it was deemed too weak. Most of the pellets formulated using the original chemistry required a compression of 1.0 metric ton to ensure whole pellets.

Heating Procedure: Strength and Microporosity

The heating procedures were evaluated based on the strength and the microporosity of the pellet after heat treatment. The preheating step was added to improve strength as described in chapter 3. The merits of the heating procedures were also evaluated based

on the strength of the pellets after heating. The pellets remained intact with no significant cracking during heating. Higher temperatures led to sintering and created stronger pellets. This was qualitative comparison as no quantitative strength test has been done.

The maximum temperature of the heating had a direct impact on the microporosity of the samples. The cumulative pore volume was measured using nitrogen adsorption in conjunction with a BJH correlation and is plotted against the maximum sintering temperature in Figure 5.2. The data fit a correlation $y=0.0012x^2-2.6701x+1433.7$ where x is the maximum sintering temperature and y is the cumulative pore volume. The microporosity decreased drastically from maximum temperatures between 700°C and 1000°C for pellets with the same chemistry and molding procedures. At 700°C the porosity is 0.171 cc/g which drops down to 0.006 cc/g when the sintering temperature is increased to 1000°C. The intermediate temperatures of 800°C and 900°C show the decreasing trend. A sintering temperature of 800°C was chosen for investigation with the pellets created using the new chemistry. This temperature gave a reasonable strength to the pellets without drastic loss in porosity.

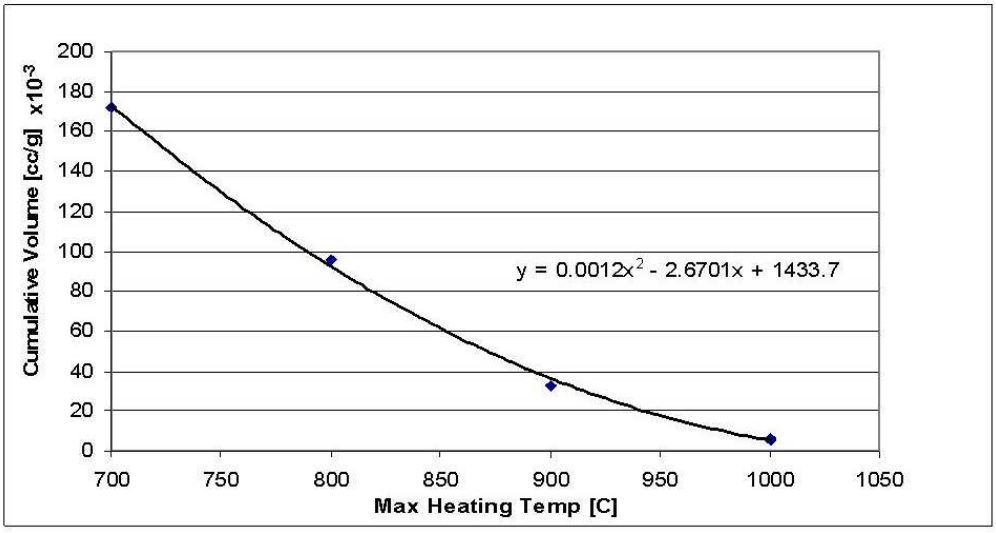

Figure 5.2 Specific Cumulative Micropore Volume vs. Maximum Sintering Temperature

Chemistry: Chemical Composition

Raman Spectroscopy identified the composition of the first pellets. Two pellets were tested and found to closely resemble the Raman spectra for rutile and anatase-TiO_2. This confirmed suspicions that the original chemistry did not form the desired network. Figure 5.3 shows the Raman spectra from two pellets made using the original chemistry along with the spectra for both anatase and rutile TiO_2 where the y-axis is the intensity (Int) of light for that wavelength. Pellet 1 appears to be mostly anatase TiO_2. Four matching anatase peaks can be seen from left to right. However, there are no rutile peaks. The spectra for the second pellet has peaks of both anatase and rutile TiO_2 indicating the presence of both phases of TiO_2 in the pellet. This probably occurred due to the different heating procedures this pellet underwent. Peaks for CaO and $CaTiO_3$ are markedly absent in these spectra. Because of the minute amount of CaO the original chemical procedures had to be modified.

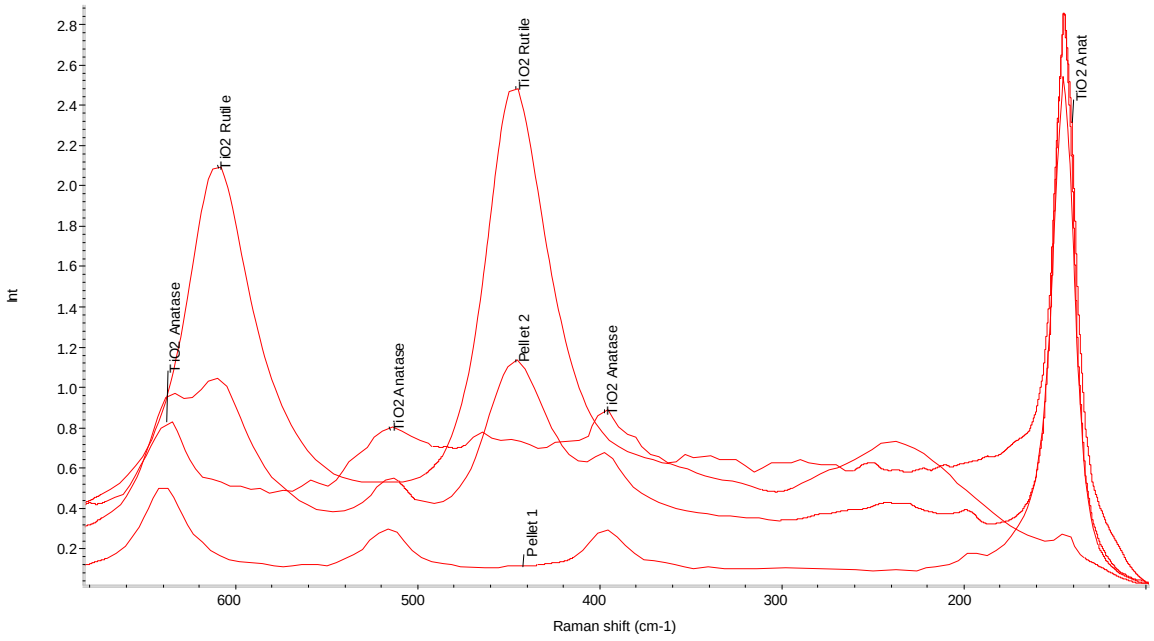

Figure 5.3 Raman Shift Spectra of Anatase and Rutile TiO_2 and Two Representative Pellets Made Using the Original Chemistry

Correlations from Modified Chemistry

Correlations were made between the characteristics of the new pellets (made using the modified chemistry) and the procedural parameters. Figure 5.4 illustrates how the characteristics are used to evaluate the parameters in this modified procedure. Refer to Table 5.1 for parameters within each main procedural step.

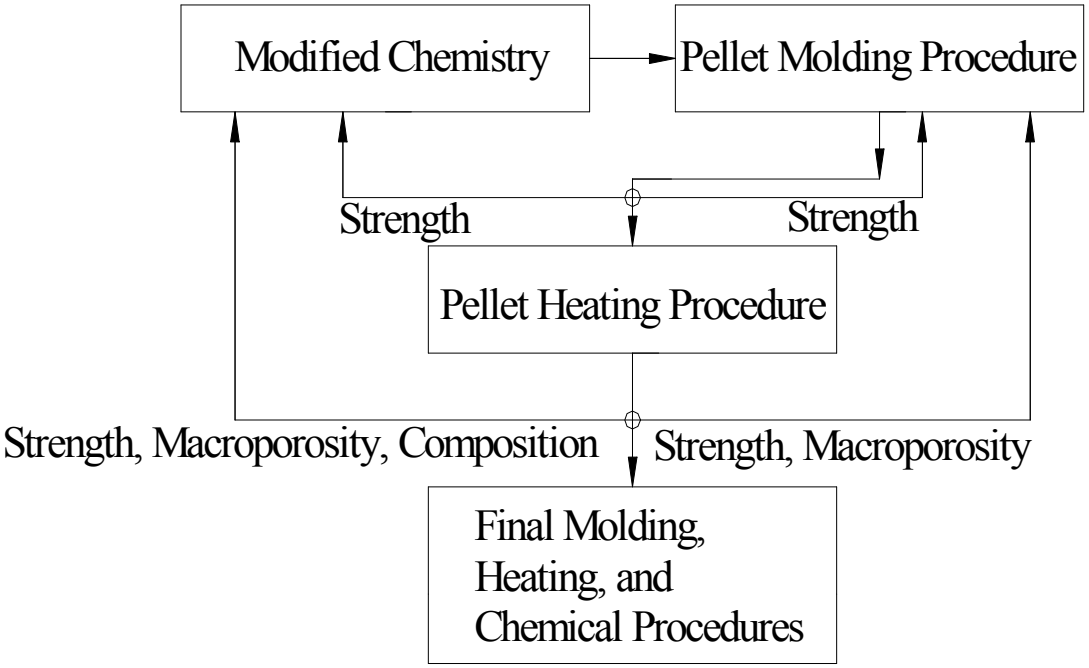

Figure 5.4 Visual Flow Diagram of How Characteristics were Used as Feedback to Modify the Parameters Using the Modified Chemistry

Molding Procedure: Strength and Macroporosity

The new pellets required a compression force of only 0.25 metric tons to hold together as compared to 1 metric ton for the previous pellets. This improvement is considerable because increased strength at lower compression will result in greater porosity for these pellets.

A comparison between new pellets compressed at 0.5 metric tons and 0.25 metric tons was conducted. The pellets were made with a 2 to 1 ratio between calcium and titanium and heated to 800°C using the same heating scheme. The size of the pores seems to remain in the same range indicated by the differential distribution which peaks around 100nm. However, the specific cumulative pore volume for the pellets was approximately 0.15cc/g less at the 0.5 metric ton compression. This is shown in Figure 5.5 by the smooth curves increasing right to left to a maximum at 10 nm. For reference a larger version of this graph can be found in Appendix F, (Figure F.2).

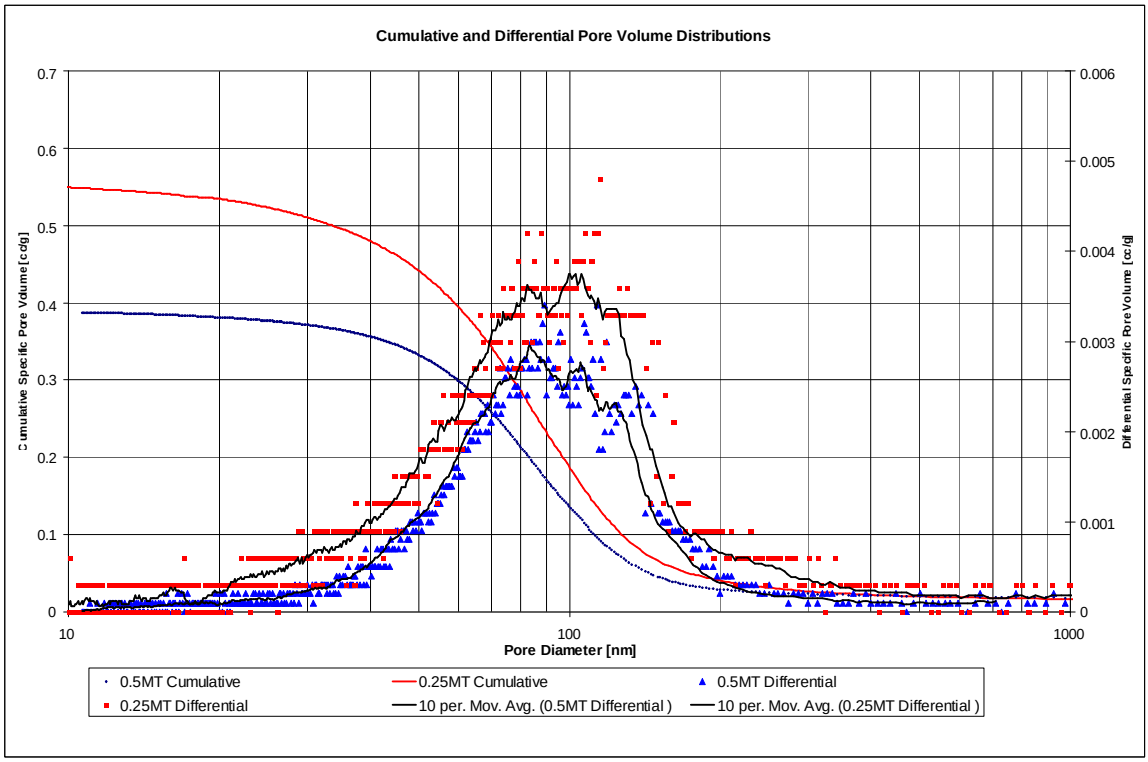

Figure 5.5 Comparison of Cumulative and Differential Specific Pore Volume Distribution for New Pellets Compressed at 0.25 and 0.5 Metric Tons.

Chemistry: Macroporosity, Microporosity, Composition, and strength

Using the modified chemistry a network of CaO and CaTiO3 was synthesized. An attempt was made to use Raman Spectroscopy to verify the existence of $CaTiO_3$ and

CaO. At first the sample spectra obtained were inconclusive as their peaks did not match either those of the pure CaO spectrum or $CaTiO_3$ spectrum as expected. One possible reason for this may be electrical interaction that may occur in the samples. Since the scale of mixing using the alkoxide chemistry is at the molecular level, which may alter the electronic response. This would affect the Raman spectroscopy as it uses light scattering that can be affected by slight variations in the electric fields of the samples. Appendix E (Figure E.2) shows the comparison of a sample made using the modified chemistry, Pure CaO and Pure $CaTiO_3$. The samples were also compared to spectra from $CaCO_3$, $Ca(OH)_2$, TiO_2-rutile, and TiO_2-anatase to identify if any of these substances was present. There did not appear to be any strong matches in the samples formulated with the new chemistry and these compounds. One sample did have a small matching peak with $CaCO_3$ indicating a small percentage of $CaCO_3$ (~2-5%). The florescence of the samples generate broad peaks which hide the species identifying peaks.

A second attempt to use the Raman spectroscopy revealed strong matching peaks for $CaTiO_3$ for two different pellet powders. These powders were made using a 2 to 1 ratio between calcium and titanium and heated to 1000°C. The only difference between the two pellets was the temperature of preheating. Pellet 1 was preheated at 430°C whereas pellet 2 was preheated at 600°C. Figure 5.6 shows the matching of the peaks. More Raman shift spectra are presented in appendix E including the full spectra of the piece shown in Figure 5.6. It should also be noted that for this spectra the intensity value (Int) is meaningless as the spectra were offset and scaled differently to show matching peaks. There were no strong peaks in the spectra matching CaO, but a non-fluorescing spectrum for CaO could not be obtained.

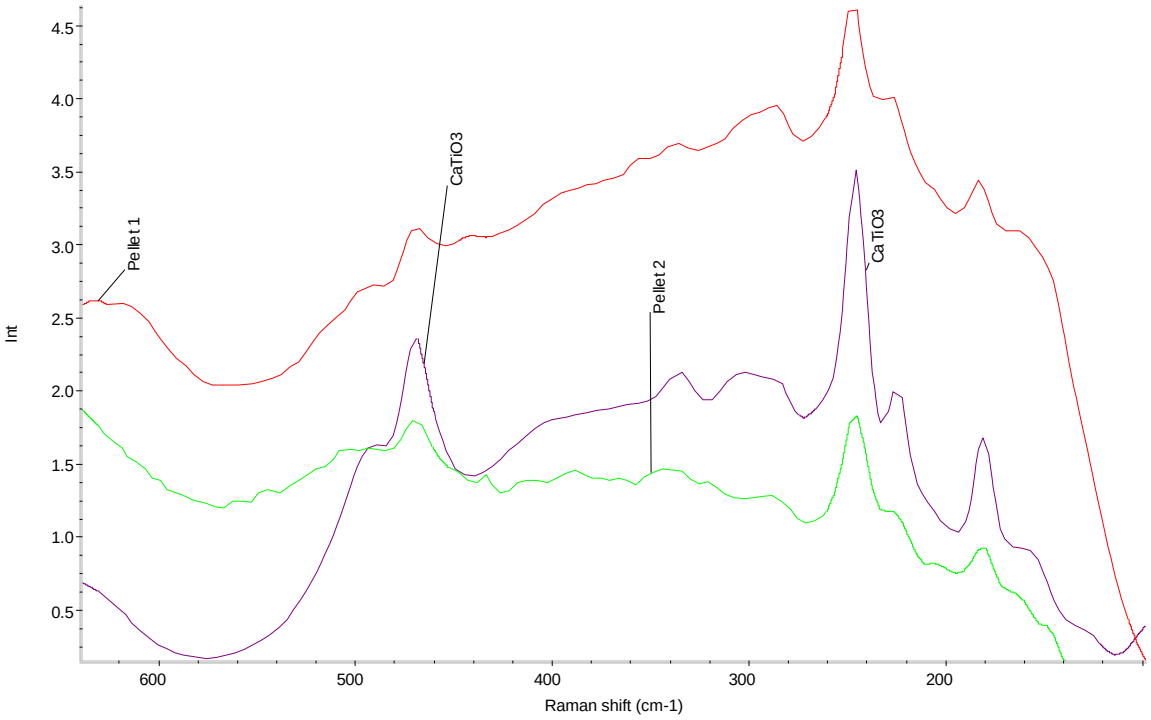

Figure 5.6 Raman Shift Spectra for CaTiO3 and Two Sample Pellets

The existence of CaO and $CaTiO_3$ in a sample made from the modified chemistry was verified through X-ray diffraction (XRD) because of the inconclusive data from the first try at Raman Spectroscopy. The signature peaks of $CaTiO_3$ and CaO have been identified in the XRD taken for this sample (Figure 5.7). In addition to the XRD verification, the amounts of CaO in the pellets were found using the chemical testing procedure described at the end of chapter 4. Results from the chemical testing procedure can be seen in Table 5.2 for many different samples.

In Table 5.2 the values for the %CaO are calculated based on the assumption that calcium only exists as CaO and neglects the possibility of $CaCO_3$ or $Ca(OH)_2$. The assumption is poor at low temperatures. The existence of $CaCO_3$ and $Ca(OH)_2$ is evident in the high percent error in the Modified Chemistry Powder 2 data for the unheated and 430°C heated runs. However, this seems to be a reasonable assumption when the

maximum heating temperatures is 1000°C. The temperature drives the dissociation of any $Ca(OH)_2$ or $CaCO_3$ that may be present. Thus, the results show that the presence of CaO is close to the expected percentage based on the stoichiometric relationships between calcium and titanium.

The standard samples of CaO and $CaTiO_3$ justify the validity of the test. CaO and $CaTiO_3$ are within 2% and 3% of their theoretical values respectively. The $CaTiO_3$ in the pellet powder can also be seen unreacted at the bottom of the sample container. One other point of interest is that the samples made with powder from the original chemistry do not indicate any appreciable reaction. This again confirms the minute amount of Ca in these pellets.

Table 5.2 Results of Quantitative Chemical Composition Testing Procedures

Experimental Parameters			%CaO		
Sample Description	**Ca/Ti**	**Max Heating Temp**	**Exp.**	**Theor.**	**%Error**
Mod. Chem. Powder 1	1	430°C	9.0%	0.0%	9.0%
Mod. Chem. Powder 1	1	430°C	8.7%	0.0%	8.7%
Mod. Chem. Powder 2	2	1000C	45.4%	50.0%	9.2%
Mod. Chem. Powder 2	2	430C	25.5%	50.0%	49.1%
Mod. Chem. Powder 2	2	unheated	30.7%	50.0%	38.6%
Mod. Chem. Powder 3	2	1000C	47.1%	50.0%	5.8%
Mod. Chem. Powder 4	3	1000C	58.7%	66.7%	12.0%
Original Chem. Powder 1	~0	900C	0.6%	0.0%	0.6%
Original Chem. Powder 2	~0	1000C	0.3%	0.0%	0.3%
Pure CaO	N/A	none	98.3%	100.0%	1.7%
Pure CaO	N/A	none	98.0%	100.0%	2.0%
Pure CaTiO3	1	none	3.3%	0.0%	3.3%

The ratios of calcium to titanium in the chemical formulation were varied to determine its affect on the strength, composition, macroporosity and microporosity. Both the macroporosity and microporosity decreased with an increase in the calcium to titanium ratio. These pore volumes are compared to those reported by Sakurai et al. (1995) in Figure 5.8. In order to have a direct comparison the pore volume was normalized by the volume of the respective pellets. Spheres of 5mm diameter were used

for Sakurai et al. because that was recorded in their papers and cylinders of 3/16" diameter and 5/16" length were used for this work. Note that the microporosity in the new pellets is greater than those reported by Sakurai et al. The macroporosity for the new pellets however is less. This is a little misleading in that much of the porosity recorded in the micropores was very close to the transition between micro and macro pores at 0.1 to 0.2 microns. This can be seen in the differential and cumulative distributions for these ratios in Appendix F, Figure F.1. These pores can be manipulated by changing some of the procedural parameters to yield more macropores. Graphite which was not introduced in our pellets will also help to increase the porosity in the macropore region and micropore region.

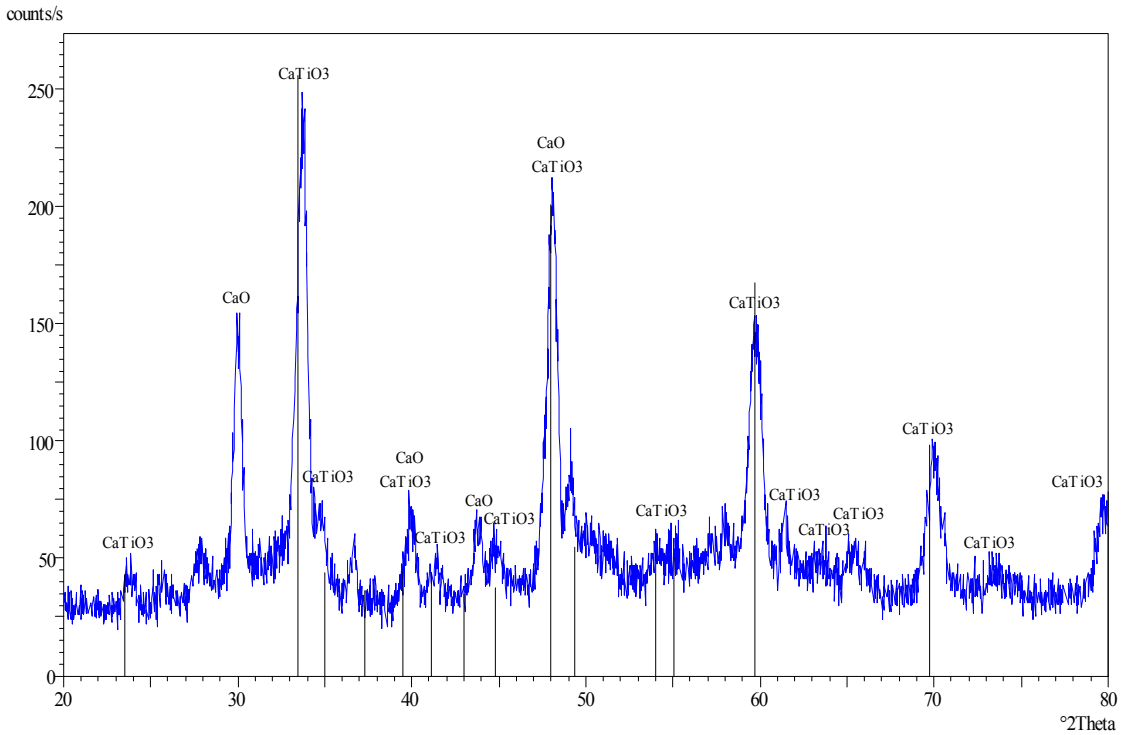

Figure 5.7 X-ray Diffraction Data with Peaks Verifying the Presence of Both Calcium Oxide and Calcium Titanate

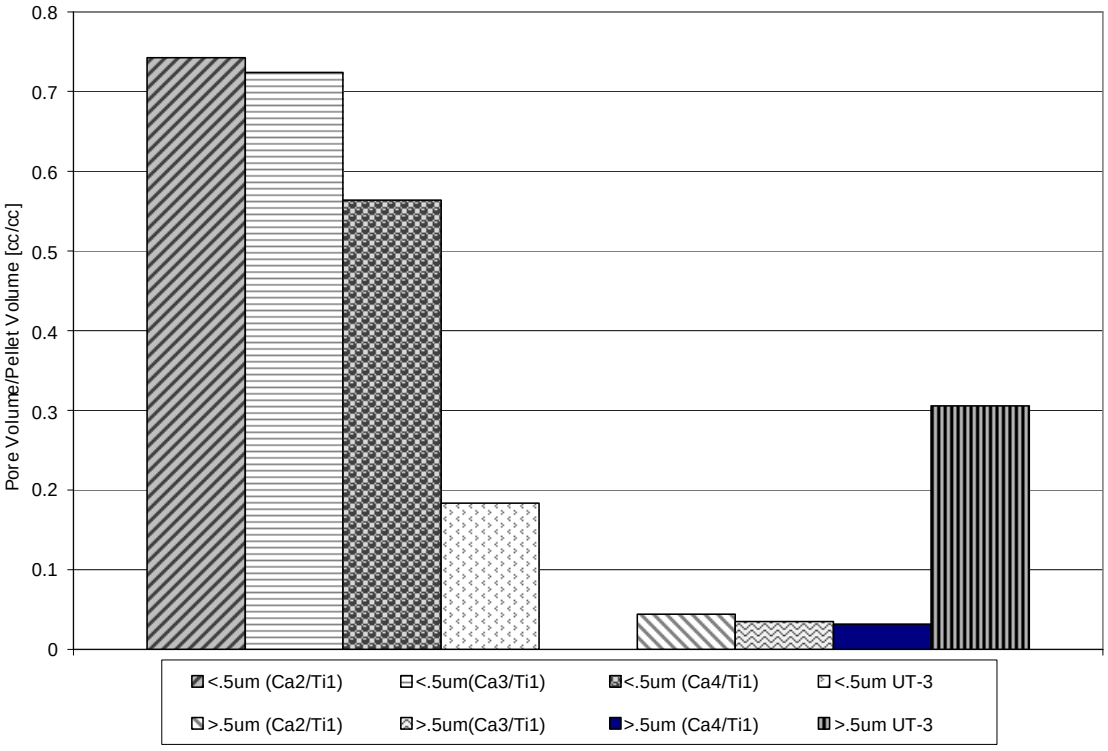

Figure 5.8 Comparison of Micropore and Macropore Volume of Pellets Made with Ratios of Different Calcium to Titanium Ratios with UT-3 (Sakurai et al., 1995) Porosity Results

The strength of the pellets generally decreased with an increase in the calcium to titanium ratio. The pellets seemed to be more fragile and had more cracks for a ratio of 3 and 4 (Ca:Ti, molar). This was expected because a greater ratio decreases the percentage of titanium which is the element which forms the substrate structure. When the percent of titanium is decreased it is, therefore, expected that the integrity will also decrease.

Heating Procedures: Composition, Strength, and Porosity

The heating procedures were evaluated based on the characteristics of composition, strength, and macroporosity. A comparison of the porosities can be seen in Figure 5.9 (Enlarged as Figure F.3). The cumulative and differential specific pore volumes are shown. The differential distribution seems to be flatter when 900°C and

1000°C heating temperature were used. This indicates that the pore volume is distributed amongst a greater range of pore sizes. The 800°C heated pellets had a much narrower pore volume distribution. The pore volume was highest in 800°C heated pellet. However, the maximum difference in the cumulative pore volume, is only about 0.05 cc/g between the 800°C and 900°C heated pellets. These pellets used a 2 to 1 ratio between calcium and titanium and were compressed into pellets using a 0.25 metric tons force. All the pellets were also preheated at 430°C.

The 900°C and 1000°C pellets were actually weaker than the 800°C pellet in this case. The reason for this is believed to be $Ca(OH)_2$ and/or $CaCO_3$ dissociating at their dissociating temperatures of 580°C and 898°C respectively.. Two slight modifications to the heating process were made.

1. The preheat temperature was raised to 600°C to eliminate any calcium hydroxide that might be in the pellet.
2. The ramp time from 700°C to the maximum sintering temperature was extended to 2 hours to slow the formation and escape of carbon dioxide as calcium carbonate dissociates.

The pellets made using these modifications seemed to be just as strong if not stronger than the 800°C heated pellets. The composition of the pellets was quantitatively measured using chemistry by the procedure outlined at the end of chapter 4. Table 5.2 Shows values for different ratios and heating schemes

Optimum Parameters

There are many parameters which can effect the characteristics of the pellets. The most important characteristics—reactivity and degradation—have yet to be studied. What may seem the optimum based on the characteristics of strength, porosity, and composition may not even last one cycle in a reactor. Even with just the characteristics

explored in this work it is difficult to weight each characteristic as they are interdependent. With these considerations Table 5.3 presents what are thought to be the optimum of the varied parameters based on the data collected.

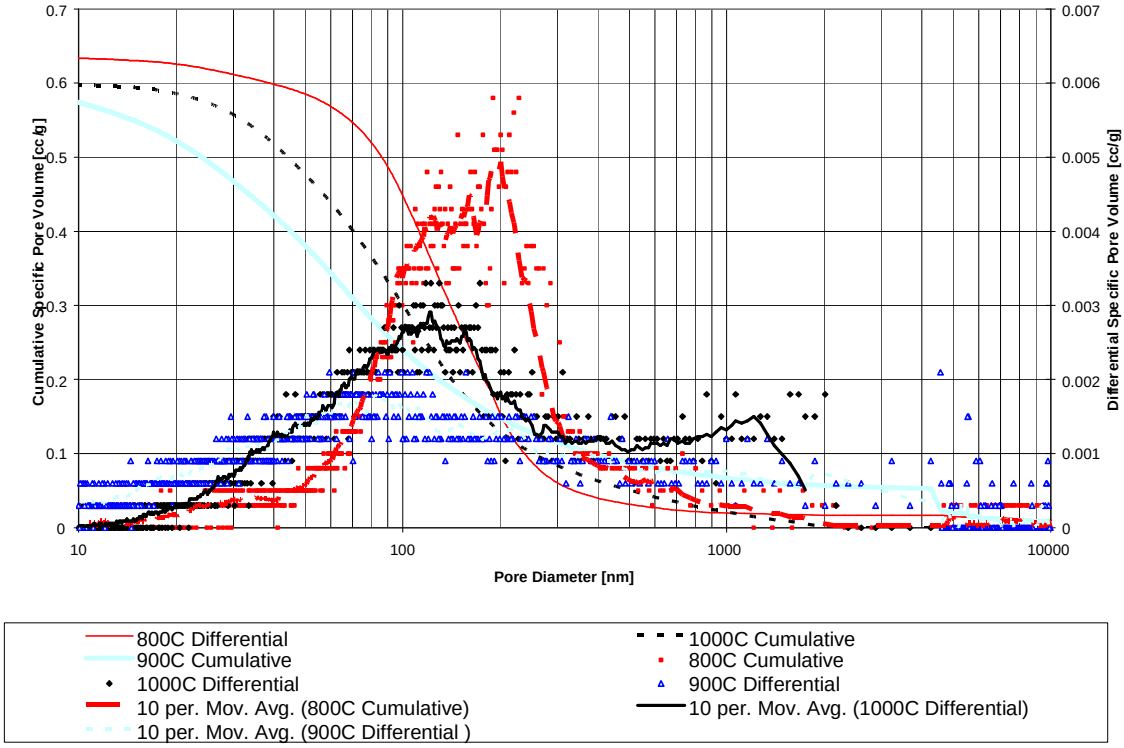

Figure 5.9 Comparison of Cumulative and Differential Specific Pore Volume Distribution for New Pellets Sintered at Different Temperatures.

Table 5.3 Optimum Parameters

Use Modified Chemistry Scheme	2Ca:1Ti
Precursor Preheating Temp.	600C
Molding Compression Force	0.25 MT
Sintering Temperature	900C
Slow Temp. Ramping Scheme	2hrs

The modified chemistry is used to create the pellets. A 2 to1 ratio between calcium and titanium was chosen. This was in large part to ensure that adequate $CaTiO_3$ network is generated to make the pellets structure strong to endure the reactor environment. The preheating temperature was to eliminate volatiles that may affect the

strength when the pellet is heat treated. The compression force was picked because it is thought that it would help the porosity and give an acceptable strength. The 900°C sintering was chosen because it strengthens the pellet but does not decrease the porosity greatly. It is also thought that this would dissociate any $CaCO_3$ so that the CaO content would be increased.

This work has focused on cylindrical pellets, though there are many different shapes and sizes of pellets that are used in industry. The question has been raised, "Can these characteristics be maintained if a different pellet shape or size is used?" This question can not be answered simply. Some characteristics will always be maintained while others will vary slightly depending on the pellet making procedure. The composition for example will always remain the same if the same chemistry and heating procedures are used. The strength and porosity, however, may change in different pellet shapes and sizes. The consolidation force used to compress the pellets will greatly affect the macroporosity and the strength as shown earlier in this chapter. The shape could also contribute to the macroporosity. Generally, macropores are found closer to the surface of the pellets. This means that the shapes with a larger surface area to volume ratio you would expect to have greater macroporosity per unit volume. The size of the pellet also makes a difference in the porosity. Pore clogging and sintering occur in the pellets because of the procedural steps. Because of this less pores are accessible further into the pellet. Thus, if pellets with the same surface area to volume ratios and different volumes are compared the one with the smaller volume will yield a higher specific pore volume. The strength of the pellets obviously can depend on shape. For instance an annular pellet will probably not be as strong as a cylindrical one. There are many established

techniques for creating these pellets and the only true way to see the effect of a new shape and/or molding procedure on the characteristics is to study them.

CHAPTER 6
RECOMMENDATIONS FOR FUTURE WORK

Teo et al. (2005) encourage those studying the UT-3 thermochemical cycle and other thermochemical cycles to examine whether it is worth investigation. Their analysis suggests a much lower efficiency than reported by the original UT-3 researchers. Based on this analysis it seems research effort should possibly be focused elsewhere.

Though, this view is held by some in the research community, there may yet be some potential for the UT-3 thermochemical cycle. The main limiting factor on the efficiency of the cycle are the high operating temperatures at which the reactions take place. Improving the chemistry of the system using some sort of catalyst may be a necessary step to make the UT-3 thermochemical cycle practical. A catalyst that would lower the activation energy of the reactions should be sought. Assuming such a catalyst exists, this may improve the thermodynamics of the system enough to warrant a closer look at the feasibility of the UT-3 thermochemical cycle.

Much work can be done on the UT-3 thermochemical cycle in addition to finding a catalyst. The scope of the suggested future work will focus on the development of the CaO pellets and the reactions that occur in them. Much other work can be done in the areas mentioned in chapter 1 in the history of the UT-3 thermochemical cycle section.

The subsequent work should finish characterizing the calcium oxide pellets. The reactivity, degradation, and cyclic strength should be investigated through the bromination reaction. The parameters of the pellet production procedure may have to be modified in order to obtain desired characteristics. After the pellets have been studied on

an individual basis with satisfactory results a procedure to mold the pellets in a more sophisticated manner should be developed. The procedure and equipment should allow for mass production of pellets quickly so that enough for a small fixed bed reactor can be made. A large number of pellets should be made and placed together in a fixed bed reactor to determine how the pellets will perform.

Short Term Plan

Investigation into Reactivity

One of the most important characteristics is the reactivity. The reaction rates and conversion of the two calcium based reactions should be determined through experimentation and compared to those reported in the literature. These should both be studied and an investigation of methods to increase conversion or reaction rates should be done. Reactivity should be measured and correlated to different operating parameters including temperature, pressure, gaseous reactant concentration, and flow rate.

Reaction rates

The limiting reaction rate should be determined. The rate found should be compared to that in the literature. The pellet production procedure may need to be modified to increase the reaction rates. Creative strategies to improve the kinetic rates should be explored. It should be determined if the diffusion to and from the internal surface of the pellet or the surface reaction itself is the limiting step in the reaction. If it is, modifications in the pellets should be made that will improve diffusion. The shape and size of the pellets could be changed to decrease the thickness which the gaseous reactants and products have to diffuse. Increasing the macroporosity will also help with diffusion rates. Increasing microporosity to increase the amount of available reaction sites could also help the reaction kinetics. If the limiting rate is the surface reaction only

a few things can be done. Concentration of reactants should be increased in the pellets even if a slight compromise in porosity is sacrificed. Little modification to the pellet can be done beyond this.

If there is no limiting step but rather the limit is a combination of surface reaction and diffusion, the optimum characteristics should be found. It may be beneficial to first make the pellets porous enough to eliminate the diffusion part of the limit. If successful the reactant percent should be increased until it starts affecting diffusion significantly. In this way the reaction rates can be increased.

Conversion

Conversion is also affected by composition and porosity. Porosity allows for more sites for reactions and more availability to the reactant. This results in a greater conversion. A higher concentration of the solid reactant can also increase the gas phase conversion if not the conversion within the pellet.

Investigation of Degradation

The performance of the pellets should be investigated over a number of cycles to see if the reactivity degrades from one cycle to the next. This is very important due to the cyclic nature of the UT-3 thermochemical process. If a pellet only has a 1% conversion after five cycles it will not be practical for the UT-3 cycle. These pellets need to have a relatively constant cyclic reactivity in order to make the process viable. The two main causes of degradation are reduction in structural strength with each cycle and sintering of particles. Both of these processes either clog or collapse pores reducing pore area to which the gaseous reactants can access. This ultimately reduces reactivity over a number of cycles.

Investigation of Cyclic Strength

Another characteristic that could be quantified is the structural strength of the pellet. This should be quantified before and after a set of cycles to determine how the strength varies with the number of cycles. The porosity can be drastically reduced if the pellets do not maintain their structure.

Creative Engineering

The pellets may be improved upon with some creative engineering. As mentioned above shape and size of the pellets can be modified. Also different chemistry can be employed to yield better characteristics. A thin surface coating of titania may be added to increase structural strength. These are just a few of number of strategies that can be taken. If the pellets do not have acceptable characteristics other portions of the research may not be worthwhile.

Long Term Plan

Mass Production of Pellets

In order to study the pellets in a fixed bed reactor a large number of pellets have to be made. The present procedure is slow and unsophisticated. Once acquainted with the procedure the process takes approximate 5 minutes per pellet after the powder has been made. The pellets often are not uniform shape and sometimes break. For a fixed bed reactor with and inside diameter of 4cm and a desired height of 10 cm, approximately 460 pellets would be needed if the packing order was only 50%. This would take approximately 39 hours to make the pellets. Obviously, a more sophisticated procedure is necessary to study the pellets in a reactor.

Pellet Performance in a Fixed Bed Reactor

Once the pellets are found to have acceptable characteristics a large number of pellets should be produced and tested in a small fixed bed reactor to investigate the system performance. Studies should be done to evaluate the bulk characteristics of the pellets. Reactivity, conversion and degradation are the characteristics on which analysis should be based. The ideal operating parameters should be found including temperature, pressure, gaseous reactant concentration, and flow rate. Correlations should be found between reactivity and operating parameters.

CHAPTER 7
SUMMARY AND CONCLUSIONS

A procedure was developed for production of the calcium oxide solid reactants for the UT-3 thermochemical cycle. The procedure developed includes methods of chemical formulation, drying, molding, and heat treatment. The chemical procedures have been changed significantly in order to obtain the correct composition of the precursors. Preheating procedures were added to the drying procedures to eliminate volatiles breaking the pellets formed with the precursors. A mold for the molding procedure was fabricated, tested, and redesigned to produce a dependable tool to produce pellets. A reliable molding procedure was developed to make the pellets. A heating scheme was created to strengthen the pellets using temperatures above the maximum operating temperatures of the reactions of 760°C.

Analytical techniques were used to assess this procedure by measuring the porosity and composition of the pellets. Porosity measurement tools that were used are nitrogen adsorption and mercury porosimetry. Composition tools include X-ray diffraction, Raman Spectroscopy, and chemical tests. Strength was also evaluated quantitatively. Correlations between the parameters and the characteristics of composition, porosity, and strength were used to determine the optimum parameters for the procedure.

The suggested optimum parameters are as follows:

1. Use the modified chemistry with a 2 to 1 calcium to titanium ratio

2. Use a preheating temperature of 600°C.

3. Use a molding compression force of 0.25 metric tons

4. Sinter the pellets at 900°C using the slow temperature ramping scheme.

These parameters may change significantly based on further characterization of the reactivity and degradation of the pellets in the reactor environment.

Further studies are necessary to realize the potential of the UT-3 thermochemical cycle. These studies should include further characterization of the calcium oxide pellets, a search for a catalyst for the reactions, mass scale production of pellets, and bulk characterization of the pellets in a fixed bed reactor.

APPENDIX A
CHEMICAL PROPERTIES

Table A.1 Chemical Properties of Various Solid and Liquids Used in This Project

Chemical Name	Chemical	Color	BP/MP	Density	MW
SOLIDS					
Calcium Metal	Ca	Black/Gray	840C	1.6	40.08
Calcium Bromide	CaBr2	White	806C	1.7	199.9
Calcium Carbonate	CaCO3	White	898C**	2.8	100
Calcium Oxide	CaO	White	4658C	3.3	56
Calcium Hydroxide	Ca(OH)2	White	580C**	2.24	74
Calcium Titanate	CaTiO3	Light Brown	1975C	4.1	136
Titanium Oxide-anatase	α-TiO2	White	1855C	3.8	80
Titanium Oxide-rutile	TiO2	White	3000C	4.2	80
LIQUIDS/VOLATILES					
Ethanol	C2H5OH	colorless	79C	0.8	46
Dionized Water	H2O	colorless	100C	1	18
Titanium Isopropoxide	Ti (C3H7O)4	colorless	232C	0.962	284
Bromide	Br2	dark brown	59C	3.11	160
Hydrobromic Acid	HBr	dark orange	-66.8C		80.912

APPENDIX B
RAMAN SPECTROMETER

A Nicolet Magna 760 Bench with Spectra Tech Continuum IR Microscrope and FT Raman module was used. Below is a picture of the module. The Raman Spectra were taken with a laser intensity of 1.06mW and a gain of 4. Powders of each pellet type were pushed into melting point capillary tubes and a fastening piece designed to hold them was used.

Figure B.1 FT Raman Module

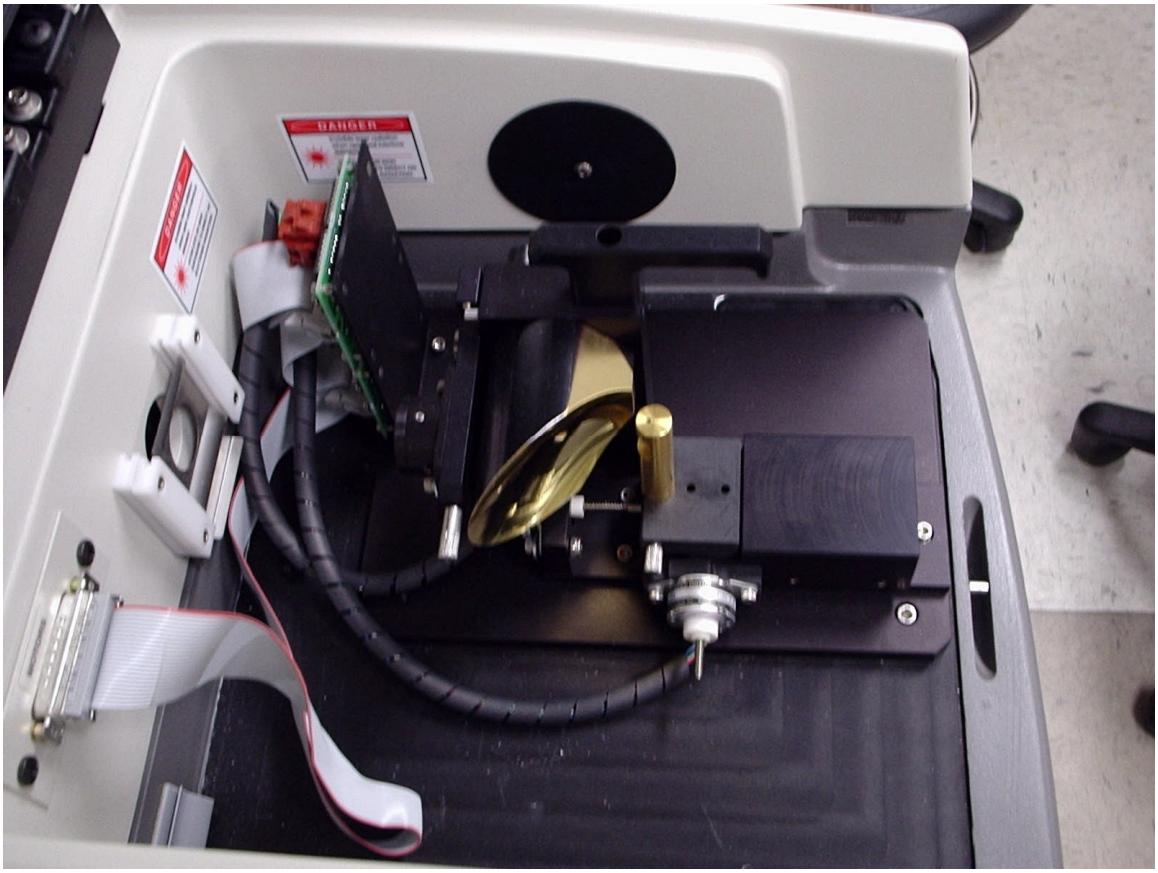

Figure B.1 Inside of FT Raman Module

APPENDIX C
PELLET MAKING PROCEDURES

Original Chemistry

1. Weigh X grams of Calcium
2. Measure Y mL of Ethanol
3. Put both ethanol and calcium in large beaker along with a magnetic stir rod.
4. Cover the solution with plastic using rubber bands to securely fasten
5. Put mixture on a magnetic stirrer and stir for 10 days
6. After 10 days the mixture should be a white cloudy mixture (if more time is needed stir longer). If possible let all the Ca metal react (black pieces)
7. Measure Y*18/40 mL of titanium isopropoxide and add to mixture, stir 5 min
8. Measure Y*12/40 mL of dionized water and add to mixture, stir 5 min
9. Pour contents of beaker into a container or containers with large surface area to dry overnight (preferably ~1" in height or less)
10. Leave fume hood fan on overnight

Modified Chemistry

1. Clean and Dry flask, condenser, and other equipment.
    a. Wipe petroleum jelly out with a paper towel with acetone on it.
    b. Wash with water and brushing out using a brush.
    c. Wash out with dionized water after a thorough rinse.
    d. About every 10 runs an acid bath cleaning should be done to dissolve and residue from the side of the flask.

2. The calcium sample is measured on the electronic scale and then dropped into the flask through the outlet with the nitrogen and thermometer.

3. Joints to condenser and adaptor are coated with a thin layer of petroleum jelly to prevent seizing. Then the joints and stopper are put in place. (MAKE SURE TO COVER ALL RUBBER, OR DO NOT US IT AS IT AFFECTS THE CHEMISTRY)

4. The nitrogen valves are opened to allow a very small flow to the flask.

5. Water to the condenser is turned on. (or condenser is filled with water)

6. Wait 5 minutes for nitrogen to purge system.

7. Anhydronous ethanol is extracted by syringe from its container and discharged into the system through the silicon septa.

8. The heater is turned on to raise the temperature of the mixture to between 72°C and 76°C. A noticeable reaction occurs in this temperature range.

9. An equilibrium point is found so that the temperature and the nitrogen settings are such that the temperature remains 72°C-76°C.

10. The mixture is diluted using the same amount of anhydronous ethanol as in step 5.

11. Titanium isopropoxide is extracted from its container via syringe. The correct proportion is injected into the flask again through a new hole in the septa.

12. The mixture is heated between 72°C and 76°C for 30 minutes (1hour).

13. A solution of ethanol and dionized water is made in a beaker.

14. A syringe is used to insert the water ethanol solution into the flask in order to maintain an oxygen free environment. A reaction occurs immediately causing most of the mixture to turn white in color.

15. The liquor was heated for 1 hour and then poured into a petri dish.

Table C.1 Chemical Ratios Used in Modified Chemistry

Step #	Chemical	Ammount	Molar Ratio (to Ca)
2	Calcium	.6 grams	1
7	Anhydronous ethanol	30mL	35
10	Anhydronous ethanol	0-10mL	0-12
11	Titanium Isopropoxide	2.2/1.5/1.1 mL	1/2 or 1/3 or 1/4
14	20% Water in Ethanol Sol.	1.8 in 7.2 mL	6.7 in 6.2

Drying and Preheating

16. The liquor was left for 18 to 20 hours under an exhausting fume hood to dry by evaporation. The powder was mostly dry but had noticeable moisture.

17. Place some of the powder into hanging crucible and put it in furnace

18. Set furnace temperature to 430°C for 1 hour (This removes any volatiles that may be present)

19. Take hanging crucible out of furnace using clamp (BE CAREFUL VERY HOT)

20. Place hanging crucible on aluminum plate to cool for 5 minutes

21. Dump contents of crucible into a Petri dish

22. (Start other heating procedures if necessary)

23. Molding

24. Take base mold and put it on steel plate on the counter

25. Take a small amount of powder from the petri dish and put it in the base mold hole.

26. Compact the powder using a plunger by hand. (Add cap to plunger and compress)

27. Add more powder

28. Repeat steps 20 and 21 until bottom of plunger with cap just barely penetrates into the mold

29. Properly align steel plate, base mold, plunger, and cap and place on the hydraulic press platform

30. Pump press until resistance is felt.

31. Watch force meter and continue to pump until desired force. (recommend ~.25 MT for new chemistry)

32. Watch the force meter and hold the force at desired force for 1 minute by slight increase in force as powder slowly compacts (Be careful not to over load the plunger as it will yield the plunger and the base mold)

33. Take off assembled mold and separate both cap and plunger and mold (may need pliers, but should not be difficult with pliers)

34. Insert longer plunger into cap and assemble with base mold

35. Flip the assembly so that the cap is on the bottom.

36. Place the hollow cylinder on top so its hole is concentric with the hole in the base mold.

37. Place the assembly on the hydraulic press so that the hollow cylinder is concentric with both the hole in the base mold and the rings on the top plate of the hydraulic press.

38. Slowly pump the press so that the pellet is pushed into the hollow cylinder on the top of the mold.

39. Carefully remove the assembly and take the hollow cylinder off vertically.

40. You should have a solid pellet with a height about half of the base mold

41. Heating Procedures

42. A program for the furnace was made (consult ATS Furnace Controller for procedure)

    a. Tune-Last-Yes→ Tune Mode

    b. Parameter Check multiple times until "Ramp and Soak" is selected

    c. Yes→ Program parameters using arrow keys up and down use parameter check to go to next parameter

    d. Select 1 cycle and hit NO when "assured soak" is displayed

    e. "End Tune" should appear. Hit TUNE/Return and the program is saved.

    f. Press START to start the program

43. Pellets were place in the quartz crucible on the quartz hanger.

44. The quartz hanger was place into the furnace.

45. The furnace program was set to run.

46. The pellets are carefully taken out of the furnace after the run is complete.

47. The pellets were weighed using the electronic scale

48. The pellets were put in petri dishes which were labeled.

APPENDIX D
PELLET CHARACTERIZATION PROCEDURES

Nitrogen Adsorption

Outgassing Procedure

49. Place the large sample cell on scale and tare scale

50. Put pellets in sample cell and place on scale

51. Record mass of pellets

52. Take sample cell with pellets inside to Quantachrome NOVA 1200 machine

53. Make sure no one is running a sample in the analysis station

54. Use key pad to load outgasser

    a. Press 3 for out gas stations

    b. Press 1 for load outgasser

    c. Press 1 for vacuum outgas

    d. The machine will pressurize the system and then you will be instructed to put sample cell on the outgas station

55. Unscrew and take off the plug and o-ring screw assembly

56. Put plug with the other plugs to the side

57. Put heating mantle on cell and then secure with metal clip

58. Put the o-ring screw assembly on the cell

59. Move the whole unit (sample cell, mantle, screw assembly) to the outgas station.

60. Secure assembly by screwing the o-ring screw assembly into the outgas station.

61. Hit any key on the keypad to continue to outgas

62. Turn on the heating mantle and set it to 200°C

63. The sample will be outgased until you manually interrupt it. Generally, the samples were outgassed overnight.

64. Go to the keypad

    a. Press 3 for outgasser

    b. Press 2 for unload outgasser

    c. The system will pressurize and will instruct you to remove the sample cell.

65. Remove the sample cell by unscrewing the o-ring screw assembly

66. Replace the plug in place of the sample cell assembly and repeat step 11 and 12

67. Hit any key on the keypad and the NOVA will evacuate the system

Full Isotherm Analysis Procedure

68. Have NOVA 1200 Disk, Outgassed Sample, and mass of sample ready

69. Put Disk into the disk drive of the NOVA 1200

70. Go to key pad

    a. Press 2 for analyze sample

    b. It will pressurize system and instruct you to place sample on the analysis station

71. Take off plug and o-ring screw assembly

72. Carefully place spacer in the sample cell

73. Secure the sample cell into the analysis station with the o-ring screw assembly

74. Take out the small plug behind the analysis station. This gives the machine a reference for the ambient pressure.

75. Fill the large dewar with liquid nitrogen and rotate the stand do the dewar is under the sample cell

76. Go to key pad

    a. Press any key to continue

b. Name the sample (Enter Date)

c. Enter User ID (enter 1 or whatever number)

d. Input the sample mass and press enter

e. Press 0 to measure the density of the material

f. Enter Cell number (62 or 50 for large cells)

g. Enter Setup (50)

h. Press Enter until Analysis Start

77. Make sure to use the cover with the hole in to cover the dewar

78. The dewar will raise automatically

79. The process will take anywhere from 5-10 hours to complete

80. The analysis will be complete when the dewar is lowered and the system is pressurized

81. The keypad screen will go back to the main menu.

82. At this point follow instruction for removal of the sample and replacement of the plug outlined in 17-18 of the outgassing section

Figure D.1 Quantachrome NOVA 1200 Machine for Nitrogen Adsorption with Small Sample Cell and Dewar

Quantachrome Mercury Porosimeter

Pore Volumes were recorded from approximately 1 psia to 60000 psia.

Filling Apparatus Procedure

1. Have pellets and measured mass ready
2. Turn on vacuum pump
3. Turn on Mercury Porosimeter
4. Fill the mercury trap with liquid nitrogen
5. Put pellets in small sample cell (different from BET cell)
6. Take vacuum grease and put around the edge of the cell
7. Place metal top on cell gently and twist to ensure a good seal
8. Place rubber O-rings on bottom and top of the cell.
9. Put Teflon casing on the cell to seal the container and tighten the O-ring (Hand Tight is sufficient)
10. Unplug the filling apparatus
11. Put Metal sheath on the sample cell. There is an O-ring at the beginning so you have to put a little bit to get it through.
12. Put assembly in the filling apparatus
13. There is a piece to secure assembly. Find this and screw it on the assembly to lock it in place.
14. Attach the alligator clip to the lead on the back of securing piece.
15. Turn the valve to vacuum and slowly open the rate control valve to gradually reduce the pressure in the filling apparatus
16. Change the control knob on the volume to FA (filling apparatus). Also adjust the calibration from 296 to 317.
17. Unplug the cord with to the pressure section. Plug it into the FA.
18. Zero both the pressure and the volume control

19. Check the pressure in the filling apparatus. Adjust the valve to allow for a faster flow rate.

20. After the pressure is less then 50mm of Hg close the rate control valve.

21. Adjust the screw stop on the filling apparatus to allow the chamber of the filling apparatus to angle so that the mercury can be filled up the capillary tube.

22. Switch the flow valve to the vent position

23. Re zero the volume on the mercury porosimeter

24. Slowly open the rate control valve to raise the pressure in the chamber of the filling apparatus while monitoring the zeroed volume.

25. As soon as the volume starts to change close the rate control valve

26. Adjust the chamber of the filling apparatus so that the capillary tube is horizontal and lock it in place using the screw stop

27. Go to the computer

    a. "C:\" Should appear, Type "CD Poro" then hit return

    b. "C:\Poro\" should appear, type "poro2pc" then hit return

    c. This should open a program, hit return

28. Consult Gary Scheifelle for operation of the program

29. Start Data Acquisition on the computer program

30. Slowly increase the pressure by opening the rate control valve

31. On the monitor there should be a plot of the pore volume vs. pressure

32. When the pressure is approximately 14.7 PSIA close the rate control valve

33. Switch the flow control valve to PRESSURE and open the pressure needle valve

34. Slowly open the rate control valve to increase the pressure in the chamber

35. The maximum pressure is about 23 PSIA close the rate control valve at this time.

36. Switch the flow control valve to VENT

37. Slowly open the rate control valve to decrease the pressure in the chamber

38. Once ambient pressure has been reached press the end button on the keyboard to finish the run

39. At this point the assembly can be taken out of the filling apparatus

    a. Hold the end of the filling chamber while unclipping the alligator clip and unscrewing the securing piece.

    b. Slide the cell and metal sheath out of the chamber making sure to always point it up

    c. Plug the chamber

40. Take off the metal sheath.

High Pressure Procedure

41. Fill the top half of a centimeter of the capillary with oil via a syringe, be sure to eliminate any bubbles. This may require you to extract some mercury from the capillary via syringe. Discard this mercury in the clean container if in fact it has not been contaminated with oil.

42. Put the Teflon spacer on the assembly.

43. Put the large metal sheath on the assembly.

44. Place assembly so the oil is up into the high pressure chamber

45. Carefully, lower the top of the high pressure chamber into place

46. Screw the top of the high pressure chamber into place

47. Press and hold the oil fill button and watch the excess oil for bubbles. Wait until there are no bubbles for 15 seconds

48. Switch the pressure connection cord back to its original position

49. Switch the knob on the volume section to HIGH PRESSURE and adjust the calibration to 296.

50. Zero both the pressure and the volume

51. Go to the computer to set the program up

52. Press the start button when directed to do so by the computer program. The machine will run automatically. Just incase of accident, be a safe distance away when the pressure on the machine is at high pressures.

53. Press the end button on the keyboard when the run has ended.

54. Save the data files to report files.

55. Exit program by pressing the escape key multiple times.

56. Once in DOS follow the commands

    a. "C:\Poro\" should appear, type "CD .."

    b. "C:\" should appear, type "CD porodata"

    c. "C:\Porodata" should appear, type "DIR"

    d. This will give you a long list, type "copy SA5####*.* A:"

    e. This will copy the files with the name SA5#### and any ending to the floppy disk drive for which you should have a disk

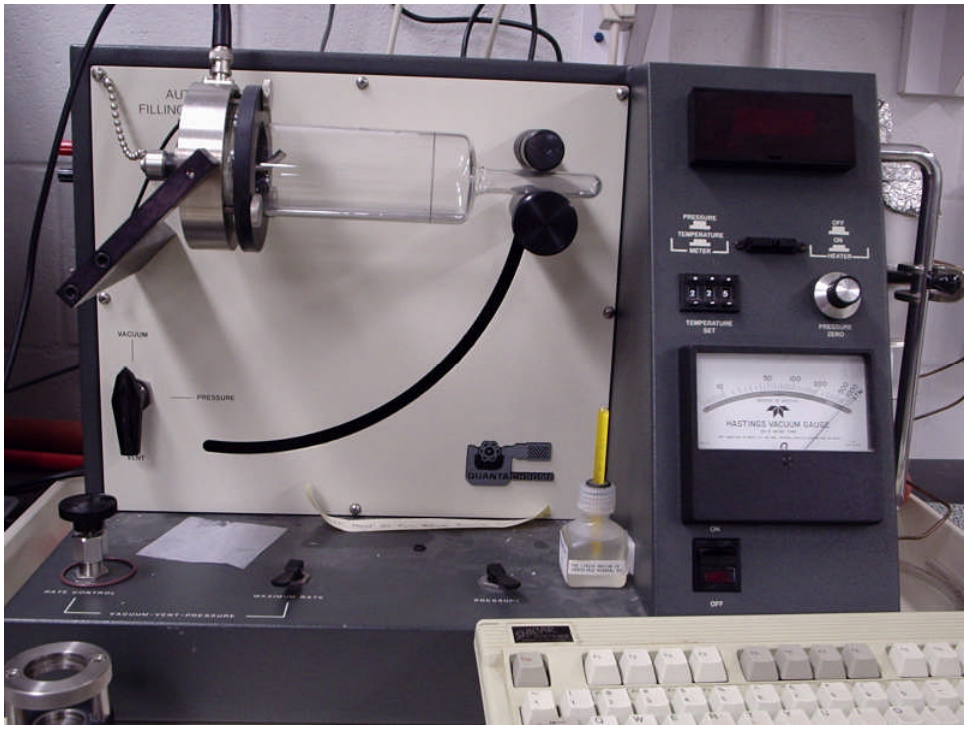

Figure D.3 Quantachrome Mercury Porosimeter Filling Apparatus

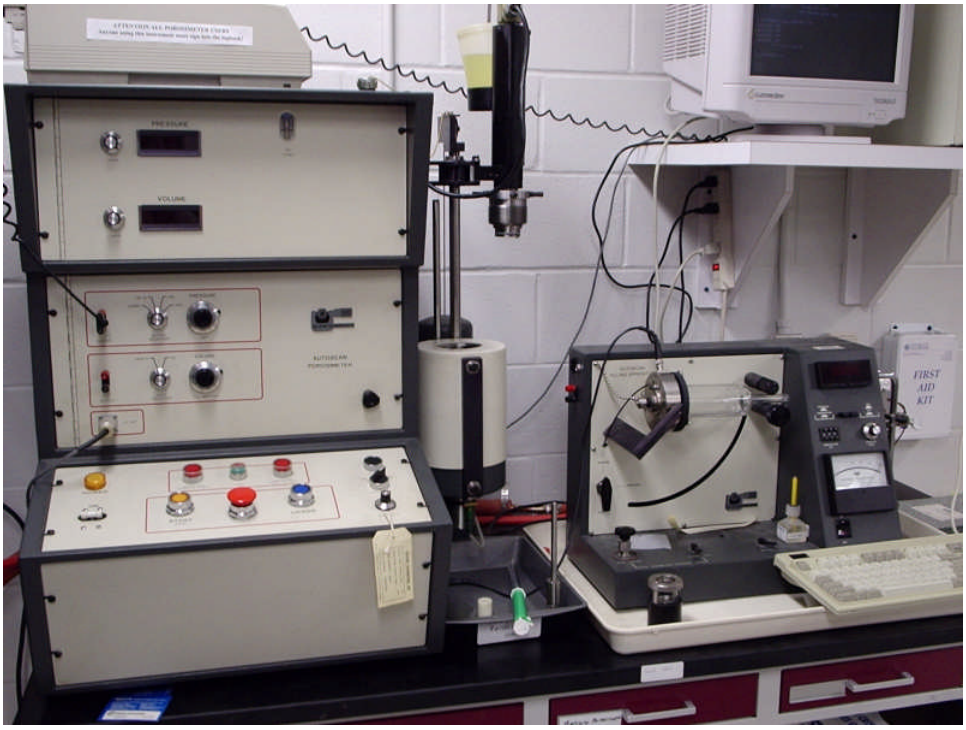

Figure D.2 Quantachrome Mercury Porosimeter

APPENDIX E
RAMAN SPECTRA

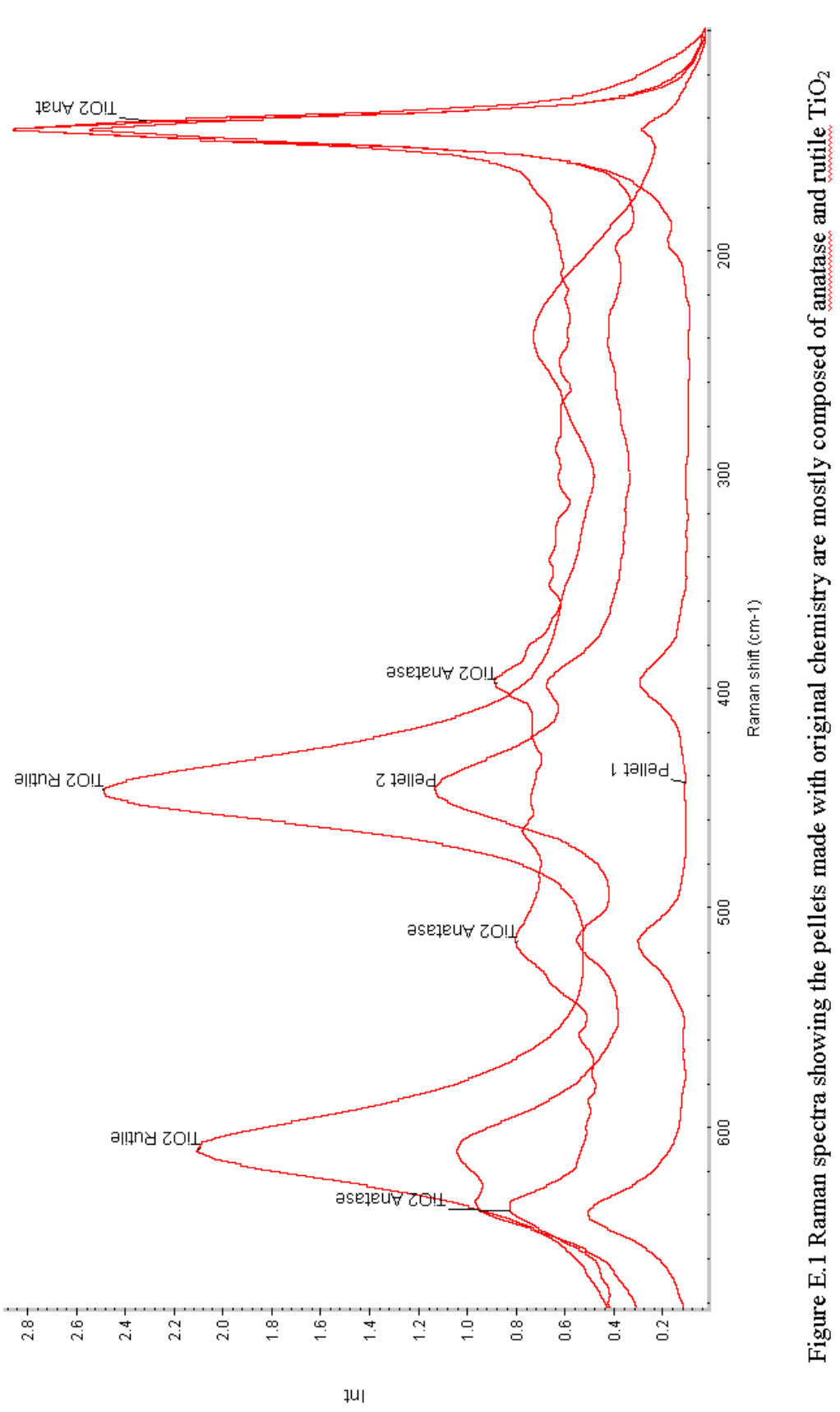

Figure E.1 Raman spectra showing the pellets made with original chemistry are mostly composed of anatase and rutile TiO_2

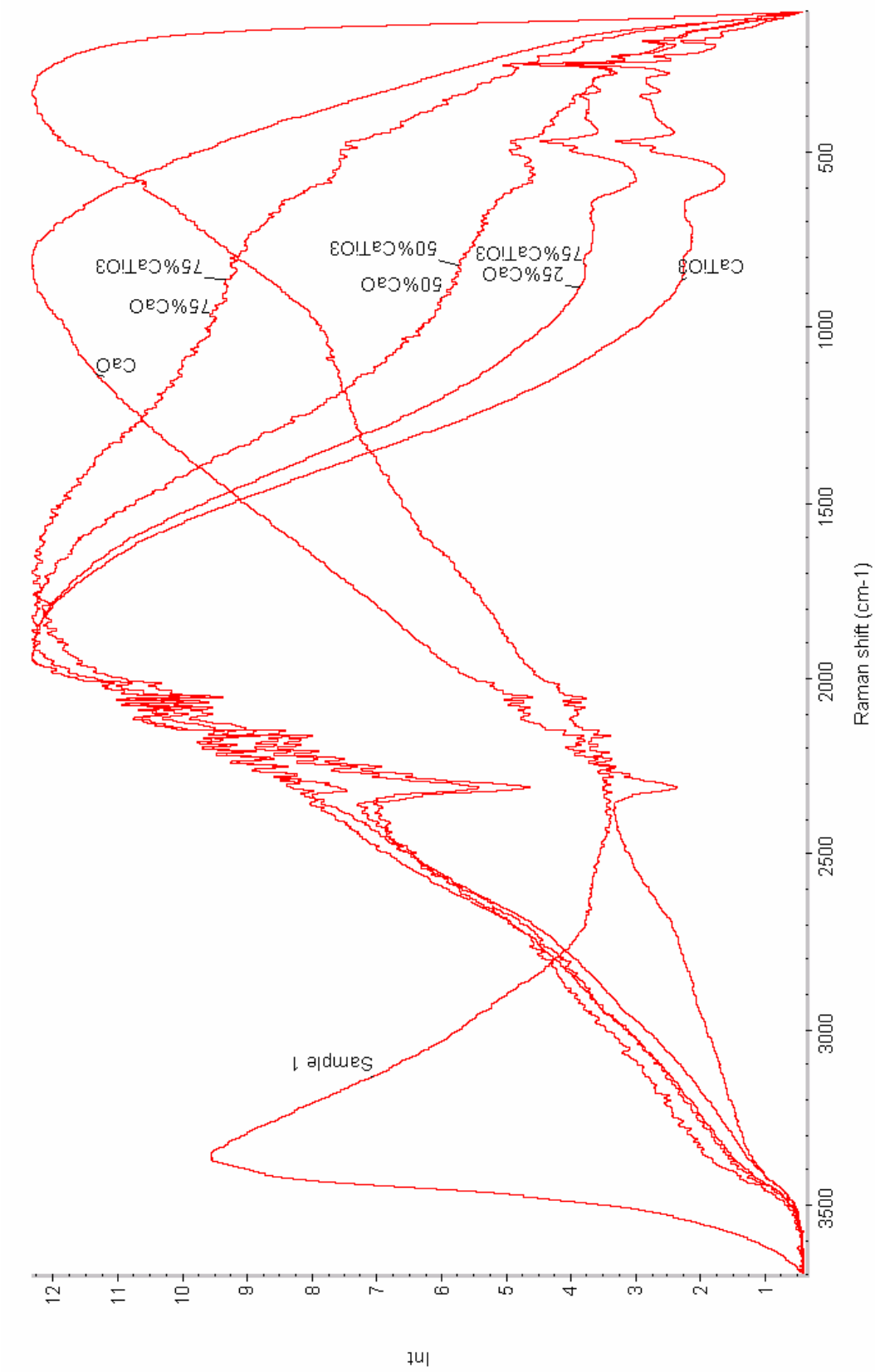

Figure E.2 Raman spectra showing the fluorescence hiding the characteristic peaks of a sample made using the modified chemistry

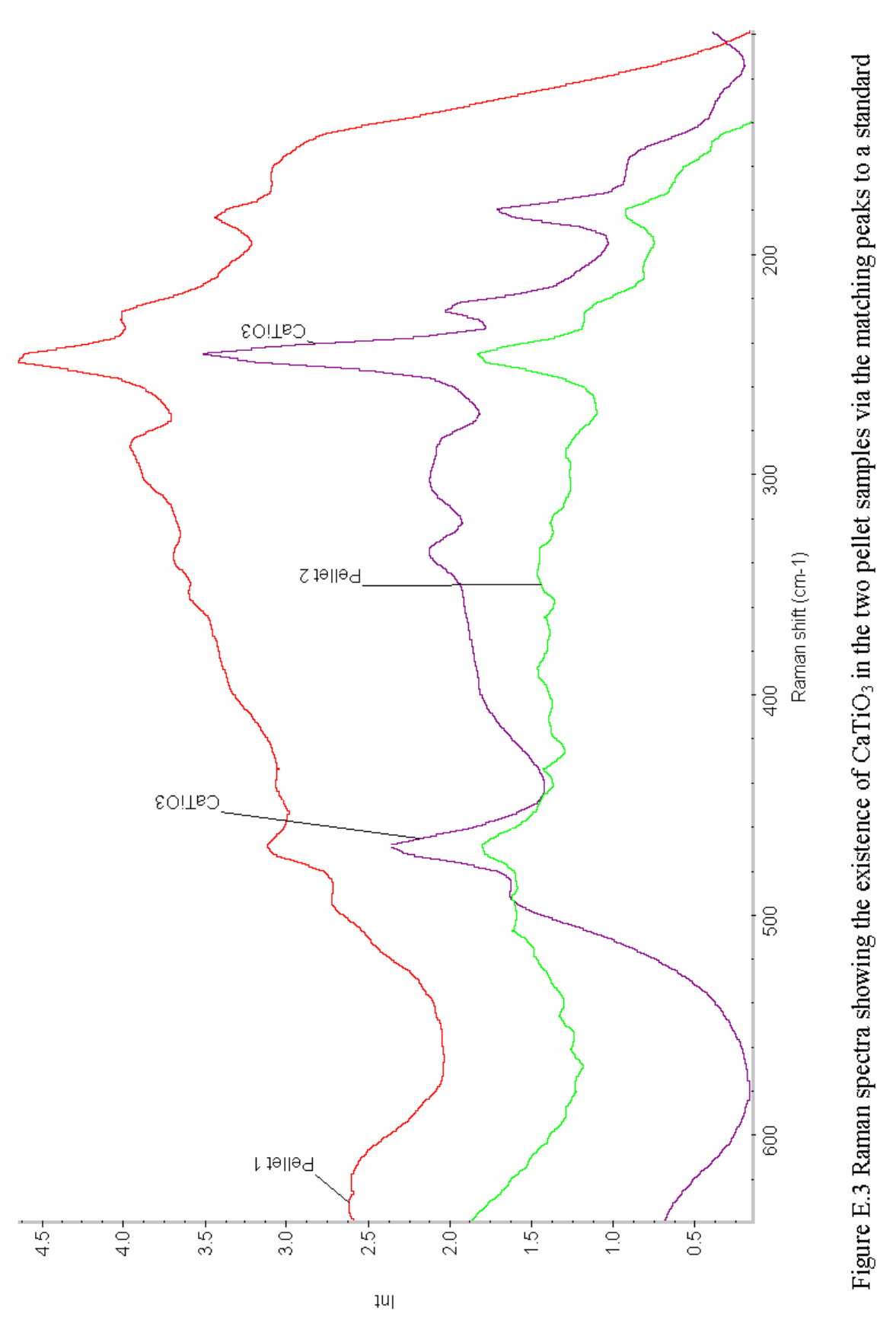

Figure E.3 Raman spectra showing the existence of $CaTiO_3$ in the two pellet samples via the matching peaks to a standard

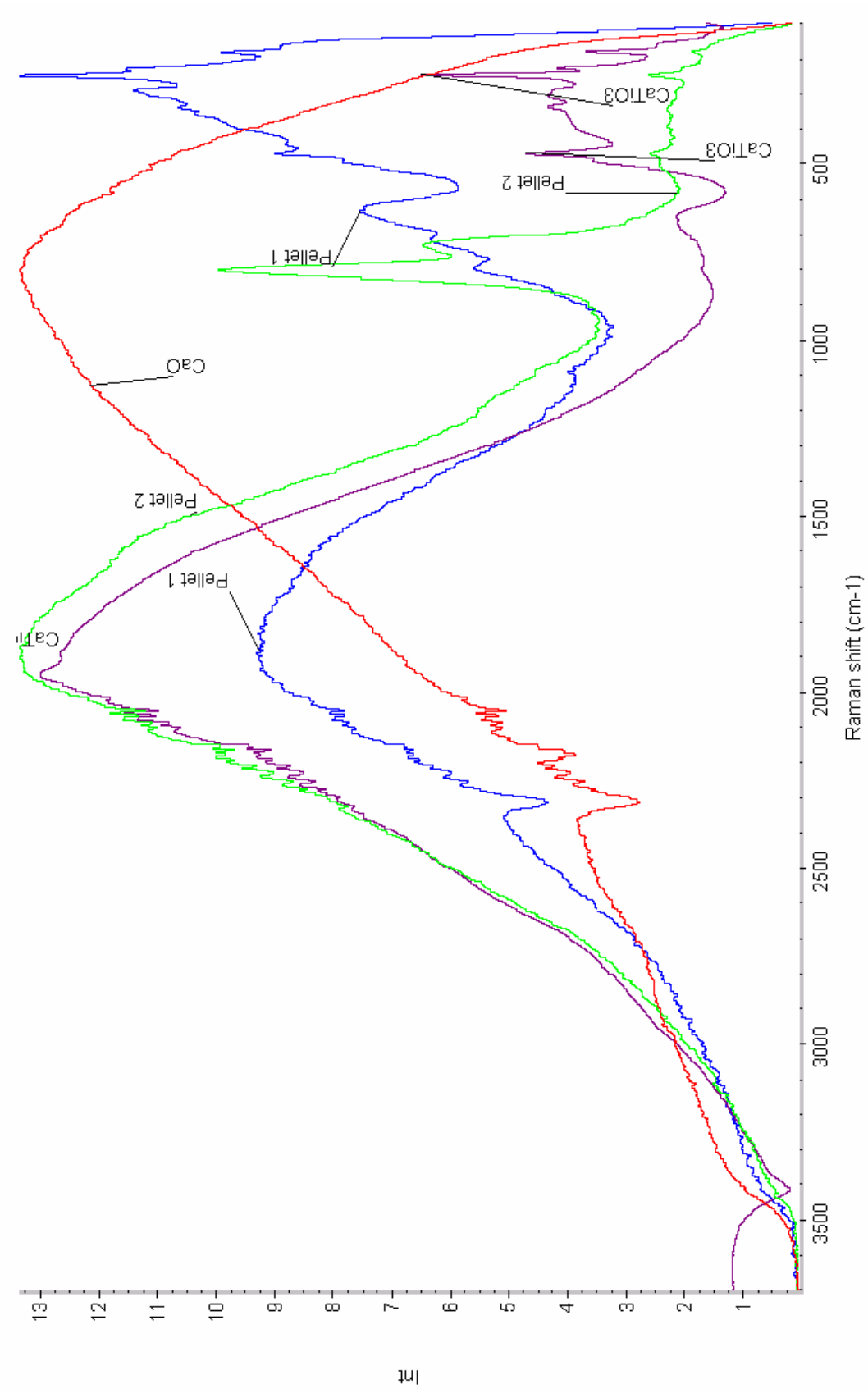

Figure E.4 Full Raman spectra showing the existence of $CaTiO_3$ in the two pellet samples via the matching peaks to a standard

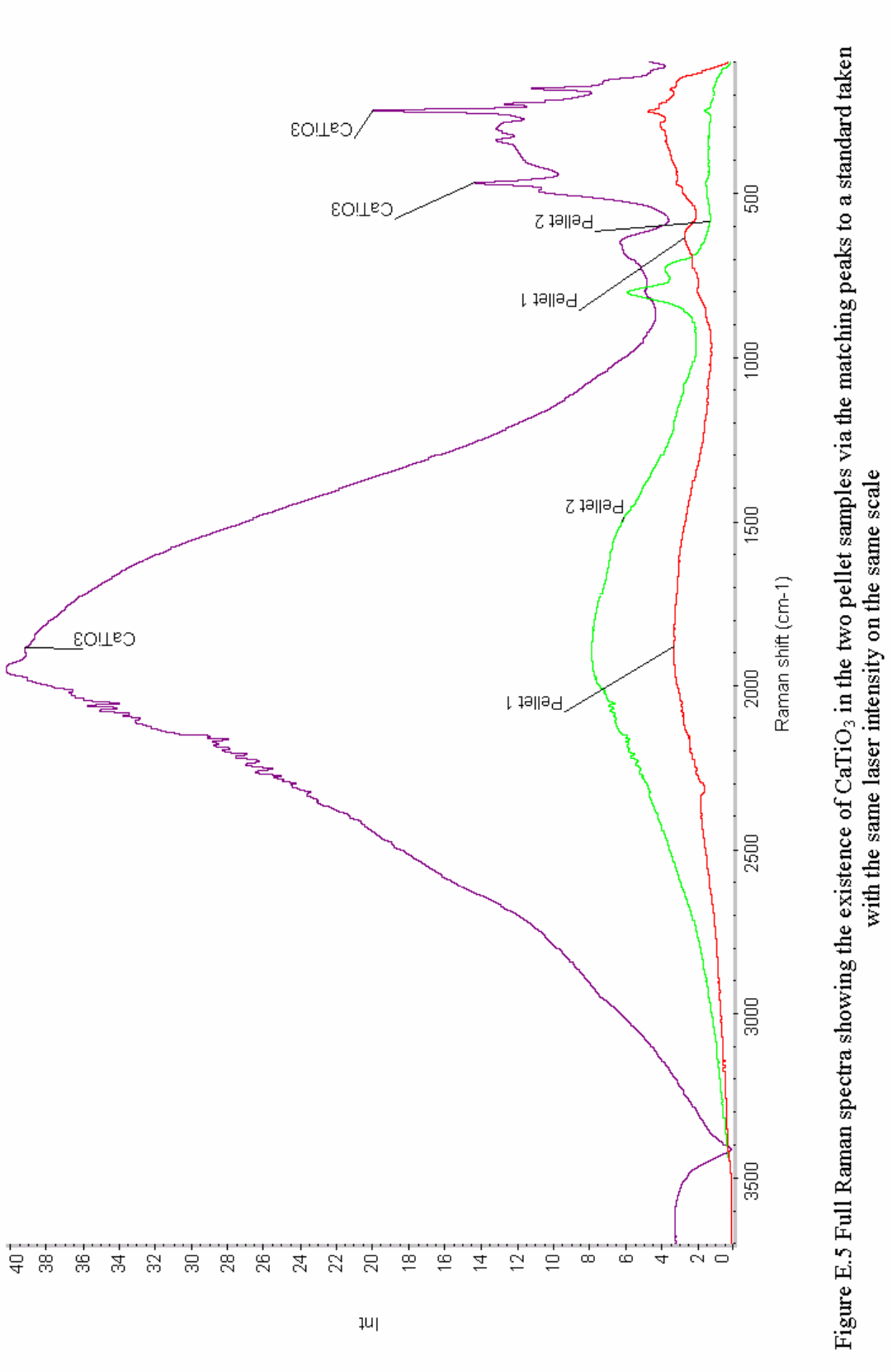

Figure E.5 Full Raman spectra showing the existence of $CaTiO_3$ in the two pellet samples via the matching peaks to a standard taken with the same laser intensity on the same scale

APPENDIX F
MERCURY POROSIMETRY DISTRIBUTIONS

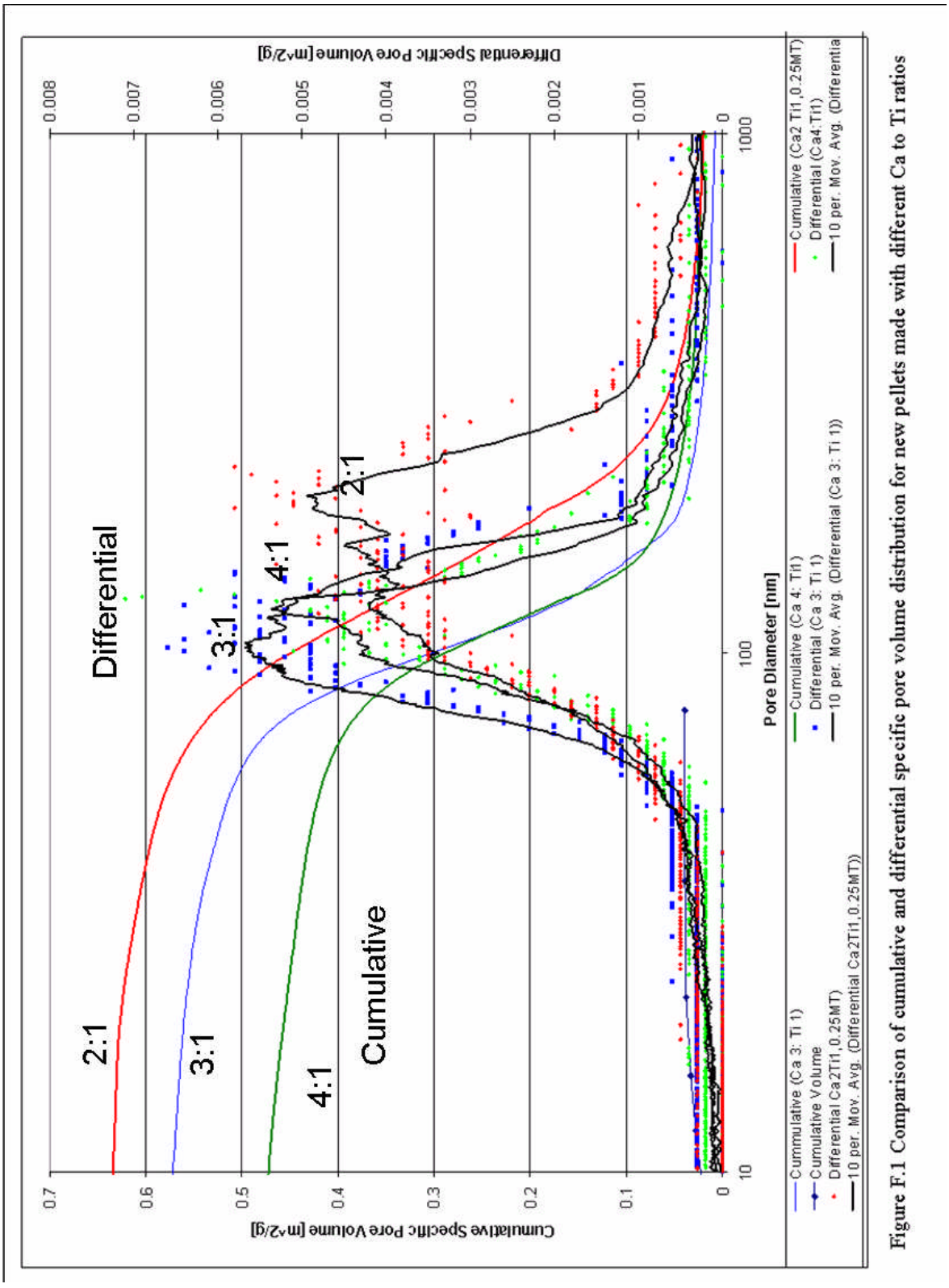

Figure F.1 Comparison of cumulative and differential specific pore volume distribution for new pellets made with different Ca to Ti ratios

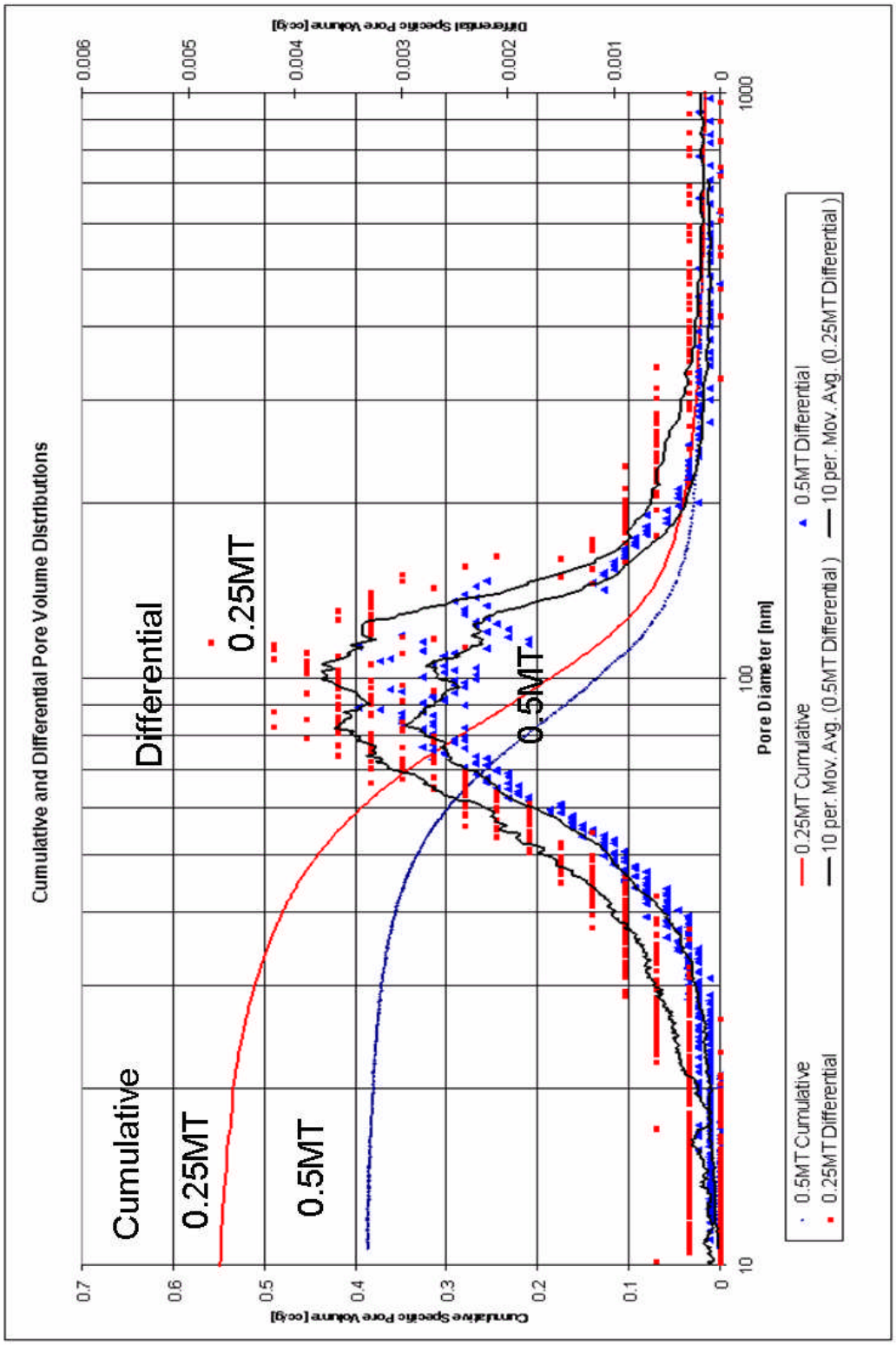

Figure F.2 Comparison of cumulative and differential specific pore volume distribution for new pellets compressed at 0.25 and 0.5 metric tons.

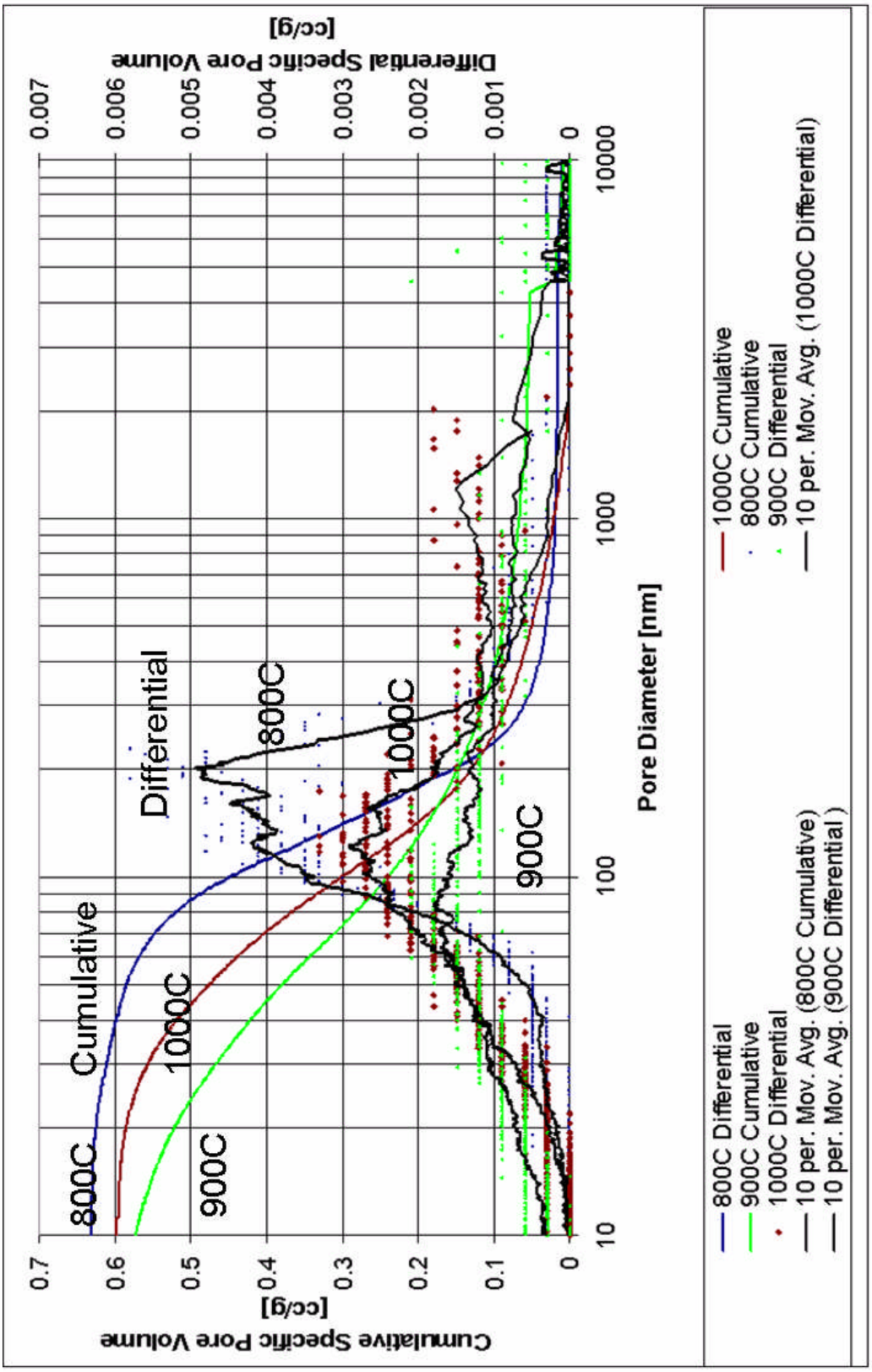

Figure F.3 Comparison of cumulative and differential specific pore volume distribution for new pellets sintered at different temperature

LIST OF REFERENCES

Aihara, M., Nagai, T., Matsushita, J., Negishi, Y., and Ohya, H., 2001, "Development of Porous Solid Reactant for Thermal Energy Storage and Temperature Upgrade Using Carbonation/Decarbonation Reaction," *Applied Energy*, Vol. 69, pp.225-238.

Aihara, M., Sakurai, M., Tsutsumi, A., and Yoshida, K., 1992, "Reactivity Improvement in the UT-3 Thermochemical Hydrogen Production Process," *International Journal of Hydrogen Energy*, Vol. 17, No.9, pp.719-723.

Aihara, M., Umida, H., Tsutsumi, A., and Yoshida, K., 1990, "Kinetic Study of UT-3 Thermochemical Hydrogen Production Process," *International Journal of Hydrogen Energy*, Vol. 15, No.1, pp.7-11.

Aochi, A., Tadokoro, T., Yoshida, K., Kameyama, H., Nobue, M., and Yamaguchi, T.,1989, "Economical and Technical Evaluation of UT-3 Thermochemical Hydrogen Production Process for an Industrial Scale Plant," *International Journal of Hydrogen Energy*, Vol. 14, No. 7, pp.421-429.

Amir, R., Sato, T., Yoko Yamamoto, K., Kabe, T., and Kameyama, H.,1992, "Design of Solid Reactants and Reaction Kinetics Concerning the Iron Compounds in the UT-3 Thermochemical Cycle," *International Journal of Hydrogen Energy*, Vol. 17, No.10, pp.783-788.

Amir, R., Shiizaki, S., Yamamoto, K., Kabe, T., and Kameyama, H., 1993, "Design Development of Iron Solid Reactants in the UT-3 Water Decomposition Cycle Based on Ceramic Support Materials," *International Journal of Hydrogen Energy*, Vol. 18, No.4, pp.283-286.

Barrett, E.P., Joyner, L.G., and Halenda, P.P.,1951, " The Determination of Pore Volume and Area Distributions in Porous Substances. I. Computations from Nitrogen Isotherms," *Journal of the American Chemical Society*, Vol. 73, pp. 373-380.

Brinker, J.C. and Scherer, G.W., *Sol-Gel Science: The Physics and Chemistry of Sol-Gel Processing*, New York, Academic Press Inc.

Brinker, J.C., Sehgal, R., Hietala, S.L., Desphande, R., Smith, D.M., Loy, D., and Ashley, C.S., 1994, *Journal of Membrane Science*, Vol. 94, p. 85.

Brown, L., Besenbruch, G., Schultz, K., Showalter, S., Marshall, A., Pickard, P., and Funk, J., 2002, "High Efficiency Generation of Hydrogen Fuels Using Thermochemical Cycles and Nuclear Power," AIChe 2002 Spring National Meeting, Topical TH- Nuclear Engineering

Brunauer, S., Emmett, P.H., and Teller, E., 1938, "Adsorption of Gases in Multimolecular Layers," Journal of American Chem. Soc.," Vol. 60, pp. 309-319.

Cox and Williamson, 1977-1979, *Hydrogen, Its Technology & Implications*, Volume 1 Cleveland, CRC Press

Ehrensberger, K., Frei, A., Kuhn, P., Oswald, H.R., and Hug, P., 1995, "Comparative Experimental Investigations of the Water Splitting Reaction with Iron Oxide $Fe_{1-y}O$ and Iron Manganese Oxides $(Fe_{1-x}Mn_x)_{1-y}O$," *Solid State Ionics*, Vol. 78, pp. 151-160.

Frostburg, A., 1997-2005,*General Chemistry Online :Glossary* accessed 05 March. 2005. <http://antoine.frostburg.edu/chem/senese/101/glossary/a.shtml>

Funk, J., 2001 "Thermochemical Hydrogen Production: Past and Present," *International Journal of Hydrogen Energy*, Vol. 26, No. 1, pp. 185-190.

Goswami D. Y., Ingley H. S., Goel N., Mirabal S. T., 2003, "Hydrogen Production", Chapter11, Advances in Solar Energy, Vol. 15, D.Y. Goswami, Editor-in-Chief, pp. 405-458.

Haueter, P., Moeller, S., Palumbo, R., and Steinfeld, A., 1999, "The Production of Zinc by Thermal Dissociation of Zinc Oxide-Solar Chemical Reactor Design," *Solar Energy*, Vol. 67, Nos.1-3, pp. 161-167.

Kameyama, H., Sato, T., Amir, R., Yoshida, K., Aihara, M., Sakurai, M., Tadokoro, Y., Kajiyama, T., Yamaguchi, T., and Sakai, N., 1992, "Cycle Simulation of the UT-3 Thermochemical Hydrogen Production Process," *International Journal of Hydrogen Energy*, Vol. 17, No.10, pp.789-794.

Kameyama, H., Tomino,Y., Sato, T., Amir, R., Orihara, A., Aihara, M., and Yoshida, K., 1989, "Process Simulation of "MASCOT" Plant Using the UT-3 Thermochemical Cycle for Hydrogen Production," *International Journal of Hydrogen Energy*, Vol. 6, No. 5, pp.567-575.

Kameyama, H., Yoshida, K., 1978, "Br-Ca-Fe Water-Decomposition Cycles for Hydrogen Production," *Proceedings of the 2nd World Hydrogen Energy Conference*, pp. 829-850.

Kameyama, H. and Yoshida, K., 1981, "Reactor Design for the UT-3 Thermochemical Hydrogen Production Process," *International Journal of Hydrogen Energy*, Vol. 6, No. 6, pp.567-575.

Kaneko, H., Hosokawa, Y., Kojima, N., Gokon, N., Hasegawa, N., Kitamura, M., and Tamaura, Y., 2001, "Studies on Metal Oxides Suitable for Enhancement of the O_2-Releasing Step in Water Splitting by the $MnFe_2O_4$-Na_2CO_3 System," *Energy*, Vol. 26, pp. 919-929.

Kaneko, H., Ochiai,Y., Shimizu, K., Hosokawa, Y., Gokon, N., and Tamaura, Y., 2002, "Thermodynamic study based on the phase diagram of the Na_2O-MnO-Fe_2O_3 system for H_2 production in three step water splitting with Na_2CO_3/ $MnFe_2O_4$/ Fe_2O_3," *Solar Energy*, Vol. 72, No. 4, pp. 377-383.

Livage, J., Henry, M., and Sanchez, "Sol-gel Chemistry of Transition Metal Oxides," C., *Prog. Solid St. Chem*., Vol.18, pp. 259

Meier, A., Ganz, J., Steifield, A., 1996, "Modeling of a Novel High-Temperature Solar Chemical Reactor," *Chemical Engineering Science*, Vol. 51, No. 11, pp.3181-3186.

Morooka, S., Kim, S.S., Yan, S., Kusakabe, K., and Watanabe, M., 1996, "Separation of Hydrogen from an H_2-H_2O-HBr System with a SiO_2 Membrane Formed in Macropores of an α-Alumina Support Tube," *International Journal of Hydrogen Energy*, Vol. 21, No.3, pp.183-188.

Nakayama, T., Yoshioka, H., Furutani, H., Kameyama, H., and Yoshida, K.,1984 "MASCOT—A Bench-scale Plant for Producing Hydrogen by the UT-3 Thermochemical Decomposition Cycle," *International Journal of Hydrogen Energy*, Vol. 9, No. 3, pp.187-190.

Ohya, H., Nakajima, H., Togami, N., Aihara, M., Negishi, Y., 1994, "Separation of Hydrogen from Thermochemical Processes using Zirconia-Silica Composite Membrane," *Journal of Membrane Science,* Vol. 97, pp. 91-98.

Ohya, H., Nakajima, H., Togami, N., Ohashi, H., Aihara, M., Tanisho, S., and Negishi, Y., 1997, "Test of One-Loop Flow Scheme for the UT-3 Thermochemical Hydrogen Production Process," *International Journal of Hydrogen Energy*, Vol. 22, No.5, pp.509-515.

Sakurai, M., Aihara, M., Miyake, N., Tsutsumi, A., and Yoshida, K., 1992, "Test of One-Loop Flow Scheme for the UT-3 Thermochemical Hydrogen Production Process," *International Journal of Hydrogen Energy*, Vol. 17, No.8, pp.587-592.

Sakurai, M., Bilgen, E., Tsutsumi, A., and Yoshida, K., 1996a, "Adiabatic UT-3 Thermochemical Process for Hydrogen Production," *International Journal of Hydrogen Energy*, Vol. 21, No.10, pp.865-870.

Sakurai, M., Bilgen, E., Tsutsumi, A., and Yoshida, K., 1996b, "Solar UT-3 Thermochemical Cycle for Hydrogen Production," *Solar Energy*, Vol. 57, No.1, pp.51-58.

Sakurai, M., Miyake, N., Tsutsumi, A., and Yoshida, K., 1996c, "Analysis of a Reaction Mechanism in the UT-3 Thermochemical Hydrogen Production Cycle," *International Journal of Hydrogen Energy*, Vol. 21, No.10, pp.871-875.

Sakurai, M., Nakajima,H., Amir, R., Onuki, K., and Shimizu, S.,1999, " Experimental Study on Side-Reaction Occurrence Condition in the Iodine –Sulfur Thermochemical Hydrogen Production Process," *International Journal of Hydrogen Energy*, Vol. 24, pp. 603-612.

Sakurai, M., Nakajima,H., Onuki, K., Ikenoya, K., and Shimizu, S., 2000a, " Preliminary Process Analysis for the Closed Cycle Operation of the Iodine-Sulfur Thermochemical Hydrogen Production Process," *International Journal of Hydrogen Energy*, Vol. 25, pp. 613-619.

Sakurai, M., Nakajima, H., Onuki, K., and Shimizu, S., 2000b, "Investigation of 2 Liquid Phase Separation Characteristics on the Iodine-Sulfur Thermochemical Hydrogen Production Process," *International Journal of Hydrogen Energy*, Vol. 25, pp. 605-611

Sakurai, M., Nakajima,H., Onuki, K., Ikenoya, K., and Shimizu, S., 2000a, " Preliminary Process Analysis for the Closed Cycle Operation of the Iodine-Sulfur Thermochemical Hydrogen Production Process," *International Journal of Hydrogen Energy*, Vol. 25, pp. 613-619.

Sakurai, M., Tsutsumi, A., and Yoshida, K., 1995, "Improvement of the Ca-Pellet Reactivity in UT-3 Thermochemical Hydrogen Production Cycle," *International Journal of Hydrogen Energy*, Vol. 20, No.4, pp.297-301.

Sanchez, C., Livage, J., Henry, M., and Babonneau, 1988, "Chemical Modification of Alkoxide Precursors," *Journal Non-Cryst. Solids*, Vol. 100, pg. 65.

Sasaki, M., and Hirai, T., 1995, "Corrosion Resistance of Ceramic-coated Stainless Steel in a Br_2-O_2-Ar Atmosphere," *Journal of European Ceramic Society*, Vol.15, pp. 329-335.

Steinfeld, A., Sanders, S., and Palumbo, R., 1999, "Design aspects of solar thermochemical engineering- a case study: two step water splitting cycle using the Fe_3O_4/FeO redox system," *Solar Energy*, Vol. 65, No. 1, pp. 43-53.

Sturzenegger M. and Nuesch, P., 1999, "Efficiency Analysis for a Manganese-Oxide-Based Thermochemical Cycle," *Energy*, Vol. 24, pp.959-970.

Tadokoro, Y., Kajiyama, T., Yamaguchi, T., Sakai, N., Kameyama, H., and Yoshida, K., 1997, "Technical Evaluation of the UT-3 Thermochemical Hydrogen Production Process for an Industrial Scale Plant," *International Journal of Hydrogen Energy*, Vol. 22, No.1, pp.49-56.

Teo, E.D., Brandon, N.P., Vos, E., and Kramer, G.J., 2005, "A Critical Pathway Energy Efficiency Analysis of the Thermochemical UT-3 Cycle," *International Journal of Hydrogen Energy*." Vol. 30, pp. 559-564.

Weidenkaff, Steinfeld, A.,A., Wokaun, A., Auer, P.O., EICHLER, B.,and A., Reller 1999, "Direct Solar Thermal Dissociation of Zinc Oxide Condensation and Crystallization of Zinc in the Presence of Oxygen," *Solar Energy*, Vol. 65, No. 1, pp. 59-69.

Weidenkaff, A., Reller, A., Sibieude, F., Wokaun, A., and Steinfeld, A., 2000, "Experimental Investigations on the Crystallization of Xinc by Direct Irradiation of Zinc Oxide in a Solar Furnace," *Chem. Mater.*, Vol. 12, pp. 2175-2181.

Westermarck, Sari, 2000, "*Use of Mercury Porosimetry and Nitrogen Adsorption in Characterization of the Pore Structure of Mannitol and Microcrystalline Cellulose Powders, Granules and Tablets*," accessed 19 April, 2005. <http://ethesis.helsinki.fi/julkaisut/mat/farma/vk/westermarck/useofmer.pdf >

Yoshida, K., Kameyama, H., Aochi, T., Nobue, M., Aihara, M., Amir, R., Kondo, H., Sato, T., Tadokoro, Y., Yamaguchi, T., and Sakai, N.,1990, "Reactor Design for the UT-3 Thermochemical Hydrogen Production Process," *International Journal of Hydrogen Energy*, Vol. 15, No. 3, pp.171-178

Zheng, H., Reaney, I.M., Csete de Gyorgyfalva, G.D.C., Ubic, R., Yarwood, J., Seabra, M.P., and Ferreira, V.M., 2004, "Raman Spectroscopy of $CaTiO_3$-based perovskite solid solutions," *Journal of Mater. Res.*, Vol. 19, No. 2, pp. 488-495.

BIOGRAPHICAL SKETCH

Benjamin Grant Hettinger was born in Madison, Wisconsin, in 1980. He was raised primarily in Ponte Vedra Beach, Florida. He graduated from Allen D. Nease High School in 1999 and that fall started classes at the University of Florida. He graduated magna cum laude with his Bachelor of Science in mechanical engineering from the University of Florida in December 2003. He then started graduate school at the University of Florida working on his master's in Mechanical Engineering in the area of thermal science. After graduating he plans on working at CDI Aerospace in West Palm Beach. His purpose in life is to glorify Jesus Christ his Lord and Savior.